Evaluation of Land Use and Land Cover Change Impacts on Streamflow and Sediment Yield, and Developing Best Management Practices: The Wollo Highland of Borkena Watershed in Ethiopia

Behaylu Dejen Asmare

A Thesis Submitted to
Department of Water Resources Engineering,
School of Civil Engineering and Architecture

Presented in Partial Fulfillment of the Requirements for the Degree of Master's in Water Resources Engineering (Specialization in Irrigation Engineering)

Office of Graduate Studies
Adama Science and Technology University

September, 2022
Adama, Ethiopia

Evaluation of Land Use and Land Cover Change Impacts on Streamflow and Sediment Yield, and Developing Best Management Practices: The Wollo Highland of Borkena Watershed in Ethiopia

Behaylu Dejen Asmare (ID: A/PE21006/12)

Advisor

Abdulkerim B. Serur (Ph.D.)

A Thesis Submitted to
The Department of Water Resources Engineering,
School of Civil Engineering and Architecture

Presented in Partial Fulfillment of the Requirements for the Degree of Master's in Water Resources Engineering (Specialization in Irrigation Engineering)

Office of Graduate Studies
Adama Science and Technology University

September, 2022
Adama, Ethiopia

DECLARATION

I hereby declare that this Master Thesis entitled **"Evaluation of Land Use and Land Cover Change Impacts on Streamflow and Sediment Yield, and Developing Best Management Practices: The Wollo Highland of Borkena Watershed in Ethiopia"** is my original work. That is, it has not been submitted for the award of any academic degree, diploma, or certificate in any other university. All sources of materials that are used for this thesis have been duly acknowledged through citation.

Behaylu Dejen Asmare	____________________	________________
Name of Student	Signature	Date

RECOMMENDATION OF THE ADVISOR

I, the advisor of this thesis, hereby certify that I have read the revised version of the thesis entitled **"Evaluation of Land Use and Land Cover Change Impacts on Streamflow and Sediment Yield, and Developing Best Management Practices: The Wollo Highland of Borkena Watershed in Ethiopia"** prepared under my guidance by Behaylu Dejen submitted in partial fulfilment of the requirements for the degree of Master of Science in Water Resources Engineering (Specialization in Irrigation Engineering). Therefore, I recommend the submission of the revised version of the thesis to the department following the applicable procedures.

Abdulkerim Bedewi Serur (Ph.D.)	________________	________________
Name of Advisor	Signature	Date

APPROVAL PAGE FOR THESIS

I, the advisor of the thesis entitled **"Evaluation of Land Use and Land Cover Change Impacts on Streamflow and Sediment Yield, and Developing Best Management Practices: The Wollo Highland of Borkena Watershed in Ethiopia"** by Behaylu Dejen, hereby certify that the recommendation and suggestions made by the board of examiners are appropriately incorporated into the final version of the thesis.

Abdulkerim Bedewi Serur (Ph.D.)	________________	______________
Name of Advisor	Signature	Date

We, the undersigned, members of the Board of Examiners of the thesis by Behaylu Dejen, have read and evaluated the thesis entitled **"Evaluation of Land Use and Land Cover Change Impacts on Streamflow and Sediment Yield, and Developing Best Management Practices: The Wollo Highland of Borkena Watershed in Ethiopia"** and examined the candidate during the open defense. This is, therefore, to certify that the thesis is accepted for partial fulfilment of the requirements of the degree of Master of Science in Water Resources Engineering (Specialization in Irrigation Engineering).

______________________	______________	____________
Chairperson	Signature	Date
______________________	______________	____________
Reviewer 1	Signature	Date
______________________	______________	____________
Reviewer 2	Signature	Date

Finally, approval and acceptance of the thesis is contingent upon the submission of its final copy to the Office of Postgraduate Studies (OPGS) through the Department Graduate Council (DGC) and School Graduate Committee (SGC).

______________________	______________	______________
Department Head	Signature	Date
______________________	______________	______________
School Dean	Signature	Date
______________________	______________	____________
Office of Postgraduate Studies, Dean	Signature	Date

ACKNOWLEDGMENTS

First and above all I would like to thank ‘The Almighty GOD’ for his guidance and for giving me the courage, wisdom and strength to walk unpaved way to reach this point in life during all my works and His provision to complete this work.

I would like to express my deep heartfelt gratitude to my advisor Abdulkerim Bedewi Ph.D. for his motivation, moral support, unbounded constructive comment and all rounded support he has provided me at all stages of my work.

I would also thank Ethiopian Meteorological Agency, Ministry of Agriculture, Ethiopian Mapping Agency and Ministry of Water and energy who provide me important data for the thesis. My gratitude also goes to Adama Science and Technology University (ASTU) for providing and gaining educational knowledge.

My special and great thanks goes to my beloved families who have been providing me with their love, support and encouragement the necessary help during my academic careers. Without their reliable help and advice this wouldn’t be real I am very proud to be part of such beautiful family.

I wish to show my gratitude to Mr. Kero Arigaw for giving valuable comments on different stages of the paper. Last but not least, I would like to give my deepest appreciations and acknowledgements to my beloved friends and relatives who have helped me in any form of support.

TABLE OF CONTENTS

DECLARATION i

RECOMMENDATION OF THE ADVISOR ii

APPROVAL PAGE FOR THESIS iii

ACKNOWLEDGMENTS iv

TABLE OF CONTENTS v

LIST OF TABLES viii

LIST OF FIGURES ix

LIST OF TABLES IN THE APPENDIX x

LIST OF FIGURES IN THE APPENDIX xi

ACRONYMS AND ABBREVIATIONS xii

ABSTRACT xiii

1. INTRODUCTION 1

1.1 Background 1

1.2 Statement of the Problem 2

1.3 Objective of the Study 3

1.3.1 General Objective 3

1.3.2 Specific objectives 3

1.4 Research Questions 3

1.5 Significance of the Study 4

1.6 Scope and Limitation of the Study 4

1.7 Thesis Organization 5

2. LITERATURE REVIEW 6

2.1 Land Use Land Cover Change 6

2.2 Application of RS and GIS for Land Uses Land Cover Analysis 7

2.3 Land Use Land Cover Changes Studies in Ethiopia 9

2.4 Impact of Land Use Land Cover Changes on Hydrological Response 11

2.5 Impact of Land Use Land Cover Changes on Sediment Yield 12

2.6 Hydrologic Models 13

2.6.1 Classification of hydrologic models....13

2.6.2 Model selection....15

2.6.3 Comparisons of SWAT model with other hydrological model....16

2.7 Soil and Water Assessment Tool (SWAT) Model....16

2.8 Best Management Practices (BMPs) to Reduce Sediment Yield....17

3. MATERIALS AND METHODS....20

3.1 Description of the Study Area....20

3.1.1 Location....20

3.1.2 Climate characteristics of the study area....21

3.1.3 Topography....22

3.2 Materials and Software Programs Used....22

3.3 Input Data and Methodology image....23

3.3.1 Weather data....23

3.3.2 Hydrological data (streamflow and sediment yield)....24

3.3.3 Digital Elevation Model (DEM)....26

3.3.4 Soil Data....27

3.3.5 Land use land cover data....28

3.4 Data Analysis....33

3.4.1 Filling missing data....33

3.4.2 Consistency test....33

3.4.3 Homogeneity test....35

3.5 Hydrologic Model Setup and Simulation....36

3.5.1 SWAT model setup....36

3.5.2 Hydrological component of SWAT....38

3.6 Sensitivity Analysis, Calibration, and Validation....42

3.6.1 Sensitivity Analysis....43

3.6.2 Model calibration and validation....43

3.6.3 Model performance evaluation....44

3.7 Analysis of Streamflow and Sediment Yield Responses under Changing LULC 46
3.8 Developing Best Management Practices 46
3.8.1 Baseline scenario 47
3.8.2 Filter strip 47
3.8.3 Terracing 48
3.8.4 Contour farming 48
3.8.5 Reforestation 48
3.9 Flow Chart of the Methodology 49
4. RESULTS AND DISCUSSIONS 50
4.1 Land Use Land Cover Change 50
4.1.1 Land use land cover classification accuracy assessment 50
4.2 Spatial and Temporal Distribution of LULC and Change detection 53
4.3 Streamflow Modelling 55
4.3.1 Streamflow sensitivity analysis 55
4.3.2 Streamflow calibration and Validation 57
4.4 Sediment Yield Modelling 61
4.4.1 Sediment yield sensitivity analysis 61
4.4.2 Sediment yield calibration and validation 63
4.5. Streamflow and Sediment Yield Responses to Land Use Land Cover Change 66
4.5.1 Streamflow responses to land use land cover change 66
4.5.2 Sediment Yield Responses to Land Use Land Cover Change 68
4.6 Spatial Distribution of Sediment Yield and Prioritization of Critical Sub-Basins 69
4.8 Evaluation of Best Management Practices. 74
5. CONCLUSIONS AND RECOMMENDATIONS 78
5.1 Conclusions 78
5.2 Recommendation 80
REFERENCES 81
APPENDIX 89

LIST OF TABLES

Table **Page**

Table 3.1 below shows weather stations used for this study including their class and location. 24

Table 3.2 Symbols and areal coverage of the soils in Borkena watershed 28

Table 3.3 Land use and land cover categories identified at the study area 30

Table 3.4 Overall recommended performance ratings (Moriasi *et al*., 2007) 46

Table 4.1 1990 image Accuracy assessment calculation of land use change analysis 51

Table 4.2 2006 image Accuracy assessment calculation of land use change analysis 52

Table 4.3 2020 image Accuracy assessment calculation of land use change analysis 52

Table 4.4 the spatial distribution of the major LULC classes in 1990, 2006 and 2020 54

Table 4.5 Shows the best optimized fitted parameters value during calibration 57

Table 4.6 Statistical analysis for streamflow calibration and validation periods 61

Table 4.7 Sediment yield parameters sensitivity rank 63

Table 4.8 Average annual basin water balance value and change 68

Table 4.9 Modified SWAT parameters 72

Table 4.10 Summary of sediment reduction with filter strip, parallel terracing, contour farming and reforestation simulation. 74

Table 4.11 Comparison best management practices in the study area 74

LIST OF FIGURES

Figure **Page**

Figure 3.1 Map of the Study Area 20

Figure 3.2 Mean monthly precipitation characteristics of the study area 21

Figure 3.3 Mean monthly maximum and minimum temperature characteristics of the study area. 22

Figure 3.4 Mean monthly flow of Borkena (swamp outlate) stations (1990-2015) 25

Figure 3.5 Sediment rating curve for Borkena swamp gauging Station 26

Figure 3.6 Slope map of the study area 27

Figure 3.7 Soil map of the study area 28

Figure 3.8 Consistency checking for the six Rainfall stations within and around the catchment.... 34

Figure 3.9 Sub-basins of the study area 37

Figure 3.10- Flow chart of the overall methodology 49

Figure 4.1 Land use land cover type map of (a) 1990, (b) 2006, and (c) 2020 53

Figure 4.2 Streamflow sensitive parameters 56

Figure 4.3 Observed and simulated streamflow hydrograph for calibration (a) and scatters plot of observed Vs simulated flow for calibration (b) and simulated vs observed average monthly flows generated from SWAT CUP during calibration (c) 59

Figure 4.4 Observed and simulated streamflow hydrograph for validation (a) and scatters plot of observed Vs simulated flow for simulation (b) and simulated vs observed average monthly flows generated from SWAT CUP during simulation (c) 60

Figure 4.5 p-value and t-stat for sensitivity analysis of sediment yield.......... 62

Figure 4.6 Observed and simulated sediment yield hydrograph for calibration (a) and scatters plot of observed Vs simulated Flow for calibration (b) and simulated vs observed sediment yield generated from SWAT CUP during calibration (c) 64

Figure 4.7 Observed and simulated sediment yield hydrograph for calibration (a) and scatters plot of observed Vs simulated flow for calibration (b) and simulated vs observed sediment yield generated from SWAT CUP during calibration (c) 65

Figure 4.8 Annual simulated streamflowat different LULC.......... 66

Figure 4.9 Mean monthly streamflowat different LULC.......... 67

Figure 4.10 Mean monthly sediment yield for 1990, 2006 and 2020 LULC 69

Figure 4.11 Spatial distribution of (a) surface runoff and (b) sediment yield in the study area 70

Figure 4.12 Comparison of best management practices in critical sub-basins 75

Figure 4.13 Comparison of best management practices sediment yield spatial distribution 77

LIST OF TABLES IN THE APPENDIX

Table **Page**

Appendix A.1 Average annual rainfall of station in the study area 89
Appendix A.2 Parameters used in a streamflow sensitivity analysis 91
Appendix A.3 Parameters used in sediment yield sensitivity analysis 92
Appendix A.4 Sub basins Surface Runoff and Sediment Yield distribution 93
Appendix A.5 Monthly average basin water balance value 94

LIST OF FIGURES IN THE APPENDIX

Figure **Page**

Appendix B.1 Homogeneity test plot at station Kombolcha...95
Appendix B.2 Homogeneity test plot at station Kemisse 95
Appendix B.3 Homogeneity test plot at station Majete 95
Appendix B.4 Homogeneity test plot at station Cheffa 96
Appendix B.5 Homogeneity test plot at station Dessie..96
Appendix B.6 Homogeneity test plot at station Harbu 96

ACRONYMS AND ABBREVIATIONS

BMPs	Best Management Practices
CN	Curve Number
DEM	Digital Elevation Model
ENVI	Environment for Visualizing Images
ERDAS	Earth Resource Data Analysis System
ETM	Thematic Mapper
ETM+	Enhanced Thematic Mapper Plus
FAO	Food and Agricultural Organization
GCP	Ground Control Point
GIS	Geographical Information System
GWQ	Groundwater Flow
HRUs	Hydrologic Response Units
LATQ	Lateral Flow
LST	Land Satellite
LULC	Land Use Land Cover
m.s.l	Mean Sea Level
MoWE	Ministry of Water and Energy
MSS	Multispectral Scanner
MUSLE	Modified Universal Soil Loss Equation
NMA	National Meteorological Agency
NSE	Nash-Sutcliffe Efficiency
OLI	Operational Land Imager
PBIAS	Percent Bias
R^2	Coefficient of Determination
RS	Remote Sensing
SCS	Soil Conservation Service
SRTM	Shuttle Radar Topography Mission
SUFI-2	Sequential Uncertainty Fitting Version 2
SURQ	Surface Runoff
SWAT	Soil and Water Assessment Tool
UTM	Universal Transverse Mercator

ABSTRACT

LULC change has been identified as a major research priority around the world, with multi-directional consequences for both human and natural systems. Borkena watersheds were among the most vulnerable natural systems and continue to face a number of difficult issues in water and land resource management as a result of rapid population growth, urbanization, and industrialization. The overall objective of this research was to assess the impact of LULC change on streamflow and sediment yield, as well as to develop best management practices (BMPs), which are critical for long-term sustainable water and land resources management and development in the Borkena watershed. The LULC change analyses for three periods (1990, 2006 and 2020) were performed using ERDAS Imagine 2014 with a maximum likelihood classifier. The SWAT hydrologic model is used to investigate the impact of LULC change on streamflow and sediment yield, as well as to identify and prioritize critical sub-watersheds whose annual sediment yield limit ranges above the tolerable one for developing watershed best management practices. The SWAT model's performance in simulating catchment hydrology and sediment yield was evaluated using sensitivity, uncertainty analysis, calibration, and validation with coefficient of determination (R^2), Nash Sutcliff efficiency (NSE), and % bias (PBIAS) standard statistical indices. The SWAT model was calibrated and verified to evaluate the effect of LULC change streamflow and sediment yield in this watershed. Using SWAT-CUP, a SWAT model's streamflow and sediment yield were calibrated for the years 1990–2007 and validated for 2008–2015. The statistical analysis results revealed that the observed and simulated values of streamflow and sediment yield agree20d well with R^2 =0.82, NSE =0.69, PBIAS = -17.3, P-factor = 0.71, and R-factor = 1.64 for streamflow calibration and R^2 =0.81, NSE =0.65, PBIAS = -14.3, P-factor = 0.6, and R-factor = 1.86 for streamflow validation. Similarly, for sediment yield calibration, R^2= 0.81, NSE= 0.72, PBIAS= -14.6, P-factor = 0.61, and R-factor = 0.71 and R^2 = 0.8, NSE = 0.7, PBIAS = -17.2, P-factor = 0.72, and R-factor = 1.02 for sediment yield validation. Cropland increased from 25.50 to 32.30%, settlement increased from 1.30 to 7.80%, and bareland increased from 0.01to 2.90% between 1990 and 2020, according to a land cover change analysis. While forest declined from 47.20 to 32.70%, grassland declined from 8.30 to 5.40%, and shrubland declined from 17.50 to 4.80%. As a result of LULC changes, changes in streamflow and sediment yield were observed. Based on this, simulated model outputs using 1990, 2006, and 2020 LULC showed an increase in average annual water yield of 35.3 mm (4.7%) and 56.5 mm (7.2%) between 1990 and 2006, respectively, while sediment yield increased by 4.4 t/ha (81.4%) between 1990 and 2006, and by 2.8 t/ha (28.2%) between 2006 and 2020. Based on the average annual simulated sediment yield using 2020 LULC, the six critical sub-watersheds with annual sediment yield limit ranges above the tolerable limit were identified and prioritized for effective watershed management. As a result, four BMPs, namely filter strips, terracing, contour farming, and reforestation, were developed for critical sub-watersheds to reduce sediment yield. The results revealed the terracing management option reduce the sediment yield up to 72.32%. Implementing filter strips with 5m and 3 m wide indicates 57.12% and 50.67% reduction respectively. Contour farming alternative reduce the sediment yield up to 63.56% whereas, reforestation has given the least reduction that is 33.81%. Therefore, applying terrace management option in critical sub-watershed is the most effective practice for reducing sediment yield in the Wollo Highland of Borkena Watershed in Ethiopia.

Keywords: LULC Change; SWAT Model; Streamflow; Sediment Yield; BMPs; Wollo Highland of Borkena Watershed

1. INTRODUCTION

1.1 Background

Changes in land use and cover have a significant impact on several hydrological processes such as infiltration, evaporation, and interception, which affect soil moisture levels, runoff generation (both process and volume), and streamflow regimes. The hydrological regime and rainfall-runoff mechanisms are altered as a result of land use and land cover because it alters some hydrological parameters, such as vegetation interception, soil water content, and surface evapotranspiration (Li *et al*., 2007). In this sense, the change in land use and land cover (LULC) is a significant factor in the global environment (Prakasam, 2010).

Numerous hydrological studies have demonstrated how LULC changes have impacted the hydrology of different watersheds across the world. In addition, LULC variations can modify the amount of infiltration and runoff (Houghton *et al*., 1995). More specifically, the increased volume of surface runoff and peak discharge of streamflow brought on by urbanization's increased impermeable surface prevents precipitation from penetrating the soil to the aquifer and increases both of these factors, which can put people at danger of floods. Second, increased streamflow has the potential to pollute streams and other water bodies by picking up significant quantities of soil pollutants, which frequently include fertilizers and pesticides. Third, another effect is eroded sediment from building sites and agricultural land.

One of Ethiopia's biggest environmental issues is changing land use (Tsegaye, 2019). Any activity that reduces the ability of land resources to provide critical ecosystem services and results in severe erosion problems is referred to as "land degradation" (Hurni *et al*., 2010). High rates of soil erosion, sediment transport, and loss of agricultural nutrients have all been significantly influenced by poor land use practices and inadequate management systems. Few actions have been made thus far to address these issues. The most heavily used basin in Ethiopia is the Awash basin.

Because of the fast population growth, urbanization, and industrialization, Borkena watersheds are among the most delicate natural systems and continue to face a number of difficult problems in the management of land resources (Tekle and Hedlund, 2000). For many years, people have altered a land cover to serve their intended purposes. One of the primary factors influencing the change in land use in the Borkena Watershed is the rapid rate of population growth (Shawl, 2020).

It can also be used to model soil and water loss in small watersheds with an agricultural predominance. In the SWAT model, the watershed is divided into subbasins to facilitate modeling or estimation of flow, sediment, or nutrient transport.

The SWAT model was used to simulate the streamflow and sediment yield of Borkena watershed. It is a semi-distributed physical-based hydrological model that has been commonly used for investigating the impacts of land use land cover change on water resources around the world (Garg *et al*., 2017). By combining GIS, RS, and a physically based semi-distributed SWAT model, the study primarily focuses on analyzing the effects of LULC changes on streamflow and sediment yield and creating best management practices (BMP) in the Borkena watershed, the highland of Wollo.

1.2 Statement of the Problem

Extreme rainfall incidents, whose characteristics are difficult to objectively assess in terms of frequency, intensity, duration, and spatial extent, reflect meteorological drought and flood (Vasiliades and Loukas, 2009). Flooding, drought, and the loss of ecosystem services are just a few of the serious water resource issues Ethiopia is facing (Wassie, 2020) Ethiopia's biggest issue is also soil degradation. Erosion was increased by deforestation, excessive grazing, and inadequate land management. Many farmers cultivate sloppy or hilly land in Ethiopia's highlands, which leads to top soil being swept away during the rainy season's torrential downpours. Pressure on land resources due to the rapidly expanding population has even led to forest destruction and overgrazing.

Due to the fast development of population, urbanization, and industry, Borkena watersheds among the most delicate natural systems experience a variety of difficult problems in land resource management (Tekle and Hedlund, 2000). Rapid changes in land use have a significant impact on the water balance because they modify the ecosystem. The most predominant and widespread issues in the basin are land degradation, which includes the loss of top fertile soil, flood risk during the rainy season (on kemisie), and a lack of water supply for irrigation during the dry season (Metaferia, 2019). In recent years, severe floods in the affected areas damaged homes and other infrastructure, resulted in mortalities, and had an impact on socioeconomic operations. As a result, there is a clear need for hydrological approaches and tools that can evaluate the expected impact of land cover changes on a catchment's hydrologic response. It is difficult to quantify the overall yearly runoff volume and sediment yields leaving the watershed.

Therefore, watershed management is the most crucial strategies to handle the above-mentioned scenario as it aids in reducing land degradation, increasing vegetation cover, and increasing the productivity of the watershed region (Taddese, 2001). For the management of sedimentation and usage of water resources, a thorough assessment of the streamflow and sediment yield analyses of the watershed is necessary.

1.3 Objective of the Study

1.3.1 General Objective

The main objective of the this study was to evaluate the effects of land use land cover changes on streamflow and sediment yield**,** and Identification of Management practices in Borkena River watershed.

1.3.2 Specific objectives

In order to achieve the main objective of the study, the following specific objectives are set:

- To assess spatiotemporal variations of land use land cover changes of Borkena Watershed from 1990 to 2020 historical time period.
- To evaluate the performance of the SWAT hydrologic model in simulating streamflow and sediment yield in the Borkena watershed.
- To assess the impact of land use land cover change on stream flow and sediment yield.
- To develop best watershed management practices to reduce sedimentation issue in the Borkena Watershed.

1.4 Research Questions

In order to meet the research objectives of the study, the following four research questions were formulated;

- What is the general trend of LULC over the three selected periods?
- How successfully does the SWAT hydrologic model simulate streamflow and sediment yield in the Borkena watershed?
- What is the change in stream flow and sediment yield under changing land use and land cover over the study area?
- What are the best management practices to reduce sediment yield in the study area?

1.5 Significance of the Study

LULC has a profound impact on the functioning of socioeconomic and environmental systems, with considerable tradeoffs for sustainability, food security, biodiversity, and people's and ecosystem's vulnerability to global change consequences (Kassa, 2009; Wolde *et al*., 2021). In Ethiopia, most parts of the regions face threats concerning food production that mostly affects the rural livelihood mainly due to an increase in population on one hand and inappropriate resource management on the other hand. However, there is no systematic research on techniques that deal with impact analysis of LULC on hydrological regime and identifying sediment prone areas at a watershed level and sub-watershed level in the study area.

Hence, the knowledge of how LULC influences streamflow, sediment yield and identifying sediment hotspot areas will enable policymakers and planners to formulate watershed management actions to minimize the adverse effect of future land-use changes on hydrological regimes. Besides, it is important to have a good understanding of the effect of historic LULC on hydrologic response to predict the future LULC change effects on water resources. This study will play its role by providing important information on LULC change and its impact on the streamflow and sediment yield as well as the best watershed management practices to alleviate sediment yield entering into Borkena River.

1.6 Scope and Limitation of the Study

The scope of this study would be limited to evaluating the impact of land use/land cover change impacts on streamflow and sediment yield, model performance evaluations, and application of the model on the selection of sediment management options. Land use land cover classification of satellite images were classified by using ERDAS Imagine Software. Model performance evaluation, calibration and validation, analysing sensitive parameters by using Automatic calibration and uncertainty analysis incorporated in SWAT2012 via the SWAT-CUP was used for this study.

The study has not considered the impacts of climate change on the hydrologic responses in the study area due to the shortest time span. In addition to this, due to limitations in streamflow and sediment yield data availability, the study has evaluated the model performance at the outlet only.

1.7 Thesis Organization

This thesis contains five chapters organized as follows: The first chapter states the introduction or background of the study, also provide the information on why this research was done as well as its objectives and highlight the significance and scope of the study. Chapter two concentrates on literatures reviewed related to this study. This section presents a brief understanding of land-use/land-cover changes, where the definition and concepts of LULC changes, the hydrological responses to LULC change, SWAT model theoretical concept and its application, and best management practices were reviewed. Chapter three describes the description of the study area including geographical location, topography, soil and climate characteristics of the study area and focuses on the methodology which includes data collection, hydrological model selection, methods of data analysis and model performance evaluation and developing BMPs were described. Chapter four describes the results and discussion of the study. Finally, chapter five deals with the conclusion of research questions and recommendations for further research direction in the study have been explained.

2. LITERATURE REVIEW

This section presents a brief understanding of land-use/land-cover changes, where the definition and concepts of LULC changes, the hydrological responses to LULC change, SWAT model theoretical concept and its application, and best management practices were reviewed.

2.1 Land Use Land Cover Change

The study of land surface change is known as land use land cover (LULC). While land cover (such as forest or desert) defines the biophysical aspects of the land surface, land use (such as agriculture, pasture, or plantation) describes how humans use land. Changes in land usage may have an impact on changes in land cover, and vice versa. Forests, shrublands, grasslands, croplands, ice and snow, urban areas, and aquatic bodies make up the majority of land cover categories. While the term "land use" refers to how people use or occupy a piece of land. Land cover conversion and modification are two ways to describe land cover change. Land cover change can be characterized as land cover conversion and modification. Land cover conversion is a change from one land category in to another and modification is a change in condition with in a land cover category (Jansen & Di Gregorio, 2002).

Use of land resources by the people gives rise to land use which varies with the purposes it serves, whether there for food production, provision of shelter, recreation, extraction and processing of materials, and the bio-physical characteristics of land itself (Parveen *et al*., 2018). Land-use change is always caused by multiple interacting factors originating from different levels of organization of the coupled human environment systems (Tadele and Forech, 2009). The mix of driving forces of land-use change varies in time and space, according to specific human-environment conditions. Lambin *et al*. (2003), described fundamental causes leading to land-use change as endogenous and exogenous.

Although exogenous variables may also have an impact, the primary causes of land-use change are primarily endogenous and include shortage of resources, increasing vulnerability, and changes in social organization. Even if the reaction of land managers to these external influences is heavily mediated by local circumstances, the other high-level reasons, such as shifting market possibilities and policy involvement, are primarily exogenous. Choubin *et al*. (2019) found that decreased soil moisture content and groundwater recharge resulted in increased overland flow, which in turn accelerated sediment detachment and transport in degraded watersheds. Land-cover change is mostly brought on by changes in land usage.

The driving forces to this activity could be economic, technological, demographic, scenic and or other factors. Hence, LULC changes is a result of complex interactions between several biophysical and socio-economic conditions which may occur at various temporal and spatial scales (Reid *et al*., 2000).

2.2 Application of RS and GIS for Land Uses Land Cover Analysis

Remote sensing and geographic information system techniques have been widely used over the world for the study of historical changes in LULC and LST analysis. Remote sensing has been used to identify vegetation cover, air pollution, LST and other surface characteristics (Wang *et al.*, 2012; Zhu, 2011). To manage the land, it is also critical to comprehend the relationship between LST and LULC. It offers a huge diversity and quantity of data on the earth's surface for in-depth research and change detection using several airborne and space borne technologies. Remote sensing technology is prepared to have an even bigger impact on monitoring land-cover change thanks to the availability of previous remote sensing data, the decrease in data cost, and the enhanced resolution from satellite platforms.

Land-use/land-cover changes can be analyzed over a period using Landsat sensors such as Landsat Multi Scanner (MSS) data and Landsat Thematic Mapper (TM) data by image classification techniques (Gudmundsson, 2001). Geographic Information System is a system designed to capture, store, manipulate, analyze, manage and present spatial or geographic data. The data type in GIS can be classified into two major groups as spatial and non-spatial data. The spatial data are the data that have location value and that non-spatial data are a data, which describe more the spatial data in the form of a table.

According to Yuan (2001), data in GIS is composed of three dimensions that mean spatial (geographic), time and attribute. Some people believe that geographic information system as the system of hardware and software, which contribute to analyze applications or information processing (Prakasam, 2010). In addition to serving as a digital repository for spatial objects (areas, points, and lines), geographic information systems are also capable of performing spatial analyses based on the relationships between these objects, including the relationships between objects that are determined by their location and geometry. There are only roughly 157 different land cover types included in the Modified United Nations Educational Scientific and Cultural Organization (UNESCO) Classifications scheme, and no research location will have every single one of them. In order to classify pixels, it will be essential to combine them into a smaller number of closely related classes based on spectral similarity (Ponce-Hernandez & Oumer, 2009).

There are two major approaches of classification which is the supervised analysis and the unsupervised analysis, form the backbone of image classification activities (Sivakami *et al*., 2010). In a supervised classification involves identifying a working out area consisting of sample pixels that belong to a known informational class. The spectral characteristics of the working out area are computed statistically. The classification algorithm is trained to categorize sample pixels on the basis of their statistical similarity to the training area characteristics. The pixels of the image arc assigned to the informational class that most closely resembles the spectral signature of the sample pixels.

In an unsupervised classification identifies spectrally similar groups or clusters within the multispectral data (Al-Doski *et al.*, 2013). Remotely sensed images are usually composed of spectral clusters that are reasonably uniform with respect to brightness in several spectral bands. Although the existence of the clusters (or classes) may not be intuitively obvious, unsupervised classification is defined as the definition, identification, labeling, and mapping of these natural or spectral classes. the desired number of groups or clusters will be inputs to the software The software then groups the pixels according to similar spectral characteristics in order of decreasing brightness. These groupings are not made on the basis of land cover, but on the similarity in spectral characteristics of the pixels.

A third method known as "hybrid classification," which combines supervised and unsupervised classification techniques, is also frequently encountered. In order to assess the quality of the classification process, it is common practice to compare the classification to geographical data that are presumed to be accurate. A classification's accuracy is often evaluated by comparing it to some reference data that is thought to properly reflect the true land-cover. The purpose of a land cover map is to depict how the land cover has changed within a watershed and to categorize the various types of land use and cover.

In order to estimate land cover changes and support impact assessments, remotely sensed imagery is essential for acquiring information on temporal trends, spatial distribution of watershed areas, and changes through time (Atasoy *et al.*, 2006). Multi temporal remotely sensed images are regarded as efficient data sources for tracking the rapid changes in land cover, identifying different types of land cover, and obtaining timely information about land cover.

2.3 Land Use Land Cover Changes Studies in Ethiopia

In Ethiopia, the availability of natural resources varies by location, as does the management style. Because of variations in biogeography and topography, there is variability. Human actions are driving changes in land use and land cover, but they are also having an impact on people (Agarwal, 2002). Different biophysical entities change as a result of LULC changes. The functions, changes, and structures of most landscapes are significantly impacted by the change in land use and cover (LULC), a complex process that is influenced by a number of interconnected processes, ranging from environmental factors to socioeconomic change (Yesuph & Dagnew, 2019b).

Over the course of several centuries, early human settlers in the Ethiopian highlands were drawn by the region's ideal agro-climatic conditions to occupy all agriculturally viable places. So, with the following clearing of forests and other vegetation, agriculture progressively spread from gently sloping ground into steeper slopes in the highlands as well as the flat swampy plains of the plateau (Esa *et al.*, 2018).

Yesuf *et al*. (2015) identified the spatiotemporal LULC changes across the lake Hayq closed drainage basin in northeast Ethiopia over 50 years from 1957-2007. They indicated that farmlands/settlements and shrublands/degraded lands increased by 43.1% and 136.9%, at an annual rate of 27.4 and 13.5 ha/yr respectively between 1957 and 2007. In contrast, bushlands, grasslands, forestlands, and lake surface area were diminished by 68.8%, 62.7%, 90.5%, and 7.6%, at a rate of 24.0, 7.6, 6.1, and 3.7 ha year/ respectively, over the five decades. Recently, Yesuph and Dagnew (2019) conducted their study at Beshillo watershed of the Blue Nile basin in the North-Eastern highlands of Ethiopia for the period 1973 to 2017. They identified seven major LULC classes, and the study's overall scenario indicates that the watershed has had highly noticeable LULC shifts in the past, which are likely to be continuing in the future due to ongoing anthropogenic activities and natural forces.

According to Kassa, (2009), the conversion of natural forests and grazing lands to croplands resulted in the reduction of these resources in his study in southern Wello. Both the Chemoga watershed in north-western Ethiopia and the Sebat-bet Gurage area in south-central Ethiopia have recorded an increase in wood lots (eucalyptus tree plantations) and cultivated land at the expense of grazing land, according to Bewket, (2014). LULC Changes that occurred from 1971/72 to 2000 in Yerer Mountain and its surrounding results an expansion of cultivated land at the expense of the grasslands (Gebrehiwet, 2004).

Daba (2018) Assessed SWAT simulated hydrological response to climate change impacts and its adaptation strategies in the upper Awash River basin. The study used the Soil and Water Assessment Tool (SWAT) hydrological model and Regional Climate Model (RCM). To investigate the hydrological impact of a possible future climate change scenario; downscaling of regional climate model (ECHAM5 with A1B emission scenario) to meteorological variables at local scale was applied for three time periods (the 2020s, 2050s, and 2080s.

Awash Basin Authority (2017) studied the Implement Integrated Participatory Watershed Management. Awash Basin were prone to watershed degradation problems. Agricultural development activity has been increasing but at the expense of forest land destruction, the total erosion generated from the basin high the result impact on downstream of Awash River with sediment deposition and flooding. The sub-basins, which have high topographical elevation, flow accelerated result of soil erosion. These problems are attributed to erosion, sedimentation and flooding. Therefore, it developed based on the planning area on the issues of erosion, sedimentation and the associated flooding hazards and their impact on the water resource infrastructures like reservoirs and natural ponds.

Girum has reported on the effects of land use and land cover changes on the hydrology of this watershed (2019). According to his report, land cover change analysis revealed that between 1986 and 2011, cultivated land increased from 8.58% to 14.25%, agricultural land increased from 9.88% to 34.82%, and urban areas increased from 1.16% to 9.94%. Between 1986 and 2011, shrub land decreased from 11.04% to 8.39%, forest decreased from 57.33% to 23.77%, grassland decreased from 10.74% to 8.74%, and wetland decreased from 1.26% to 0.09%. In this paper, the SWAT was calibrated and validated using four metrological stations from 1998 to 2001: Kombolcha, Kabie, Cheffa, and Majetie. But there was a station upstream of the watershed, it was best to include Dessie station, and each station had data from 1990 to 2016, so it was best to run the model for a long period of time.

According to many literatures, population growth has a paramount impact on the environment. For instance, population pressure has been found to have negative effect on Riverine vegetation, scrublands and forests in Kalu district (Gebrehiwet, 2004; Zeleke & Hurni, 2001) Riverine trees in Chemoga watershed, and natural forest cover in Dembecha Woreda north-western Ethiopia Zeleke and Hurni, (2001). Similarly, (Ali, 2009) report that the population growth has significant effect on land degradation, poverty and food insecurity in the northern Ethiopian highlands.

However, the majority of empirical evidence suggested that changes in land use and land cover and socioeconomic change have a strong relationship; as population grows, there is an increased need for arable land, grazing land, and fuel wood; settlement areas also grow to accommodate the rising demand for food and energy, as well as an increase in the number of livestock. Therefore, the main factors contributing to the deforestation and degradation of natural resources in Ethiopia are thought to be population pressure, a lack of awareness, and poor management (Geremew, 2013).

2.4 Impact of Land Use Land Cover Changes on Hydrological Response

The hydrological flow system of river basins is significantly impacted by LULC change. The hydrologic cycle and the properties of the land surface are closely related, according to Namarata *et al.* (2004). Variations in the vegetation cover typically have an impact on the amount of infiltration, runoff, evaporation rate, and pattern of precipitation.

Gashaw *et al.* (2018) studied effects of land-use change on the hydrological conditions of the Andassa watershed, Blue Nile Basin in Ethiopia, for the years 1985 to 2015. They noted an increase in annual streamflow (2.2%), wet seasonal streamflow (4.6%), surface runoff (9.3%), and water yield (2.4%) while a decrease in dry season streamflow (2.8%), lateral flow (5.7%), ground water flow (7.8%), and ET (0.3%) occurred over the course of their study period as a result of a steady expansion of cultivated land and settlement and a decline in forest, shrubland, and grassland. According to Shawul *et al.* (2019), in the Upper Awash Basin, the conversion of native forest, shrubland, and pasture to agriculture and urban land resulted in a relatively significant increase in surface runoff and total water yield, but also a declining trend in evapotranspiration, lateral flow, and groundwater flow. To regulate changes in runoff volume and sediment yields, several statistical papers are frequently utilized to compare different land use patterns.

Peak flows may rise as a result of a change in land use if the soil's infiltration capacity is decreased, for instance due to soil compaction or erosion, or if the drainage capacity is raised. After trees are taken down, peak flow may rise (Bruijnzeel, 1990). Large events had the smallest relative increases in storm flow following tree removal, while tiny events have the biggest. As precipitation increases, soil and plant cover have less of an impact on storm movement (Bruijnzeel, 1990). This knowledge gap about how the Borkena River's high and low discharge regimes respond to shifting land-use/cover during the study period was successfully filled by the current study.

2.5 Impact of Land Use Land Cover Changes on Sediment Yield

Soil erosion is one of the most important environmental problems among various forms of land degradation that pose a serious challenge to the food security of the population and the future development prospects of the country. The high intensity of rainfall in the highlands, as well as the disjointed topography, cause accelerated erosion, with over 70% of the highlands having a slope greater than 30% (Wagayehu & Lars, 2003).

Rocks from the earth's crust physically and chemically disintegrate to generate sediment, which is a fragmented material. Sediment yield, which is the parameter of primary concern in reservoir studies, is the total amount of fluvial sediment exported by the watershed tributary to a measurement point. It is the amount of eroded sediment discharged by a stream at any given point and refers to the amount of sediment exported by a basin over a period. Their sizes, specific gravities, and mineral makeup all differ. Once the sediment fragments have been released, they can be moved by gravity, wind, or water. Sediment is a critical pollutant in surface water that adversely affect water quality and contains other important contaminants (including nutrients, impacts of land use/ land cover Change on sediment yield and streamflow to Hydropower Reservoirs. pesticides and heavy metals) (Deshmukh *et al*., 2005).

The amount of sediment produced depends on soil erosion parameters (primarily rainfall, soil quality, land use, and terrain) as well as transit capability (Deshmukh *et al*., 2005). Since the capacity to carry sediment varies depending on the kind of land cover, sediment spread is also a function of land use. At gauging stations, the entering sediment load is typically monitored. The sediment-rating curve is determined by flow and sediment observations. The daily sediment discharge often distances several orders of magnitude, and the sediment rating curve is typically much dispersed.

2.6 Hydrologic Models

Modeling is the process of organizing, synthesizing, and integrating parts into a realistic representation of the prototype. Hydrological models are mathematical descriptions of components of the hydrologic cycle to simulate real-world hydrologic processes. However, hydrological models are in general designed to meet one of the two primary objectives. The one objective of the watershed hydrologic modelling is to get a better understanding of the hydrologic processes in a watershed and of how changes in the watershed may these phenomena. The other objective is for hydrologic prediction (Tadele, 2007). They are also providing valuable information for studying potential impacts of changes in land use and land cover or climate.

2.6.1 Classification of hydrologic models

Hydrological models vary in ways of the time step, spatial scale, whether the model simulates single events or continuously, and how different hydrological components are computed. According to Dwarakish and Ganasri (2015), watershed-scale models are further divided into lumped, semi-distributed, and fully distributed models based on their spatial distribution. The lumped modeling approach treats a watershed as a single unit for computations by averaging watershed parameters and variables over a single unit. Semi-distributed models divide the entire watershed into HRUs or sub-basins, whereas spatially variability is represented by grids in distributed models. Comparatively, semi-distributed and distributed models account for the spatial variability of hydrologic processes, input, boundary conditions, and watershed characteristics better than lumped models (Elfert and Bormann, 2010).

The models can be characterized as stochastic, deterministic, and mixed depending on how the hydrological processes are represented. The outcome of a deterministic model is exactly specified by known relationships between states and events with leaving no space for random variation. In such models, two equal sets of model input run always yield the same output under identical conditions. On the other hand, if a model has at least one component of random character which is not explicit in the model input, but only implicit or hidden it is called a stochastic model. If the model components are described by a mix of deterministic and stochastic components, the model is called a stochastic-deterministic or hybrid model (Kassa, 2009).

The hydrological models can also be classified according to whether the hydrological processes are described as conceptual, empirical, or fully physically based. Empirical models are used to establish a relationship between rainfall and runoff to predict runoff in different catchments (Chen *et al*., 2013; Shirke *et al*., 2012). Empirical models contain no physical transformation function to relate input to output; such models usually build a relationship between input and output based on hydro-meteorological data (Sarkar and Kumar, 2012). Physical processes such as subsurface flow, surface runoff, and infiltration in the watershed are not explicitly considered in empirical models, which is a major limitation. Furthermore, these numerical models are incapable of modeling the impact of vegetation changes on various hydrological components (Dwarakish and Ganasri, 2015).

Conceptual models are used for simplifications of the complex processes of a catchment. The particular components of these models often have to be described by empirical functions based on the observation of certain processes. Physically-based distributed models, on the other hand, can explicitly represent the spatial variability of important land surface characteristics including topographic elevation, slope, aspect, vegetation, and soil, as well as climatic parameters such as precipitation, temperature, and evapotranspiration distribution (Akbari and Singh, 2012).

2.6.2 Model selection

Within each class of models, there are a variety of different model architectures. Therefore, one of the issues facing the model user community is selecting a specific model structure for a specific application. Beven (2000) offered guidelines for choosing models based on their structure and outward appearances that are easily accessible, whose time and financial investments seem worthwhile, and for determining whether the model under consideration will produce the outputs required to meet the goals of a specific project. The estimated data, resources, time, and cost needed to parameterize and calibrate a model, as well as the expertise and experience needed to run these models, can also be used to describe model complexity (Dwarakish & Ganasri, 2015).

In particular, it’s necessary to identify the simplest model that will yield adequate accuracy, bearing in mind that model complexity is not synonymous with the accuracy of the results, that the model has to be characterized by flexibility, by the possibility of making it applicable under various spatial and temporal conditions and that increased accuracy has to be worth the increased effort (Kassa, 2009). The selection of a model is a key aspect in obtaining satisfactory answers to a given problem. Numerous hydrological models are currently being used to simulate the hydrological process at various geographical and temporal dimensions.

According to Cunderlik, (2009), four fundamental selection criteria must be considered based on the specific purpose of the project. These are (i) required model outputs relevant for the required purpose and thus to be estimated by the model, which questions whether the model forecasts the variables required by the project, such as peak flow, event volume, and hydrograph, long-term flows, (ii) hydrologic processes that needed to accurately predict the intended outputs using the model, raising the question of whether the model can simulate controlled reservoir operation, single event, or continuous processes, (iii) availability of input data, which questions if all of the model's inputs can be available within the project's time and cost limits, (iv) cost of the project, which questions the investment is justifiable in the context of the project's objectives or not.

2.6.3 Comparisons of SWAT model with other hydrological model

For this study the program SWAT was selected due to its continuous time scale, computational efficiency, its ability to simulate long-term impacts, its applicability to large scale catchment, distributed spatial handling of parameters and integration of multiple processes such as climate, hydrology, nutrient and pesticide, erosion, land cover, management practices, channel processes, and processes in water bodies has an important tool for watershed scale studies.

The model was applied for LULC impact assessment in different parts of the world and also in Ethiopia. It is also readily and freely available model. (Borah and Bera, 2003), compared SWAT with several other watershed-scale models. In the study, they reported that the Dynamic Watershed Simulation Model (DWSM) (Borah *et al*., 2004), Hydrologic Simulation Program-Fortran (HSPF) model (Bicknell *et al*., 1997), SWAT and other models have hydrology, sediment and chemical routines applicable to watershed-scale catchments and concluded that SWAT is a promising model for continuous simulations in predominantly agricultural watersheds.

El-Nasr *et al*. (2005) found that both SWAT and the MIKE-SHE model simulated the hydrology of Belgium's Jeker River basin in an acceptable way. However, MIKE-SHE predicted the overall variation of river flows slightly better. Srinivasan *et al*. (2005) found that SWAT estimated flow more accurately than the Soil Moisture Distribution and Routing (SMDR) model. Furthermore, in order to compare and contrast HEC-HMS and HBV with SWAT, the HEC-HMS hydrological model simulates the rainfall-runoff process of a watershed, as does the HBV model. But SWAT semi-distributed hydrological models are better at predicting the impact of land management practices on streamflow, runoff, and sediment load than other semi-distributed hydrological model (Du and Salah, 2004) .

Generally, for this study, SWAT semi-distributed models are selected because their structure is more physically based than the structure of lumped models, and they are less demanding on input data than fully distributed models.

2.7 Soil and Water Assessment Tool (SWAT) Model

The SWAT model, a semi-distributed physical simulation model, is largely used as a strategic planning tool and can forecast the effects of land use change and management actions on hydrological regimes in watersheds with shifting soil, land use, and management conditions over extended periods of time (Neitsch *et al*., 2011). The eight main components that the SWAT model simulates are: hydrology, weather, sedimentation, soil temperature, crop growth, nutrients, pesticides, and agricultural management (Neitsch *et al*., 2011).

Evapotranspiration, surface runoff, infiltration, percolation, shallow and deep aquifer flow, and channel routing are some of the major hydrologic phenomena that this model is able to represent (Arnold *et al.*, 1995). The elements of a stream determine its flow (surface runoff and ground water flow from shallow aquifer). A graphical user interface for the SWAT model is provided by the Arc SWAT extension of Arc GIS (Arnold *et al*., 1998). The interface will require access to Arc GIS compliant raster (GRIDs), vector datasets (shape files or feature classes), and database files that give specific types of information about the watershed in order to generate a SWAT dataset. Before executing the model, the required spatial datasets and database files must be ready.

In SWAT model, the water balance is the backbone of the hydrologic simulation in a watershed; and the hydrology of the watershed can be separated into two major divisions, land phase and routing phase (Arnold *et al*., 2012). Hereafter the discussion is mainly focuses on main component of SWAT model and selected options (if option selection is required) for this study. For more explanation of each component and options see SWAT 2005 model theoretical documentation (Neitsch, 2005).

A program called SWAT-CUP (SWAT Calibration and Uncertainty Tools) was created to unify different SWAT calibration/uncertainty analysis programs using a common user interface. The application can run ParaSol, SUFI2, and GLUE. The input files required to execute a calibration program are guided by the application. One calibration method is included in each SWAT-CUP project, and it is possible to repeat the process numerous times until convergence is attained. It enables the storage of calibration iterations for eventual usage in the iteration history.

2.8 Best Management Practices (BMPs) to Reduce Sediment Yield

The SWAT model is a tool that predicts the impact of BMPs on runoff, sediment and agricultural chemical yields (nutrient loss) in complex watersheds (Arnold *et al*., 1995; Arnold & Fohrer, 2005; Kode *et al*., 2014; Ullrich & Volk, 2009). The SWAT model may incorporate site-specific variables, dimensions of agricultural BMPs, and tillage methods, which is frequently beyond the capacity of most other watershed models. Identification of these crucial locations is essential for the effective and efficient application of watershed management strategies. Watershed prioritizing is the process of ranking various important sub-basins of a watershed in order to determine which of them should receive treatment and soil conservation measures first (Choto & Fetene, 2019).

Implementing a collection of best management practices (BMPs) is required to reduce the major erosion from the upper catchment and decrease the sediment delivered to the reservoir in order to lengthen the reservoir's lifespan. Agricultural and structural-based BMPs are typically favored for reducing soil loss within the sensitive parts of the watershed (Khoshru *et al*., 2020). The techniques that farmers use on the agricultural fields are referred to as agricultural BMPs. One of the many soil treatments that are regarded as BMPs to reduce surface runoff by intercepting and slowing the runoff velocity is contour farming. It entails carrying out field operations along the contour, such as tilling, planting, and harvesting, etc.

With the help of this BMP, sheet erosion and rill formation are effectively prevented or reduced, as well as the erosive force of surface runoff. Another BMP that aids in sediment setting by lowering runoff velocity and preserving soil moisture is conservational tillage. Infrastructures created on the boundaries of the land or field that are either natural or artificial are referred to as structural BMPs. The lifespan of these constructions is typically longer than three years. Several structural BMPs can be employed to prevent soil loss at the contour, depending on the slope of the landscape.

These features contribute to a shorter slope, which in turn contributes to less soil erosion. A balance between desired economic viability and environmental consequences affects how agricultural BMPs are implemented. Studies have been conducted all around the world, including in Ethiopia, to assess the efficiency of different BMPs in hotspot areas of a watershed to reduce sediment output and soil erosion. Many studies have been done to combine multi objective optimization techniques with the SWAT model to better choose and position BMPs from both an economic and environmental perspective (Adi, 2021). In contrast, very few studies were carried out in Ethiopia using hydrologic models to assess the effects of BMPs.

According to Abraham and Nadew (2018), applying filter strips and parallel terrace/stone bunds scenarios reduced the existing sediment yields by 48 and 53%, respectively, from the existing condition scenario at the subbasins and the basin outlet in Guder watershed, Blue Nile Basin in Ethiopia. Terracing, grass waterways, and vegetative filter strips are examples of this. Overall, the three management options significantly reduced the sediment yield, but filter strips saw the greatest drop. Up to 80% less silt was produced after using filter strips to treat high sediment yield sub-basins, showing that these strips had higher sediment trap efficiency than the competition. It is necessary to determine whether such BMPs are applicable to a watershed region even when their individual efficacy has been established.

3. MATERIALS AND METHODS

This chapter describes the study area with regard to location, topography, soil, and climate of the study area and focuses on the methodology, which includes data collection, hydrological model selection, methods of data analysis and model performance evaluation, and developing BMPs. These were described to evaluate the impact of land use and land cover changes on streamflow and sediment yield analysis and BMPs.

3.1 Description of the Study Area

3.1.1 Location

One of the major tributaries to the Awash River is the Borkena River. It drains from the mountainous chains and ridges found in the northern plateau, which is adjacent to the Afar rift, down to the south eastern direction, and after joining the Jara River, it finally drains the Awash River. This watershed is located in the South Wollo Zone and includes the three Woredas of Oromia Liyu Zone of the Amhara National Regional State (ANRS) of Ethiopia.

In terms of the geographic coordinate system, the Borkena watershed is located at 10° 50' 00‘ N and 39° 50' 00‘ E latitude and longitude, respectively. The total area of the watershed is estimated to be 1787 km^2.

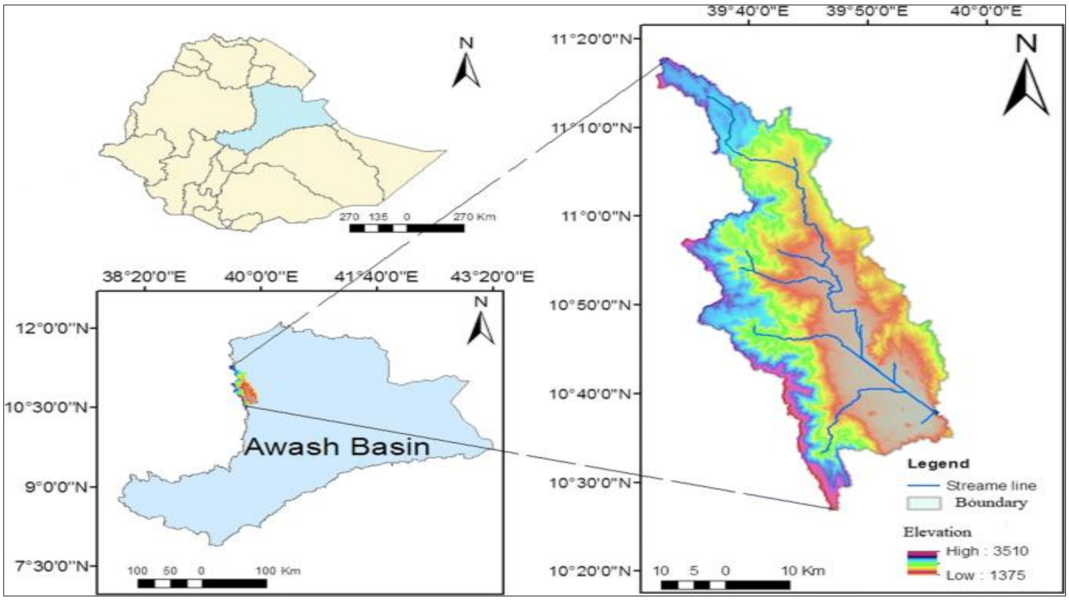

Figure 3.1 Map of the Study Area

3.1.2 Climate characteristics of the study area

The climate of Borkena watershed varies between sub-humid to subtropical and according to the traditional classification of climate which is mainly based on altitude variation, the climate is classified as “Dega and Weyna-dega”. There is a high spatial and temporal variation of rainfall in the study area. The main annual rainfall over the catchment is 1028 mm.

The main rainfall season, which accounts for around 84% of the annual rainfall, occurs from July to September, while small rains also occur from November to February (Hedlund, 2000a). The mean monthly temperature considering the Kombolcha station varies between 16.1 ^{o}C and 22.1 ^{o}C, which correspond to December and June respectively.

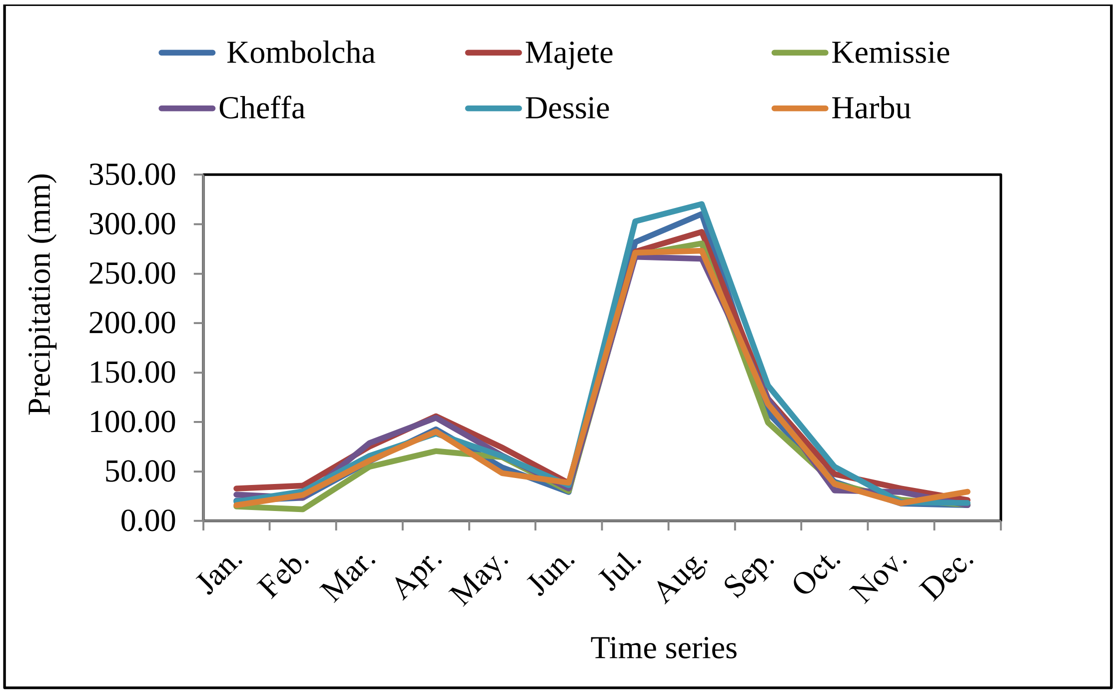

Figure 3.2 Mean monthly precipitation characteristics of the study area

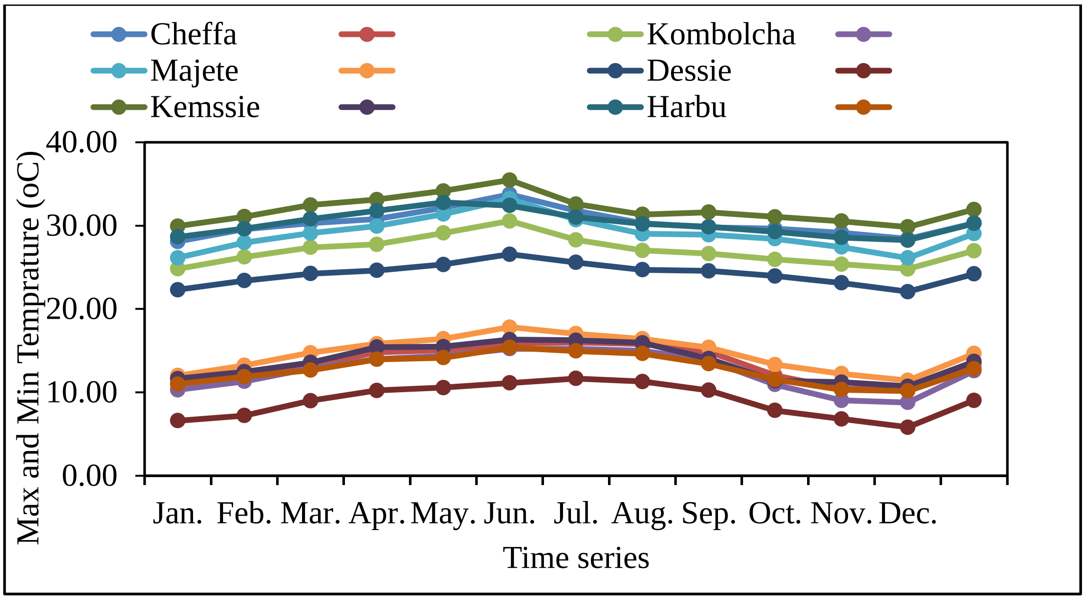

Figure 3.3 Mean monthly maximum and minimum temperature characteristics of the study area

3.1.3 Topography

The topographic variation of the area ranges from about 3510 m above m.s.l on the top of the ridge around the North West of the water divide at Kutaber about 1375 m above m.s.l at the downstream parts around the swamp outlet. Both the towns of Dessie and Kombolcha are located at an elevation of about 2660 m and 1800 m above m.s.l respectively. The fault bounded graben forms large plain areas such as the Boru plain, Alaska plain, Marim Weha plain, and large flat lands in Kombolcha and its surroundings. These plains are seasonally flooded by the Borkena (Metaferia, 2019).

3.2 Materials and Software Programs Used

Different kinds of software were employed to achieve the goals of this study. The Imagine 2014 software package was used, along with the following programs: RAINBOW, Geographical Information System (GIS), Environment for Visualizing Images 5.3 (ENVI 5.3), ArcGIS interfaced Soil and Water Assessment Tool (ArcSWAT-2012), Sequential Uncertainty Fitting version 2 (SUFI-2) algorithm in SWAT calibration and uncertainty program (SWAT-CUP), and Earth Resources Data Analysis System (ERDAS). The homogeneity test of rainfall data was conducted using RAINBOW. GIS was utilized to interface with the SWAT model and process the spatial data. SWAT 2012 and GIS 10.4 were also used for this study.

For the homogeneity test of rainfall data, RAINBOW software package was utilized. The spatial data was processed using GIS, which also served as the SWAT model interface. GIS 10.4 and SWAT 2012 were used for this study. Using the ENVI 5.3 software's radiometric correction and atmospheric correction tools, respectively, images were calibrated for radiometric and atmospheric correction. Additionally, land gaps were filled. The SWAT calibration and uncertainty program (SWAT-CUP) software package's Sequential Uncertainty Fitting version 2 (SUFI-2) algorithms was utilized for model sensitivity, calibration, and validation.

Earth Resources Data Analysis System (ERDAS) Imagine 2014 software was used to classify the images and create maps of the land use and land cover in order to track changes in the various land use and land cover categories. The standardization of the data for further analysis was accomplished through a number of data processing stages. In this study, efforts have been made to investigate the effects of changing land use change on streamflow and sediment yield in Borkena watershed.

3.3 Input Data and Methodology image

3.3.1 Weather data

For this specific study, precipitation, maximum and minimum temperatures, sunshine hours, relative humidity, and wind speed data within and around the Borkena watershed for six weather stations (Cheffa, Kombolcha, Majete Dessie, Kemssie, and Harbu) for the year 1990 to 2020 were collected from the National Meteorological Services Agency (NMSA). The climate of the watershed provides the moisture and energy inputs that control the water balance and determine the relative importance of the different components of the hydrologic components (Neitsch *et al*., 2011). SWAT also needs daily long years of climate data (precipitation, maximum and minimum temperature, solar radiation, wind speed, and relative humidity) to be input for the simulation of hydrological processes. The weather data used were represented from six stations (Cheffa, Kombolcha, Majete Dessie, Kemssie, and Harbu) for the period 1988-2020. Table 3.1 shows weather stations used in this study located in the Borkena watershed.

Table 3.1 below shows weather stations used for this study including their class and location.

No.	Station Name	Latitude (UTM)	Longitude (UTM)	Elev (M)	Elements					
					Pcp	Tmin	Tmax	RH	SR	WS
1	Dessie	1228990	569343.7	2553	Yes	Yes	Yes	No	No	No
2	Kombolcha	1225227	578392.8	1857	Yes	Yes	Yes	Yes	Yes	Yes
3	Harbu	1214960	586703.4	1507	Yes	Yes	Yes	No	No	No
4	Chefa	1197944	587992.3	1450	Yes	Yes	Yes	No	No	No
5	Kemisie	1184693	595013.9	1435	Yes	Yes	Yes	No	No	No
6	Majetie	1160369	596297.8	1573	Yes	Yes	Yes	Yes	Yes	Yes

Note, Pcp is Precipitation, Tmin is Minimum Temperature, Tmax is Maximum Temperature, RH is Relative Humidity, SR is Solar Radiation, and WS is Wind Speed.

3.3.2 Hydrological data (streamflow and sediment yield)

3.3.2.1 Streamflow data

The Borkena watershed has an outlet river discharge gauging station, which is located at 10° 03' 00‘ N and 39° 56' 00‘ E. In this study, daily flow data for the Borkena River for a period of 28-years from 1988–2015) recorded at Borkena swamp gauging station was collected from the Ministry of Water and Energy of Ethiopia (MoWE). It was used for performing sensitivity analysis, calibrating and validating the SWAT model. The missing value of the data was filled using a long year average technique with the given gaging station data.

Figure 3.4 indicates the peak flow occurs in July and August and that the minimum flow also occurs from November to February and June. This is highly related to the temporal pattern of rain fall in the study area.

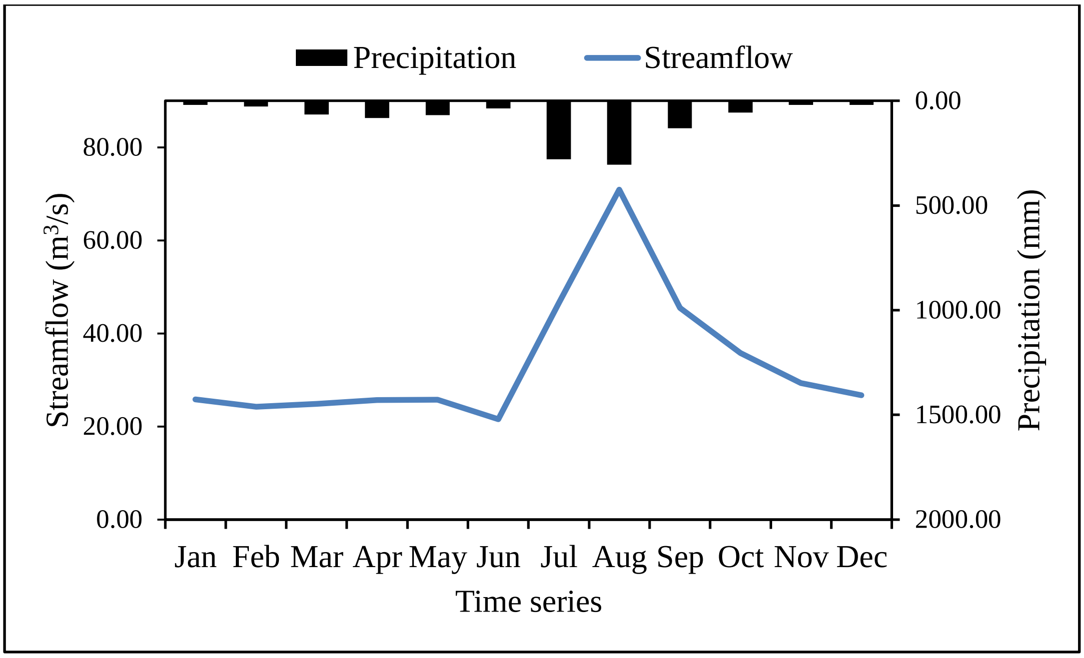

Figure 3.4 Mean monthly flow of Borkena (swamp outlate) stations (1990-2015)

3.3.2.2 Sediment data

The Ministry of Water and Energy (MoWE) collects sediment data, but no sufficient and reliable (continuous-time step) sediment yield data were recorded. In order to create an equation describing the relationship between flow and sediment, it is necessary to construct the sediment rating curve. The average relationship between discharge and suspended sediment concentration for a certain area is described by a sediment rating curve (Asselman, 2000). The linear least squares fit of the Power was used to create the sediment rating curve. The sediment rating curve and the equation created from the sediment rating curve are showed in the figure below. Rating curve Equations 3.2 developed from streamflow and sediment yield relationships are correlated with an R^2 value of 0.87.

$$Sy = 0.086 \times C \times Q \tag{3.1}$$

$$Sy = 50.31 \times Q - 18.31 \tag{3.2}$$

Where, Sy is suspended sediment yield (ton/day), C is sediment concentration in mg/l, Q is streamflow (m^3/s), and 0.086 is a conversion factor.

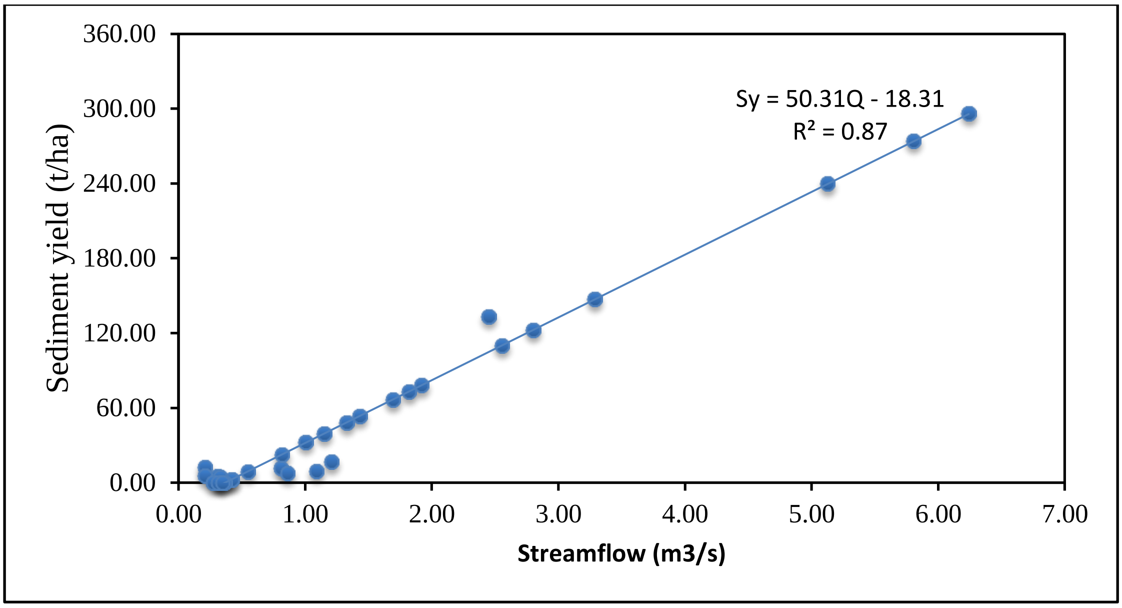

Figure 3.5 Sediment rating curve for Borkena swamp gauging Station

3.3.3 Digital Elevation Model (DEM)

Digital elevation models (DEM), which provide the elevation of each point in a given area at a particular spatial resolution, are used to describe topography. The DEM (Figure 3.1) was utilized to define the watershed and investigate the land surface terrain's drainage patterns. The DEM is used to derive stream network properties like channel slope, length, and width, as well as basin factors like slope gradient and length of the terrain's slope. By masking the shapefile of the Borkena watershed, which was later used to outline the watershed, a 30 m 30 m resolution DEM of the study region received from the Shuttle Radar Topography Mission (SRTM) was recovered using GIS software. Additionally, it is used for the land slope class classification, which was the basic parameter for the Hydrological Response Unit (HRU) definition.

As shown in Figure 3.6, the slope class found between 0-5% and 10-20% accounts for the majority of the watershed's land slope class, accounting for 33.6% and 29.0%, respectively. The remaining land slope classes, 5–10%, 20–40%, and greater than 40%, cover 19.4%, 17.7%, and 0.3% of the watershed, respectively. These different land classes show a variation of topography in the Borkena watershed.

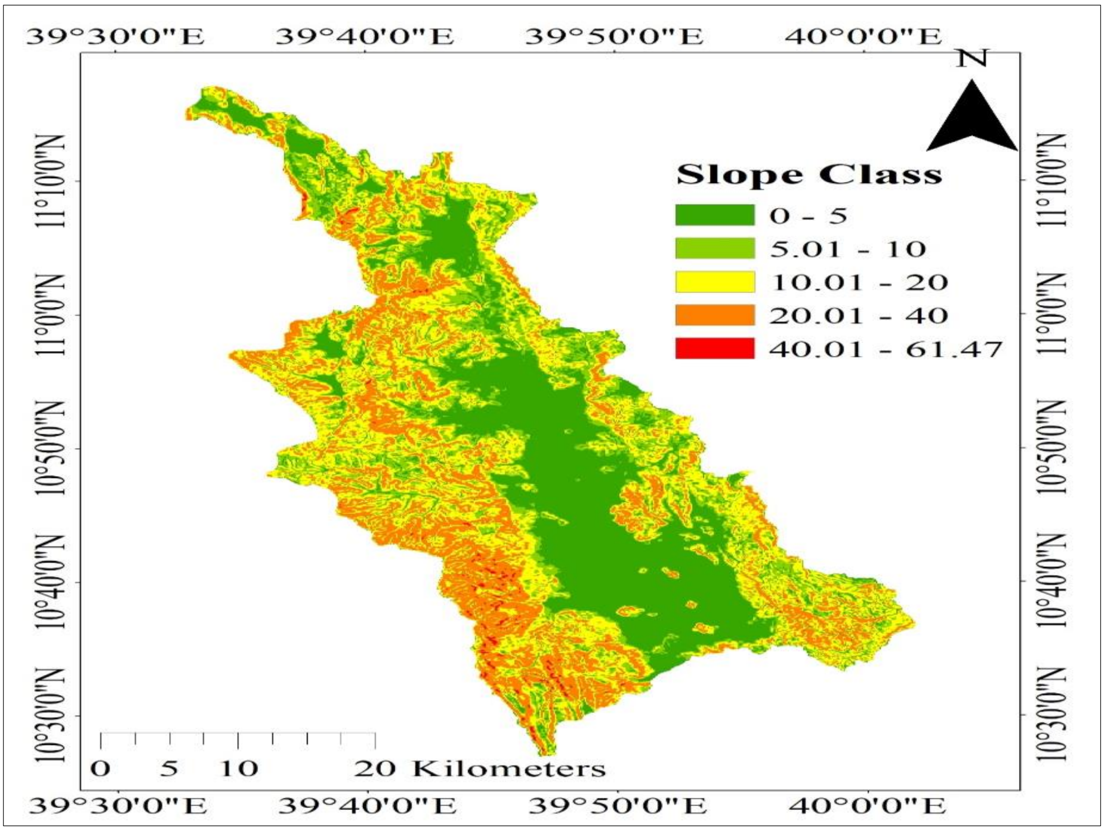

Figure 3.6 Slope map of the study area

3.3.4 Soil Data

Soil properties are one of the major inputs of data required by the SWAT model of the watershed. Eutric Leptosols, Eutric Vertisols, Lithic Leptosols, and Fibric Histosols are the four main soil types present in the basin. The soil type was determined using the FAO soil classification system. Thus, 16.7% of Eutric Vertisols, 54.5% of Lithic Leptosols, 19.8% of Eutric Leptosols, 8.9% of Fibric Histosols, and 0.16% of Eutric cambisols were produced. The major soil types found in the catchment are Eutric Leptosols, Eutric Vertisols, Lithic Leptosols and Fibric Histosols. The physical and chemical characteristics of the soil data play a large role in determining the movement of water and air within the HRU.

The soil properties such as depth of soil layer, soil texture, hydraulic conductivity, bulk density, and organic carbon content are required by SWAT for each layer of each soil type. These soil data were obtained from major world soils of the Food and Agricultural Organization (FAO, 2002). To integrate the soil map with the SWAT model, a user soil database that contains textural and chemical properties of soils was prepared for each soil layer and added to the SWAT user soil databases. The soil map of the study is presented in Figure 3.7.

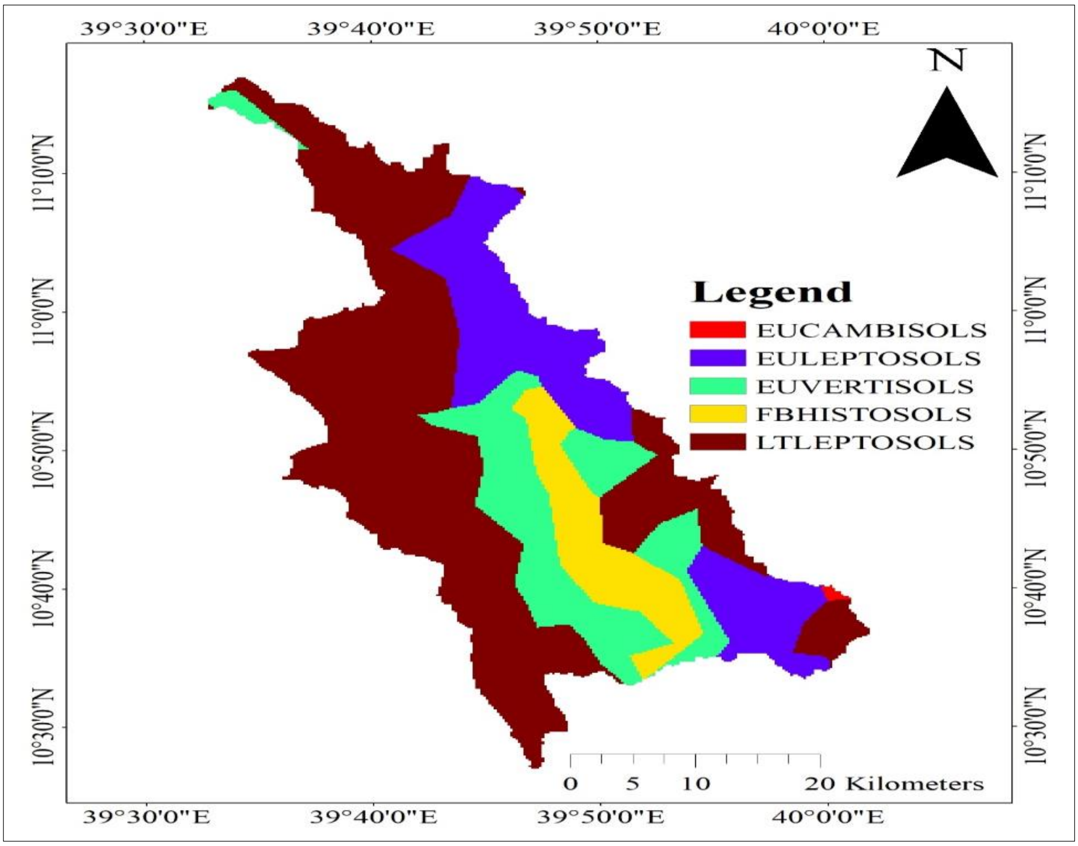

Figure 3.7 Soil map of the study area

Table 3.2 Symbols and areal coverage of the soils in Borkena watershed

Major Soil	Area (km^2)	Area Coverage (%)
Eutric Vertisols	296.6	16.7
Lithic Leptosols	967.3	54.5
Eutric Leptosols	361.7	19.8
Fibric Histosols	158.6	8.9
Eutric cambisols	2.8	0.16

3.3.5 Land use land cover data

The most crucial element affecting runoff, evapotranspiration, and surface erosion in a watershed is land use. This information is necessary for the SWAT model to represent the watershed's Hydrological Response Units (HRUs), together with a slope and soil map.

3.3.5.1 Data acquisition and preprocessing

Two multispectral satellite images of the Borkena watershed were taken for a period of three years in order to evaluate LULC changes. The 1990, 2006, and 2020 images (LANDSAT) were obtained from the United States Geological Survey (USGS) (http://.usgs.gov). In addition to employing high-resolution photography, auxiliary data was gathered, including topographic maps, ground truth information, and aerial images. images from the 1990 Landsat 5 Thematic Mapper (L5-TM), the 2006 Landsat 7 Enhanced Thematic Mapper Plus (L7-ETM+), and the 2020 Landsat 8 Operational Land Imager and Thermal Infrared Sensor (L8-OLI/TRS) all have a resolution of 30 meters.

In order to establish a more direct association between the gathered data and biophysical phenomena, satellite image pre-processing is crucial before the change detecting phenomenon. Remotely sensed data from aircraft or satellites is typically geometrically deformed due to acquisition equipment and platform movements. For geometric rectification, the satellite data were imported as images into the Arc GIS 10.4 program.

ArcGIS 10.4, ERDAS Imagine 2014, and ENVI 5.3 software packages were used in this investigation to carry out successive pre-processing tasks. Along with layer stacking, mosaicking, image gap-filling, and sub-setting, these stages also included radiometric and atmospheric corrections. Appropriate band compositions (layer stacking) were performed in order to enhance the quality and visualization of the Landsat images utilized in this investigation.

3.3.5.2 LULC classification

Classification of the image is a process conducted to catalog all pixels in an image or raw remotely sensed data into a finite number of individual LULC classes to produce beneficial thematic maps and information. After going through step-by-step processing and land cover detection, the map showing seven (croplands, grassland, shrubland, forestland, bareland, water body, and settlement) classes of land use/cover was created as shown in Table 3.3 were chosen for mapping the entire Borkena watershed area.

Table 3.3 Land use and land cover categories identified at the study area

LULC Class	SWAT Code	Description
Bareland	BARR	Land areas with low or no vegetation including rocky areas
Cropland	AGRL	Land areas used for crop cultivation area currently under crop, fallow, and land under preparation and the scattered rural settlement that is closely associated with the cultivated fields.
Forestland	FRSE	Areas covered with natural and plantation trees and sometimes mixed with enrichment plantations, forming nearly closed canopies of 70-100% cover.
Grassland	RNGE	Areas covered with grass used for grazing, as well as barelands that have little grass or no grass cover. It also includes other small sized plant species.
Settlement	URBN	Land areas where most land is covered with structures including urban and rural residential and roads
Shrubland	FRST	Land areas with scattered trees mixed with short bushes, grasses, and areas under agroforestry
Water Body	WATR	Land areas which are waterlogged, swampy throughout the year, reservoir and rivers.

Using supervised classification techniques and digital remote sensing (satellite image) data, land use/land cover classes were mapped. The major goal of categorizing satellite images was to automatically classify pixel values and convert them into the various categories or kinds of land use. The classification of satellite images was done using the ENVI software's supervised classification algorithms. When employing supervised classification, maximum likelihood was used as the parametric rule. Using the settings of the maximum likelihood statistical approach, the optimum grouping of unknown pixels was produced. In this study, supervised classification was applied for LULC classification using ERDAS Imagine 2014 software. The most important step in this procedure was selecting over 500 training samples for each Landsat image by drawing polygons around representative regions of each LULC class. For the classes (crop land,

and forest land), a minimum number of training samples were 100 because these classes have been major LULC classes in the watershed.

After supervised classification, training sites for the predefined LULC classes (Table 3.3) were developed by the visual interpretation of the Landsat images (1990, 2006, 2020) based on prior knowledge of some of the study areas, information from the previous studies, and using Google earth pro 7.3.3 software. Google Earth represents a powerful and attractive source of positional data that can be used for investigation and preliminary studies with suitable accuracy and low cost. Since Google Earth images with the high spatial resolution are free for the public, they are used directly in land use land cover mapping in small geographical extend (Tilahun & Teferie, 2015). Once the training sites were developed, the maximum likelihood classifier was applied to create spectral signatures and then used to classify all pixels in the image.

3.3.5.3 Accuracy assessment

Accuracy assessment is an important step in the image classification process. The objective of this process is to quantitatively determine how effectively pixels were grouped in to the correct features classes in the area under investigation. It is a process used to estimate the accuracy of image classification by comparing the classified map with a reference map (Choubin *et al*., 2019). The most used method is the contingency method to determine the level of accuracy, or also called the contingency matrix (confusion Matrix). The contingency matrix contain some information, there are producer's accuracy, overall accuracy, and kappa accuracy. Producer's accuracy and user's accuracy are estimators of overall accuracy.

The accuracy assessment of the classified map is the comparison of the classified image and the sampling points from the orthoimages, Google Earth Imageries and existing land cover map. Value of Producer accuracy, user accuracy, over all accuracy and kappa statistics were calculated with the Equation 3.3, 3.4, 3.5 and 3.6 respectively.

$$\text{Users accuracy} = \frac{\text{Number of correctly classfid pixels in ach cataeegory}}{\text{Total numbers of reference pixels in that category}} \times 100 \tag{3.3}$$

$$\text{Producer accuracy} = \frac{\text{Number of correctly classfid pixels in ach cataeegory}}{\text{Total numbers of reference pixels (the coloumen total)}} \times 100 \tag{3.4}$$

$$\text{Overall accuracy} = \frac{\text{Total numbers of correctly classfid pixels (Diagonal)}}{\text{Total numbers of reference pixels}} \times 100 \qquad (3.5)$$

$$\text{Kappa Cofficient (KC)} = \frac{(\text{TS}*\text{TCS}) - \Sigma\ (\text{column total}*\text{row total})}{\text{Total sampl}^2 - \Sigma\ (\text{column total} - \text{row total})} \times 100 \qquad (3.6)$$

If KC≤ 0.5 shows rare agreement, 0.5 ≤ KC ≤ 0.75 shows a medium level of agreement, 0.75 ≤ KC≤ 1 shows a high level of agreement, and K = 1 for perfect agreement (Dibaba *et al*., 2020).

3.3.5.4 LULC change detection analysis

LULC detection is the process of identifying differences in geographical surface phenomena over time. LULC change detection involves the ability to quantify spatiotemporal effects using multi-temporal data sets. The Post-classification comparison technique was chosen in this study to be employed for LULC change detection. This classification technique involves the classification of multiple date images separately to generate thematic maps, which are then compared pixel-by-pixel of corresponding classes to produce tables. This approach was selected for its advantage to minimize the possible effects of sensor and atmospheric and environmental differences between images as they are independently classified and provides more detailed information obtained from a complete matrix of LULC change (Adepoju *et al*., 2006). Pairs of the produced classified thematic maps (1990, 2006, and 2020) were compared in ArcGIS 10.4 software. Change detection of LULC was performed to understand the changing status and its magnitude of change rate for the study periods. The magnitude of change (MC) and the percentage of change (PC) for each LULC class during each period was computed based on Equations 3.7and 3.8.

$$\text{MC (ha)} = \text{A}_\text{i} - \text{A}_\text{f} \qquad (3.7)$$

$$\text{PC (\%)} = \frac{\text{A}_\text{i} - \text{A}_\text{f}}{\text{A}_\text{i}} \times 100 \qquad (3.8)$$

Where A_i is the class area at the initial time and A_f is the class area at the final time

3.4 Data Analysis

3.4.1 Filling missing data

Missing data on the hydrology and climate is frequent and causes major issues because it biases the results. The choice of the best missing data management techniques is typically a challenge for researchers. The validity and reliability of the research findings are impacted by the missing data (McKnight *et al.*, 2011). The accuracy of the results is also negatively impacted by the use of faulty missing data filling techniques. To perform a good analysis and simulation through using long time series data, handling this problem by using a highly demanded missing data filling method is a pre-request. There are a number of methods for estimating missing data, such as the arithmetic average method, normal ratio method, inverse distance method, weighting method, and regression methods.

Among those, the Inverse Distance Weighted technique was employed to estimate missing data for this study. This method's weights for each sample are inversely proportionate to its distance from the point being estimated, and it is reliable if the weather stations are situated within a 100 km radius (Lam, 1983). This method uses the observed values at other stations to estimate the missing value of an observation, which is determined by Equation 3.9. The method is fast, easy to implement, and easily tailored for specific needs.

$$P_x = \frac{\sum_i^N = 1(\frac{1}{d_i^2} p_i)}{\sum_i^N = 1(\frac{1}{d_i^2})} \tag{3.9}$$

Where Px is the estimated value, Pi is the observed value of the i^{th} neighbouring station, di is the distance from each location the point being estimated and N is the number of neighbouring stations.

3.4.2 Consistency test

The quality of the input data used for data analysis determines the quality of the outcomes for any given study. It is vital to first verify the consistency of the station's recorded data before using it. Inconsistencies would appear in the rainfall data of that station if the circumstances pertinent to its recording have changed significantly over the course of the record. From the moment the big shift occurred, this discrepancy would be apparent. The double mass curve technique was used to check a record for consistency. A common data analysis method for examining the behaviour of records produced of hydrological or meteorological data at several places is the double mass curve.

A DMC is a plot of one variable's arithmetic cumulative numbers against another variable's cumulative figures or the same variable's computed cumulative values for the same period. The DMC theory is based on the concept that a graph of one quantity's accumulation against the accumulation of the others over the same period plots a straight line since the data are proportional and the slope of the line shows the constant of proportionality between the quantities (Use *et al.*, 2021). In other words, the proportionality is not constant at all rates of accumulation if there is a large break in the slope of the double-mass curve. The graphs below show all of the points that were put on or near straight lines and were used to check the consistency of rainfall across all stations. The stations did not require any additional adjusting as a result.

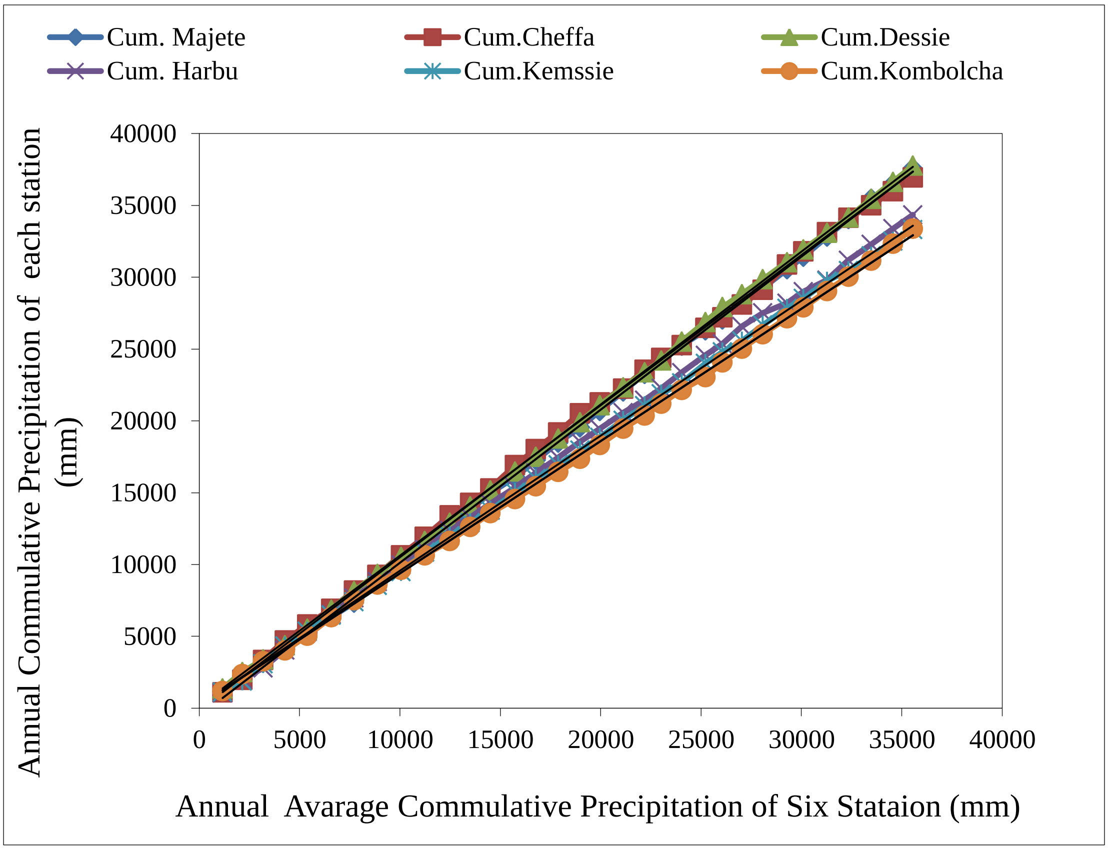

Figure 3.8 Consistency checking for the six Rainfall stations within and around the catchment.

3.4.3 Homogeneity test

Using non-homogeneous data may be increased or decreased the real representation. To know the collected data either it is homogenous or non-homogenous the data should be checked. For this study, the homogeneity test will be evaluated using software by means of frequency analysis RAINBOW (Raes *et al*., 2006). As one of the techniques for examining the homogeneity of hydro-meteorological datasets, the homogeneity restriction guarantees that the observations come from the same population. The homogeneity test provided by RAINBOW is based on the total number of departures from the mean.

The homogeneity of the data in a time series was examined by determining the maximum and range of the cumulative deviations from the mean. Equation 3.10 is used to calculate the cumulative deviations from the mean, which is one of the tests for homogeneity.

$$S_k = \sum_{i=1}^{k}(X_i - \bar{X}) \tag{3.10}$$

K= 1, 2,…,n

Where, X_i are the records from the series X_1, X_2, …, X_n and $\bar{X}$ is the mean. The initial value of S_k = 0 and last value S_k = n is equal to zero. When plotting the S_k's (also called a residual mass curve) changes in the mean are easily detected. For a record X_i above normal the S_k = i increases, while for a record below normal S_k = i decreases. For a homogenous record one may expect that the S_k fluctuate around zero since there is no systematic pattern in the deviations of the X_i from their average value X.

If the cumulative deviation crosses one of the horizontal lines, the homogeneity of the data set is rejected with 90, 95, and 99% probability. For this study, the probabilities of rejecting the homogeneity of the datasets were evaluated in the homogeneity statistics menu. Appendix B includes illustrations of the homogeneity of rainfall for each station.

3.5 Hydrologic Model Setup and Simulation

3.5.1 SWAT model setup

The SWAT model is physically based, computationally effective, semi-distributed, and capable of long-term, continuous simulation. To simulate hydrological processes, the SWAT model needs inputs for topography, soil, and land use in addition to hydro-meteorological data (Arnold *et al*., 2012). To forecast water, sediment, nutrients, and pesticides, SWAT uses geographically dispersed data on topography, soils, land cover, land management, and weather. The ArcGIS interface known as ArcSWAT now contains a GIS interface for the SWAT model that integrates several spatial data (DEM, LULC, and soil) and climate data. In this study, the GIS interfaced ArcSWAT-2012 was used to set up a SWAT model for the Borkena watershed.

3.5.1.1 Watershed delineation

The delineation of the watershed from a DEM is the initial stage in producing the SWAT model input. Using 30 m by 30 m resolution DEM data and Arc SWAT for project setup, watershed and subwatershed delineation were completed. The watershed delineation procedure involves five critical steps: DEM setup, stream delineation, outlet and inlet definition, watershed outlet selection and definition, and calculation of sub basin parameters. This is done in order to generate the necessary folders to hold all the data. Following the completion of the DEM setup and the specification of the outlet point on the DEM, the model automatically determines the flow direction and flow accumulation, leading to the calculation of stream networks, subbasin watersheds, and topographic features using the appropriate tool. For the stream definition, the threshold-based stream definition option was used to define the minimum size of the sub-basins. The watershed was sub-divided into 29 sub-watersheds using the default threshold area, which was 3100 ha.

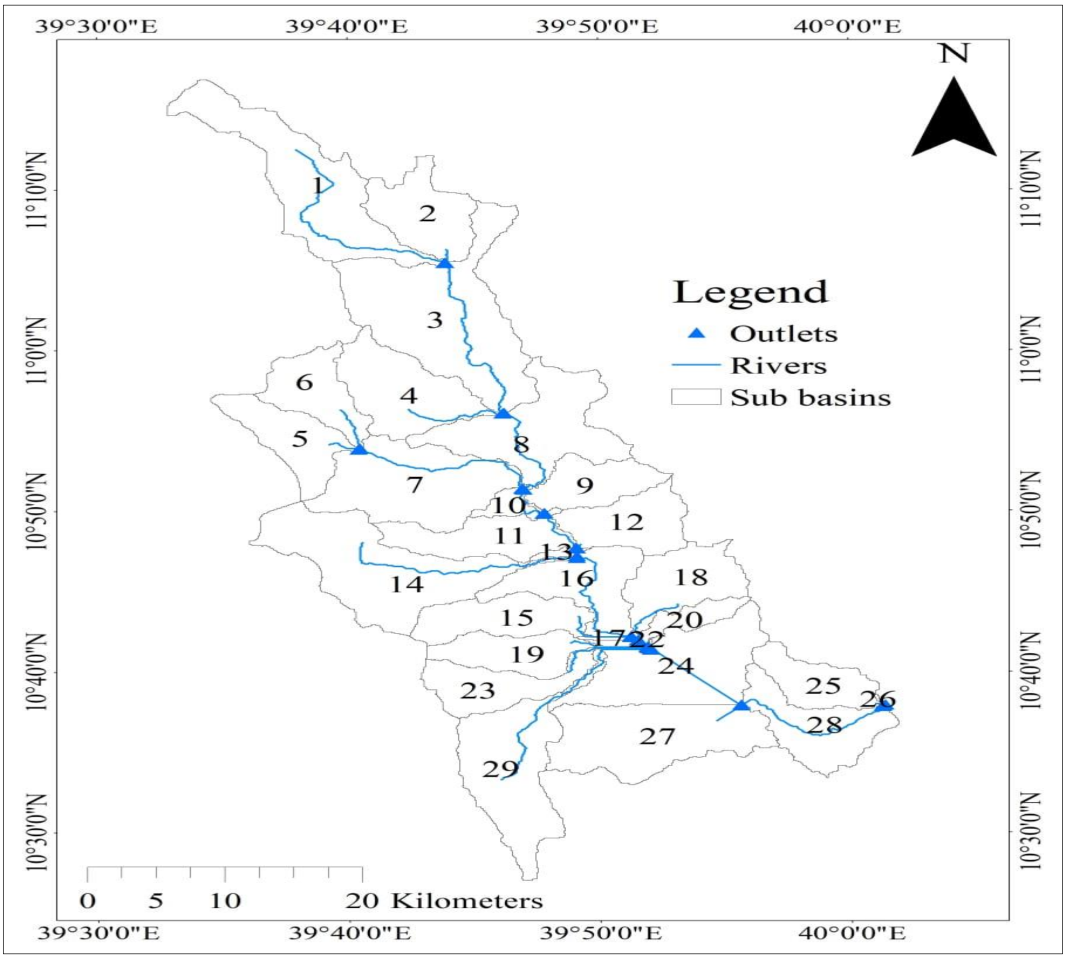

Figure 3.9 Sub-basins of the study area

3.5.1.2 Hydrological response units (HRUs) determination

To apply the Arc AWAT model, hydrologic response units (HRUs) have to be developed. An HRU is a specific mix of land use, soil, and slope classes within a sub basin. In this study, the HRU analysis option on the Arc SWAT tool bar was used to analyse slope characteristics, load maps of land use and soil, and determine the land use/soil/slope class combination in the defined sub watershed. When defining HRU distribution in the model, there are two possibilities. It relies on a particular threshold value to determine whether to allocate a single HRU or several HRUs to each sub watershed.

The Arc SWAT 2012 user manual suggests that a 5% land use threshold, 10% soil threshold, and 20% slope threshold are adequate for most modelling applications. For the HRU definition, the reclassified LULC, soil, and slope in the SWAT database were covered. To define the distribution of HRUs, multiple HRU definition options of 5% LULC, 10% soil, and 10% slope threshold were used. This means the minor LULC, soil, and slope are less than the percentage removed. As a result, the Borkena watershed was divided into 455, 473, and 536 sub-watersheds for LULC of 1990, 2006, and 2020, respectively.

3.5.1.3 Weather data

SWAT needs the daily maximum and minimum temperatures, solar radiation, relative humidity, wind speed, and precipitation values. The user has the option of reading these inputs from a file or creating the numbers using monthly average data that has been condensed over several years. With the exception of Kombolcha and Majete stations, all the stations had sparse data records for relative humidity, wind speed, and solar radiation. SWAT incorporates the weather generator (WGN) model to produce or complete gaps in measured records in response to such difficulties.

This weather generator model needs different weather parameters. The minimal data records for the other stations were produced utilizing SWAT models' weather generating capabilities at the Kombolcha and Majete stations. The missing data were filled in by assigning a missing data identifier of -99, allowing the SWAT model to generate weather data for that day based on average monthly values. After the weather parameters were prepared by using WGN, they were imported into the SWAT database to automatically generate the weather records for the rest stations.

3.5.2 Hydrological component of SWAT

Two different divisions were used to simulate the watershed's hydrology. The hydrological cycle's initial stage, the land phase, regulates how much water and sediment are loaded into each subbasins main channel. The passage of water and sediments through the watershed's network of channels to reach the outlet is the second division of the hydrologic cycle, which is known as the routing phase.

3.5.2.1 Land phase

In the land phase of hydrological cycle, SWAT simulates the hydrological cycle based on the water balance equation 3.11.

$$\mathrm{SW_t = SW_0 + \sum_{i=0}^{t}\left(R_{day} - Q_{surf} - E_a - W_{sweep} - Q_{gw}\right)} \tag{3.11}$$

Where, SW_t is the final soil water content (mm), SWo is the initial soil water content on day i (mm), t is the time (days), R_{day} is the amount of precipitation on day i (mm), Q_{surf} is the amount of surface runoff on day i (mm), E_a is the amount of evapotranspiration on day i (mm), W_{sweep} is the amount of water entering the vadose zone from the soil profile on day i (mm), and Q_{gw} is the amount of return flow on day i (mm) (Neitsch *et al*., 2011).

I. **Surface runoff**

Surface runoff, or overland flow, is a flow that occurs along a sloping surface. Using daily or sub-daily rainfall amounts, SWAT simulates surface runoff volumes for each HRU. SWAT provides two methods for estimating surface runoff: the SCS curve number method (SCS, 1972) and the Green and Ampt infiltration method (Heber Green and Ampt, 1911), even though the latter method is better at estimating runoff volume accurately for this study. Hence, the SCS curve number method has been adopted. The method is an empirical model, which is based on the following Equation 3.12.

$$\mathrm{Q_{surf} = \frac{[(R_{day} - 0.2S)]^2}{(R_{day} + 0.8S)}} \tag{3.12}$$

Where, Q_{surf} is the accumulated runoff or rainfall excess (mm), R_{day} is the rainfall depth for the day (mm), S is the retention parameter (mm). The retention parameter is defined by the Equation 3.13.

$$\mathrm{S = 25.4\left[\left(100\,\frac{1000}{CN}\right) - 10\right]} \tag{3.13}$$

Where, CN is the curve number for the day

SCS defines three antecedent moisture conditions: I-dry (wilting point), II-average moisture and III-wet (field capacity). The moisture condition I curve number is the lowest value the daily curve number can assume in dry conditions. The curve numbers for moisture conditions I and III are calculated with the Equation 3.14 and 3.15.

$$\mathrm{CN_1 = CN_2 - \frac{CN_2 - 20(100 - CN_2)CN_1}{[100 - CN_2 + \exp(2.533 - 0.0636(100 - CN_1))]}} \tag{3.14}$$

$$CN_3 = CN_2\left[\exp\left(0.00673(100 - CN_2)\right)\right] \tag{3.15}$$

Where, CN_1 is the moisture condition-I curve number, CN_2 is the moisture condition-II curve number, and CN_3 is the moisture condition-III curve number.

II. Peak runoff rate

The highest runoff flow rate that may be observed during a certain rainfall event is known as the peak runoff rate. The peak runoff rate is the maximum runoff flow rate that occurs with a given rainfall event. The peak runoff rate is an indicator of the erosive power of a storm and is used to predict sediment loss. SWAT estimates the peak runoff rate with a modified rational method Choto *et al.* (2019), as expressed in Equation 3.16. The rational method mainly assumes that if rainfall of intensity begins at time t = 0 and continues indefinitely, the rate of runoff will increase until the time of concentration. The time of concentration is the time for a drop of water to flow from the remotest point in the sub-basin to the sub-basin outlet. It is calculated as the sum of the time it takes for flow from the remotest point in the sub-basin to reach the channel and the time it takes for flow in the upstream channels to reach the outlet.

$$Q_{peak} = \frac{\alpha_{tc} * Q_{surf} * A}{3.6 * t_{conc}} \tag{3.16}$$

Where, Q_{peak} is peak runoff rate (m^3/s), α_{tc} is the fraction of daily rainfall that occurs during the time of concentration, Q_{surf} is the surface runoff (mm), A is the sub-basin area (km^2), t_{conc} is the time of concentration (hr), and 3.6 is a unit conversion factor.

III. Potential evapotranspiration

Potential Evapotranspiration is a collective term that includes evaporation from the plant (transpiration) and evaporation from the water bodies and soil. Evaporation is the primary mechanism by which water is removed from a watershed. An accurate estimation of evapotranspiration is critical in the assessment of water resources and the impact of land use change on these resources.

There are many methods that are developed to estimate potential evapotranspiration (PET). SWAT provides three options for PET calculation: Penman-Monteith (Monteith, 1965), Priestley-Taylor and Hargreaves methods. The methods have various data needs of climate variables. Penman- Monteith method requires solar radiation, air temperature, relative humidity and wind sped; Priestley-Taylor method requires solar radiation, air temperature and relative humidity; whereas Hargreaves method requires air temperature only.

For this study, the Penman-Monteith method was selected and it requires air temperature, relative humidity, solar radiation, and wind speed. The Penman-Monteith Equation (Monteith, 1965) combines components that account for energy needed to sustain evaporation, the strength of the mechanism required to remove the water vapour, and aero change and surface resistance terms and expressed by Equation 3.17.

$$\lambda \mathrm{ET} = \frac{\Delta(\mathrm{R_n} - \mathrm{G}) + \mathrm{p_a c_p} \frac{(\mathrm{e_s} - \mathrm{e_a})}{\mathrm{r_a}}}{\Delta + \gamma(1 + \frac{\mathrm{r_s}}{\mathrm{r_a}})} \tag{3.17}$$

where, R_n is the net radiation, G is the soil heat flux, (e_s - e_a) represents the vapour pressure deficit of the air, r_a is the mean air density at constant pressure, c_p is the specific heat of the air, D represents the slope of the saturation vapour pressure temperature relationship, g is the psychometric constant, and r_s and r_a are the (bulk) surface and aero change resistances.

3.5.2.2 Routing phase

The second component of the simulation of the hydrology of a watershed is the routing phase of the hydrologic cycle. It consists of the movement of water, sediment and other constituents (e.g. nutrients, pesticides) in the stream network. To route the flow in the channel network, two methods are available: variable storage and Muskingum.The variable storage method uses a simple continuity equation in routing the storage volume, whereas the Muskingum routing method models the storage volume in a channel length as a combination of wedge and prism storage. In the latter method, when a flood wave advances into a reach segment, inflow exceeds outflow and a wedge of storage is produced. The variable storage method was used for this study. The method was developed by (Neitsch *et al.*, 2011). The equation of the variable storage routing is given by:

$$\Delta V_{stored} = V_{in} - V_{out} \tag{3.18}$$

Where, ΔVstored is the change in volume of storage during the time step (m^3 water)

Vin is the volume of inflow during the time step (m^3 water), and

V*out* is the volume of outflow during the time step (m^3 water).

3.5.2.3 Soil erosion and sediment simulation

Erosion caused by rainfall and runoff is computed with the Modified Universal Soil Loss Equation (MUSLE) (Neitsch *et al*., 2011) in the SWAT model. The runoff factor in MUSLE takes the place of the rainfall energy factor. This enhances the ability to anticipate sediment yield, does away with the requirement for delivery ratios, and makes it possible to use the equation for specific storm events. Runoff is a function of antecedent moisture condition as well as rainfall energy, which improves the forecast of sediment output. With MUSLE, delivery ratios are unnecessary because the runoff factor accounts for the energy required separating and conveying sediment. To estimate sediment yield, the Modified Universal Soil Loss Equation (MUSLE) was used in the SWAT model as shown in Equation 3.19.

$$\mathrm{Sed} = 11.8\left(\mathrm{Q_{surf}} \times \mathrm{Q_{peak}} \times \mathrm{A_{hru}}\right)^{0.56} \times \mathrm{K_{USLE}} \times \mathrm{C_{USLE}} \times \mathrm{P_{USLE}} \times \mathrm{LS_{USLE}} \times \mathrm{CFRG} \tag{3.19}$$

where Sed is the sediment yield on a given day (metric tons), Q_{surf} is the surface runoff volume (mm), Q_{peak} is the peak runoff rate (m^3/s), A_{hru} is the area of the HRU (ha), K_{USLE} is the USLE soil erodibility factor (0.013 metric ton m^2 hr/ (m^3-metric ton cm)), C_{USLE} is the USLE cover and management factor, P_{USLE} is the USLE support practice factor, LS_{USLE} is the USLE topographic factor and *CFRG* is the coarse fragment factor.

3.6 Sensitivity Analysis, Calibration, and Validation

The model had to be performed after it had been set up, and the outcome of the simulation couldn't be used directly in further analyses. Instead, sensitivity analysis, model calibration, and model validation should be used to assess the model's capacity to accurately estimate the constituent streamflow and sediment production (White and Chaubey, 2011).

3.6.1 Sensitivity Analysis

Sensitivity analysis helps to improve understanding of the system being modeled, including model parameters and applicability, which raises the level of confidence in the model and its predictions. A preliminary parameter selection simplifies the calibration procedure and lowers the uncertainties associated with various parameters because the SWAT model has a large number of parameters and a number of outputs. This study used a SWAT-CUP during the sensitivity process (Abbaspour *et al*., 2007). A general interface called SWAT-CUP was created for SWAT; by using it, any calibration, level of uncertainty, or sensitivity may be operated, and programs can be quickly connected to SWAT interface.

This is demonstrated by the program links that swat cup has different algorisms of glue, parasol, and SUFI2 procedures to swat. Sequential uncertainty fits were preferred in this particular study (SUFI2). Prior to doing the sediment yield study, the streamflow sensitivity analysis was completed. The inputs consist of observed data, simulated data, and the most sensitive streamflow and sediment parameters along with their absolute lower and upper bound values. A swat-cup built-in tool that employs the global sensitivity design method was used to conduct the sensitivity analysis. Swat-cup uses t-test and p-test to rank the most sensitive parameters that correspond to the greatest change in output response. The output of a t and p test is a table with columns of t-stat and p-values.

3.6.2 Model calibration and validation

Model calibration is the process of fine-tuning or altering model parameters to match observable data as closely as possible, while accepting a certain amount of variation. In order to reach a specified objective function, it also involves changing parameter values and comparing expected outputs of interest to measured data. Specifically, SWAT-CUP, which offers a framework for making decisions and features a semi-automated Sequential Uncertainty Fitting version 2 algorithm, was used to calibrate and validate the SWAT model for streamflow and sediment yield of the watershed for the swamp station in this study (SUFI-2). The most sensitive parameters were selected for calibration, and until an acceptable level of agreement between the measured and simulated streamflows was reached, their values were iteratively modified within the permitted upper and lower limits.

After successful calibration, model validation was involved by running a model using input parameters determined during the calibration process for the component of interest (streamflow and sediment yield). Validation involves running a model using parameters that were identified during the calibration process and comparing the predictions to observed data, which were not used in the calibration. Calibration and validation were carried out by splitting the available observed data into a range of datasets. The selection of observed data periods for calibration and validation was based on the availability of relatively consistent observed data. First, the model was set to run from 1988–2015 with the initial 2 years (1988–89) as a model warm-up period that allowed the model to stabilize for further simulations. Then, the consequent phases were established as the calibration (1990–2007) and validation (2008–2015) periods.

3.6.3 Model performance evaluation

The degree of the model's goodness of fit is determined by an objective function that gauges the degree of congruence between the model's output and what is seen. The overall fit between the observed and anticipated streamflow using the SWAT model was measured for this investigation using three objective functions.

3.6.3.1 Coefficient of determination (R^2)

The coefficient of determination (R^2) expressed as the squared ratio between the covariance and the multiplied standard deviations of the observed and simulated or predicted values. Therefore, it estimates the combined dispersion against the single dispersion of the observed and predicted series. The range of R^2 lies between zero and one, which describes how much of the observed distribution is explained by the prediction. A value of zero means no correlation at all, whereas a value closer to 1 means there is a higher agreement between the simulated and the measured values. It is estimated based on Equation 3.20.

$$R^2 = \frac{\left(\sum_{i=1}^{n}[X_i - X_{av}][Y_i - Y_{av}]\right)^2}{\sum_{i=1}^{n}[X_i - X_{av}]^2[Y_i - Y_{av}]^2} \tag{3.20}$$

Where, X_i is the measured value, X_{av} is the average measured value, Y_i is the simulated value, and Y_{av} is the average simulated value.

3.6.3.2 Nash-Sutcliffe (NS) efficiency criterion

The NSE determines the relative magnitude of the residual variance compared to the measured data variance that is calculated by Equation 3.21 (Nash and Sutcliffe, 1970). The value of NSE ranges from 1 to −∞ (negative infinity) with values less than or very close to zero indicating poor model performance and values equal to one indicating perfect performance. It is defined as one minus the sum of the absolute squared differences between the predicted and observed values normalized by the variance of the observed values during the period under investigation.

$$\mathrm{NS} = 1 - \frac{\sum_{i=1}^{n}(X_i - Y_i)^2}{\sum_{i=1}^{n}(X_i - X_{av})^2} \tag{3.21}$$

Where, X_i is the measured value, X_{av} is the average measured value, Y_i is the simulated value, and Y_{av} is the average simulated value.

3.6.3.3 Percentage of Bias (PBIAS)

The average tendency of the simulated values to be more or lower than their observed counterparts is measured by the PBIAS. PBIAS should have a value of zero. PBIAS is the percentage deviation of the data under evaluation. A positive PBIAS number means the model is underestimating measured values, whereas a negative value means the model is overestimating (Gupta *et al*., 1999). The BIAS 25 is acceptable (Liew *et al*., 2007). Discharge PBIAS values less than 25 suggest an inadequate model simulation, whereas values between 10 and 15 indicate a good model simulation (Linard *et al*., 2009).

$$\mathrm{PBIAS} = 100\left(\frac{\sum_{i=1}^{n} X_i - \sum_{i=1}^{n} Y_i}{\sum_{i=1}^{n} X_i}\right) \tag{3.22}$$

Where, X_i is measured value, X_{av} is average measured value, Y_i is simulated value and Y_{av} is average simulated value.

Table 3.4 Overall recommended performance ratings (Moriasi *et al*., 2007)

Performances	R^2	NS	PBIAS
Very good	$0.70 < R^2 \le 1.\ \ 0$	$0.75 < NS \le 1.00$	PBIAS < ±10
Good	$0.60 < R^2 \le 0.70$	$0.65 < NS \le 0.75$	$\pm 10 \le$ PBIAS $< \pm 15$
Satisfactory	$0.50 < R^2 \le 0.60$	$0.50 < NS \le 0.65$	$\pm 15 \le$ PBAS $< \pm 25$
Unsatisfactory	$R^2 < 0.50$	$NS < 0.50$	PBIAS ≥ ±25

3.7 Analysis of Streamflow and Sediment Yield Responses under Changing LULC

One of the most significant aspects of this study involves simulating how LULC change may affect streamflow and sediment output in the Borkena watershed. The effects of LULC change on the hydrological responses based on 1990, 2006, and 2020 LULC inputs were assessed using the calibrated and validated SWAT model. For the years 1988 to 2015, simulation runs were carried out every month. Different spatiotemporal scales were used to assess seasonal streamflow variability and water balance component responses to LULC change. Additionally, studies on the effects of LULC modification on the variability of sediment output were conducted at various spatiotemporal scales. The relative difference between two successive periods of LULC and the related simulated hydrological responses were taken into consideration in order to analyse the transition between various historical LULC categories.

3.8 Developing Best Management Practices

Best management practices (BMPs) have been identified as an efficient way to prevent soil erosion and sediment transport in watersheds (Betrie *et al*., 1970). In order to simulate the efficiency of BMPs to minimize sediment yield, the source-level determined by the SWAT model was applied in accordance with the spatial variability of sediment yield. By altering SWAT parameters to reflect how practices affect the process that the SWAT model simulates, the best management practices were represented in the model (Waidler *et al*., 2011). However, the choice of these best management practices and the values of their parameters are site-specific and should take the realities of the research region into account (Adi, 2021; Berihun *et al*., 2020).

In this specific study, four different management scenarios (filter strips, terracing, contour farming, and reforestation) were selected and implemented in the SWAT model. The effectiveness of various BMPs scenarios was evaluated by comparing each scenario with the baseline scenario and calculating apercentageof the reduction. Equation 3.23 was used to calculate this effectiveness.

$$\text{Effectiveness}\ (\%) = \frac{(\mathrm{Y_{baseline}} - Y_{\mathrm{BMP}})}{\mathrm{Y_{baseline}}} \times 100\% \tag{3.23}$$

Where $Y_{baseline}$ and Y_{BMP} are the average annual sediment yields in the baseline scenario and the BMP scenario, respectively,

3.8.1 Baseline scenario

The baseline scenario relates to the way that land is now managed without any conservation measures. The scenario is a simulation without BMPs, and the state of the watershed as it stands was taken into account. Comparisons between the efficiency of the selected management methods and their capacity for reduction are made using the baseline scenario as a reference.

3.8.2 Filter strip

In between agriculture, grazing land, forestland, or other disturbed land, there are vegetated areas called "filter strips" that are used as a buffer. Vegetative filters or buffer filters are other names for filter strips. Filter strips can be positioned along the channel's side to help reduce the amount of silt, fertilizer, pesticides, and bacteria that enter surface runoff (Adi, 2021). For the purpose of filtering and capturing runoff, it is a strip of dense vegetation. A function of the strip's width, SWAT gives a trapping efficiency. Based on local research findings in Ethiopian watersheds, the model is able to replicate filter strip widths ranging from 1 m to 30 m. (Berihun *et al*., 2020; Bewket & Sterk, 2005; Gashaw *et al*., 2018; Lemma *et al*., 2019). The SWAT model calculates sediment trapping efficiency using Equation 3.24 (Neitsch *et al*., 2012).

$$\mathrm{trape_{effe}} = 0.367 \times \ \mathrm{FILTREW}^{0.297} \tag{3.24}$$

Where; $trap_{eff}$ is trapping efficiency and FILTERW is the width of the vegetation strips.

3.8.3 Terracing

Terracing is one of the best management techniques for reducing the sediment yields from subbasins with high sediment yields. By modifying the erosion and runoff parameters, terracing is simulated in SWAT. (For the modelling of the impact of terracing on sediment reduction, the parameters that need to be changed according on the land slope are the USLE support practise factor (USLE-P), SCS curve number (CN2), and slope length of the hillside (SLSUBBSN). The curve number (TERR CN) was altered by lowering the value by 10%, or at least six units, according to various earlier investigations (Berihun *et al*., 2022). The model determines average slope length of the sub-basin using equation 3.25.

$$\mathrm{SLSUBBSN} = (0.21 \times S + 0.9)\frac{100}{S} \tag{3.25}$$

Where SLSUBBSN is the average slope length of the sub-basin and S is the average slope of the HRU.

3.8.4 Contour farming

In order to mitigate erosion, contouring involves structure minor barriers that delay water flow and improve infiltration. By changing the curve number (CONT CN) to account for enhanced surface storage and infiltration and the USLE practice factor (CONT P) to account for decreased erosion, this scenario was simulated in SWAT. For this specific study, CN_II was adjusted by recommendations from the US, SCS (Division, 1986), and CONT_P was adjusted based on different literature reports (Dibaba *et al*., 2021).

3.8.5 Reforestation

Reforestation refers to the planting of new trees in a forest where the number of existing trees has been declining. In this study, shrubland, bare land, and reforestation of agricultural land with high sediment yield potential were all taken into account and compared to the aforementioned two possibilities. The SWAT model's Land Use Update (LUP) tool, which enables the addition of new land use updates while simultaneously deleting existing ones, was activated to carry out these operations.

3.9 Flow Chart of the Methodology

Figure 3.10 describes sequential steps of the methodologies with the data required by the SWAT model to achieve the objectives this study. The following framework illustrates the general workflow of the study.

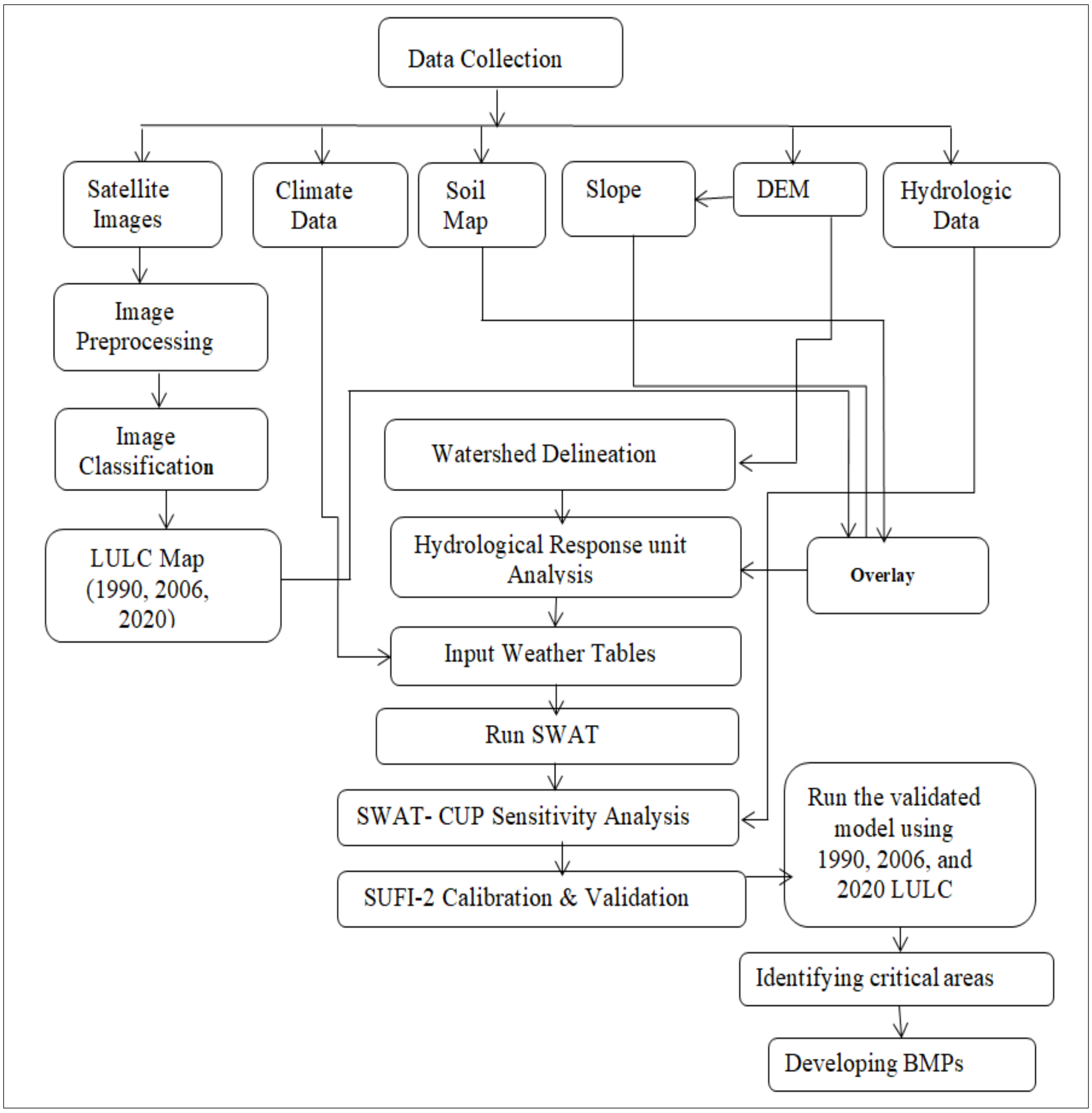

Figure 3.10- Flow chart of the overall methodology

4. RESULTS AND DISCUSSIONS

In this section, the results of the study were presented and discussed. In the first section, the results of the LULC classification accuracy and change detection analysis in the Borkena watershed were presented. In the second section, the results of the parameter sensitivity analysis, calibration and validation of the SWAT of the streamflow and sediment yield in the Borkena watershed are presented. Furthermore, streamflow and sediment yield responses to LULC change were analyzed and discussed in detail. Finally, the spatial distribution of sediment yield, the identification of critical sediment sources, and the effectiveness of different BMPs were analyzed and discussed.

4.1 Land Use Land Cover Change

4.1.1 Land use land cover classification accuracy assessment

Three cloud-free satellite images were acquired from the United States Geological Survey (USGS) website at http://glovis.usgs.gov in order to examine the land cover changes in the study watershed. The three images were taken by the Landsat TM (Thematic Mapper) in 1990, the Landsat ETM+ (Enhanced Thematic Mapper Plus) in 2006, and the Landsat-8 Operational Land Imager (OLI-8) in 2020, all at a resolution of 30 meters. Accuracy evaluations were performed on these LULC images to see whether the resulting map and the real ground conditions matched.

The user, producer, overall, and kappa coefficient accuracy of the classification as well as its accuracy were evaluated using metrics obtained from the error matrices. The accuracy evaluation is used to ascertain the accuracy of the land use classification result. The contingency method, often known as the contingency matrix, is the most popular technique for assessing accuracy (confusion matrix). The producer's accuracy, overall accuracy, and kappa accuracy are three types of information that are included in the contingency matrix. The overall accuracy estimates are based on both producer and user accuracy. The accuracy perceived from the producer's perspective is known as "producer accuracy," whereas user correctness is known as "user accuracy."

Accordingly to the analysis, the overall accuracy results of the classified images were 90.19%, 87.18%, and 86%, respectively, for the year’s maps of 1990, 2006, and 2020. On the other hand, based on the result, the overall accuracy was confirmed to be in the acceptable range. The resulting classification of land use and land cover maps of the three periods had a Kappa statistic of 0.88, 0.85, and 0.83, for the periods 1990, 2006, and 2020, respectively, which indicated a high level of agreement because the values were greater than 0.75. The user, producer, overall accuracy assessment, and kappa coefficient for the 2020 LULC classification are presented, in Tables 4.1, 4.2, and 4.3, respectively.

Table 4.1 1990 image Accuracy assessment calculation of land use change analysis

LULC	BS	CL	FL	GL	Set	SHL	WB	Total Samp.	Corrected sample	UA (%)
BS	35	0		5		2		42	35	83.3
CL	0	42					1	43	42	97.7
FL	1		45	0				46	45	97.8
GL			2	24		3		29	24	82.7
Set	1			0	23	0	0	24	23	95.8
SHL					5	15	0	20	15	75
WB		1		0	0	0	9	10	9	90
Total	37	43	47	29	28	20	10	214	193	
PA (%)	94.6	97.7	95.7	82.7	82.1	75	90		OAA (%)	90.2
Overall Kappa Statistics = 0.88										

Note, (BS=Bair soil, CL= Cropland, F= forest, GL= Grassland, Set= Settlement, SL= Shrubland, WB= Water body, PA= Producer Accuracy, UA= User Accuracy and OAA= overall Accuracy)

Table 4.2 2006 image Accuracy assessment calculation of land use change analysis

LULC	BS	CL	FL	GL	Set	SHL	WB	Total Sampl	Corrected sample	UA (%)
BS	21	0	2	1	1	0	0	25	21	84
CL	0	39	1	1	2	2	0	45	39	86.7
FL	1	1	30	0	1	1	0	34	30	88.2
GL	2	0	1	28	0	0	1	32	28	87.5
Set	1	1	1	0	21	0	0	24	21	87.5
SHL	1	0	1	1	0	18	0	21	18	85.7
WB	0	1	0	0	0	0	13	14	13	92.9
Total	26	42	36	31	25	21	14	195	170	
PA (%)	80.8	92.9	83.3	90.3	84	85.7	92.9		OAA (%)	87.2
Overall Kappa Statistics = 0.85										

Table 4.3 2020 image Accuracy assessment calculation of land use change analysis

LULC	BS	CL	FL	GL	Set	SHL	WB	Total Sample	Corrected sample	UA (%)
BS	30	0	5	0	0	1	0	36	30	83.33
CL	0	35	0	8	0	0	0	43	35	81.4
FL	1	3	25	0	0	0	0	29	25	86.21
GL	2	0	1	24	0	0	1	28	24	85.71
Set	1	1	1	0	29	0	0	32	29	90.63
SHL	1	0	1	0	2	23	0	27	23	85.19
WB	0	0	0	0	0	0	11	11	11	100
Total	35	39	33	32	31	24	12	206	177	
PA (%)	85.7	89.7	75.8	75	93.6	95.8	91.7		OAA (%)	85.92
Overall Kappa Statistics = 0.83										

4.2 Spatial and Temporal Distribution of LULC and Change detection

The map displaying seven classifications of land use and land cover (cultivation, grassland, shrubland, forestland, barelands, water bodies, and settlement) was created as shown in the figure 4.1. The study's findings indicated that the watershed has experienced considerable LULC change. It discloses an increase in cropland, settlements, and bareland while showing a decline in forestland, grassland, shrubland, and water. The Land use land cover maps of (a) 1990, (b) 2006, and (c) 2020 in the watershed are presented in Figure 4.1.

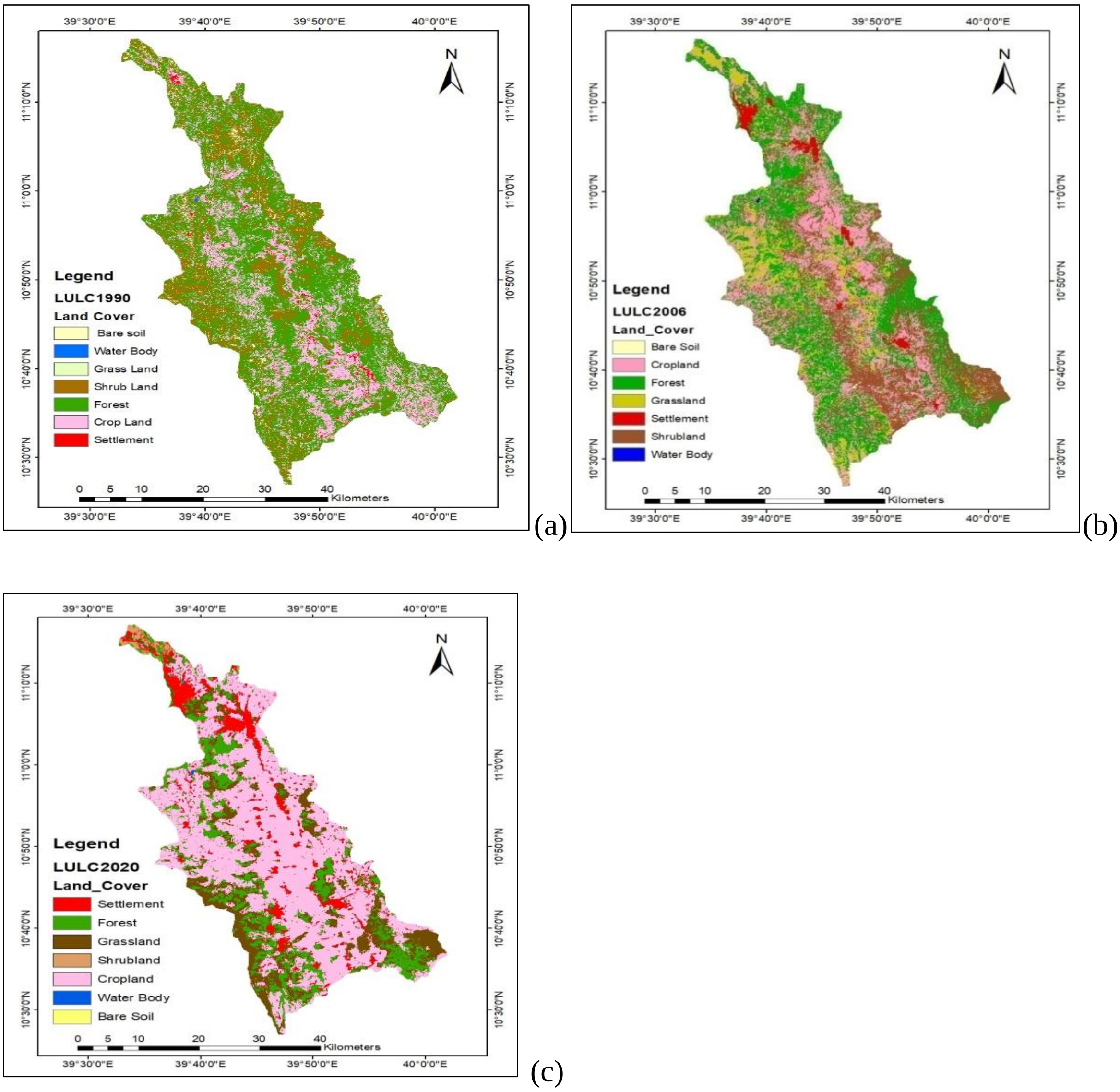

Figure 4.1 Land use land cover type map of (a) 1990, (b) 2006, and (c) 2020

In the year 1990, the Borkena watershed was dominated by Forestland (47.2%) followed by cropland (25.5%), shrubland (17.5%) and grassland (8.3%) while settlement area, water body, and bare land accounted for 1.3%, 0.1%, and 0.1% of the watershed respectively. Cropland was also dominant in 2006, accounting for 40.5% of the watershed, followed by forestland (30.4%), shrubland (16.6%), and grassland (7.8%), while settlement area, bareland, and water body accounted for 4.5%, 0.7%, and 0.1%, respectively. Also, In the year 2020, cropland was dominant with an area coverage of (57.8%), followed by forestland (14.5%), shrubland (12.6%), and settlement area (9.1%) in the watershed, respectively, whereas grassland, bareland and water bodies are minor as compared with cropland, forestland, shrubland, and settlement areas. The temporal distribution of the major LULC classes in 1990, 2006, and 2020 is shown in Table 4.4.

Table 4.4 the spatial distribution of the major LULC classes in 1990, 2006 and 2020

Land use land cover types	1990		2006		2020		LULC change					
							1990-2006		2006-2020		1990-2020	
	Area (km^2)	(%)	Area (km^2)	(%)	Area (km^2)	(%)	km^2	(%)	km^2	(%)	km^2	(%)
Bareland	1.8	0.1	2.7	0.2	53.6	3.0	0.9	0.1	50.9	2.8	51.8	2.9
Cropland	455.7	25.5	723.7	40.5	1033.0	57.8	268.0	15.0	309.3	17.3	577.3	32.3
Forest	843.3	47.2	543.4	30.4	259.3	14.5	-299.9	-16.8	-284.1	-15.9	-584.0	-32.7
Grassland	148.2	8.3	139.8	7.8	51.5	2.9	-8.4	-0.5	-88.3	-4.9	-96.7	-5.4
Settlement	24.1	1.3	80.4	4.5	163.1	9.1	56.3	3.2	82.7	4.6	139.0	7.8
Shrubland	312.3	17.5	296.5	16.6	225.9	12.6	-15.8	-0.9	-70.6	-4.0	-86.4	-4.8
Water Body	1.6	0.1	0.5	0.0	0.7	0.0	-1.1	-0.1	0.1	0.0	-1.0	-0.1

Note: Negative and positive signs indicate the decrease and increase of LULC class, respectively.

The most significant LULC changes were found in the land use types classified as forestland, cropland, grassland and settlement as shown in Table 4.4, when compared with the LULC data of the years 1990, 2006, and 2019. During the 16 year time interval from 1990-2006, the area coverage of cropland, settlement area and bare land increased by 268 km^2 (15%), 56.3 km^2 (3.2%), and 0.9 km^2 (0.1%) respectively. while forestland, shrubland, grassland, and water bodies diminished between 1990 and 2006 by 299.9 km^2 (16.8%), 15.8 km^2 (0.9%), 8.4 km^2 (0.5%), and 1.1 km^2 (0.1%) respectively. Most forest areas lost were converted to cropland (14.4%) and about 2.4% to settlement areas. The area of forestland, grassland, shrubland, and water bodies decreased by 584.0 km^2 (32.7%), 96.7 km^2 (5.4%), 86.4 km^2 (4.8%), and 1.0 km^2 (0.1%), respectively, between 1990 and 2020.

The available forest was mainly deforested; this is mainly because of the cutting of trees for various uses, such as firewood and agricultural purposes. Cropland, settlement area and bareland, on the other hand, increased by 577.3 km^2 (32.3%), 139.0 km^2 (7.8%), and 51.8 km^2 (2.9%), respectively, in the majority of the watershed between 1990 and 2020. This change could be linked to the high population growth that caused the increase in demand for new agricultural land. The settlement area also changed significantly between 1990 and 2020 by 7.8% due to the rapid development of settlement area such as the expansion of the town. The growth of these urban centres can be attributed to the high rate of rural urban migration.

Similar, Metaferia (2019), Amsalu *et al*. (2007), and many others reported that cultivated land and urban area was expanded at the expense of natural forest cover due to the higher rate of population growth. Therefore, population growth is the driving factor to LULC change in Borkena watershed which leads to significant alteration of streamflow and sediment yield LULC.

4.3 Streamflow Modelling

4.3.1 Streamflow sensitivity analysis

Estimating the rate of change in a model's output with respect to changes in watersheds that clearly differ in its hydrologic sensitivity is the goal of the sensitivity study (Reungsang *et al*., 2005). Utilizing observed data and the Sequential Uncertainty Fitting (SUFI-2) technique, which is connected to the SWAT Calibration Uncertainty Program, or SWAT-CUP, sensitivity analysis was carried out on the SWAT flow parameters at a monthly time step. The most sensitive factors in the study area were determined by taking into account all flow parameters.

As a consequence, nineteen factors were chosen for sensitivity based on manual ArcSWAT training and literature reviews. The absolute SWAT value, which is depicted in Appendix A.3, serves as the basis for the ranges of variation for these parameters. Following a number of simulations, SWAT-CUP outputs the rank order of parameter sensitivity based on its t-statistic and p-value. The p-value associated with the highest value of t-stat shows the rejection of the hypothesis that a rise in the parameter's value causes a substantial increase in the variable response and the lowest value of t-stat indicates the ratio of the high parameter coefficient to standard error (Abbaspour *et al.*, 2017). The ten most sensitive hydrologic flow parameters during calibration and validation in the watershed are given in Figure 4.2.

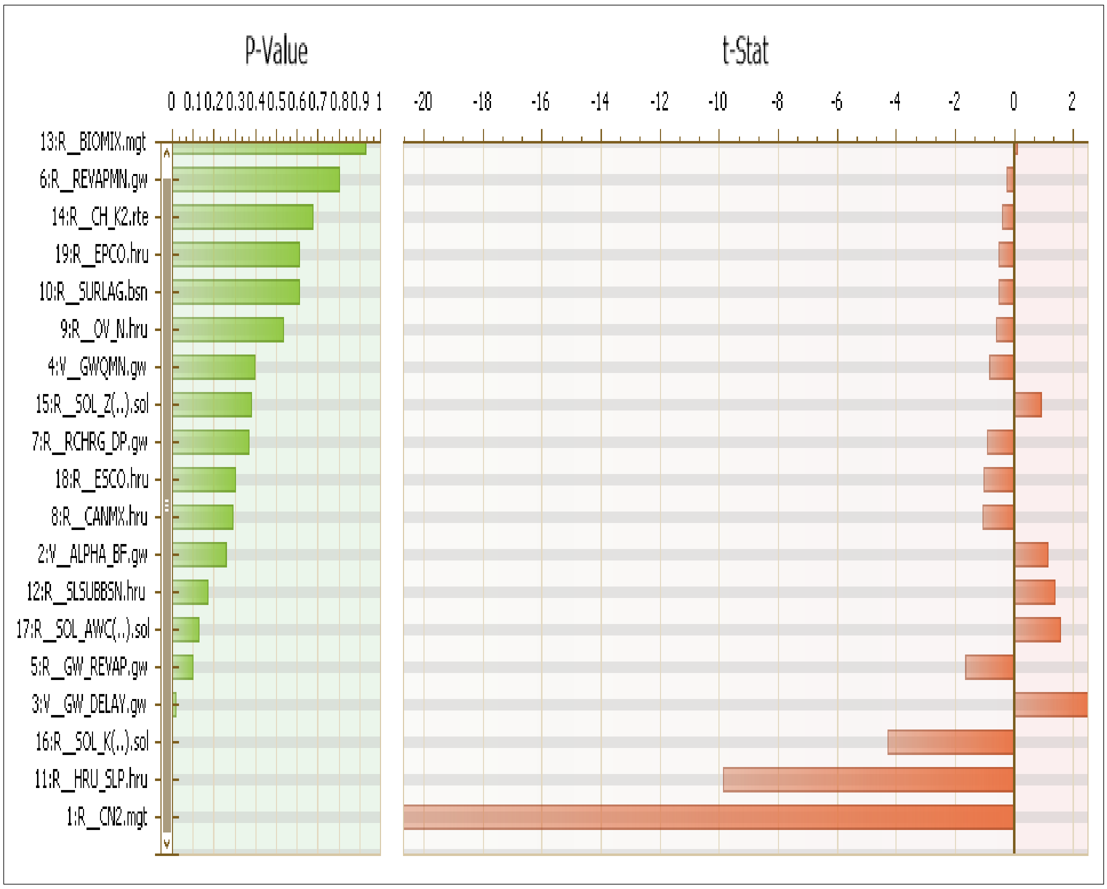

Figure 4.2 Streamflow sensitive parameters

According to Figure 4.4, the most sensitive flow parameter in the Borkena watershed was found to be the moisture condition II curve number (CN2), which was then followed by the average slope steepness (m/m) (HRU SLP.hru), saturated hydraulic conductivity of the soil layer (SOL K), delay time for aquifer recharge (GW

DELAY.gw), groundwater "revap" coefficient (GW REVAP.gw), available water capacity of the soil (ESCO).

Table 4.5 Shows the best optimized fitted parameters value during calibration

Rank	Parameter_Name	Fitted_Value	Min_value	Max_value
1	R__CN2.mgt	-0.124	-0.132	-0.024
2	R__HRU_SLP.hru	0.738	0.659	0.825
3	R__SOL_K(..).sol	-125.228	-190.688	183.371
4	V__GW_DELAY.gw	541.120	439.812	570.532
5	R__GW_REVAP.gw	0.119	0.108	0.123
6	R__SOL_AWC(..).sol	0.920	0.819	0.959
7	R__SLSUBBSN.hru	145.370	132.346	151.641
8	V__ALPHA_BF.gw	0.764	0.747	0.880
9	R__CANMX.hru	19.400	17.100	35.500
10	R__ESCO.hru	0.684	0.578	0.693

4.3.2 Streamflow calibration and Validation

The two years from 1988 to 1989 were utilized as a warm-up period when comparing the streamflow between the observed and simulated discharge values over 18 years' means of time-steps between 1990 and 2007 on a monthly basis. Every step of the model simulation, with the corresponding parameters written out, tested the model's performance at each gauging station. In order to get independent agreements between measured and simulated streamflow for gauged sub-basin, the parameter values were varied repeatedly within the permitted limits.

R^2, NSE, and PBIAS at swamp gauged station was used to assess the effectiveness of the SWAT model. With R^2 of 0.8, NSE of 0.7, and PBIAS -17.3 values, the calibration for monthly flow demonstrated that there is a good agreement between the measured and simulated flows. P-factor = 0.71 and R-factor = 1.64 are the values for the uncertainty measure throughout the calibration period. Similar to the calibration for monthly flow demonstrated that there is a good agreement between the measured and simulated flows. P-factor = 0.71 and R-factor = 1.64 are the values for the uncertainty measure throughout the calibration period. The validation period has also shown a good agreement between monthly measured and simulated flows. For model validation, the remaining observed streamflow data of Borkena River from 2008 to 2015 were used. The performance indicator result shows the model performing well during validation. The value of the swamp outlet was $R^2 = 0.8$, NSE = 0.65, and PBIAS =-14.3, Pfactor = 0.6, and R-factor = 1.84. Observed and simulated streamflow hydrographs and scatter plots at Swamp stations during calibration and validation are illustrated in Figures 4.3 and 4.4, respectively.

Similarly, calibration and validation results were reported by different studies that conducted in Ethiopian region. For example, Haile and Assefa (2012) reported that the SWAT model showed a good agreement between observed (ENS=0.76 and R^2=0.85) and simulated (ENS=0.72 and R^2=0.79) streamflow for calibration and validation in Angerb watershed.

.

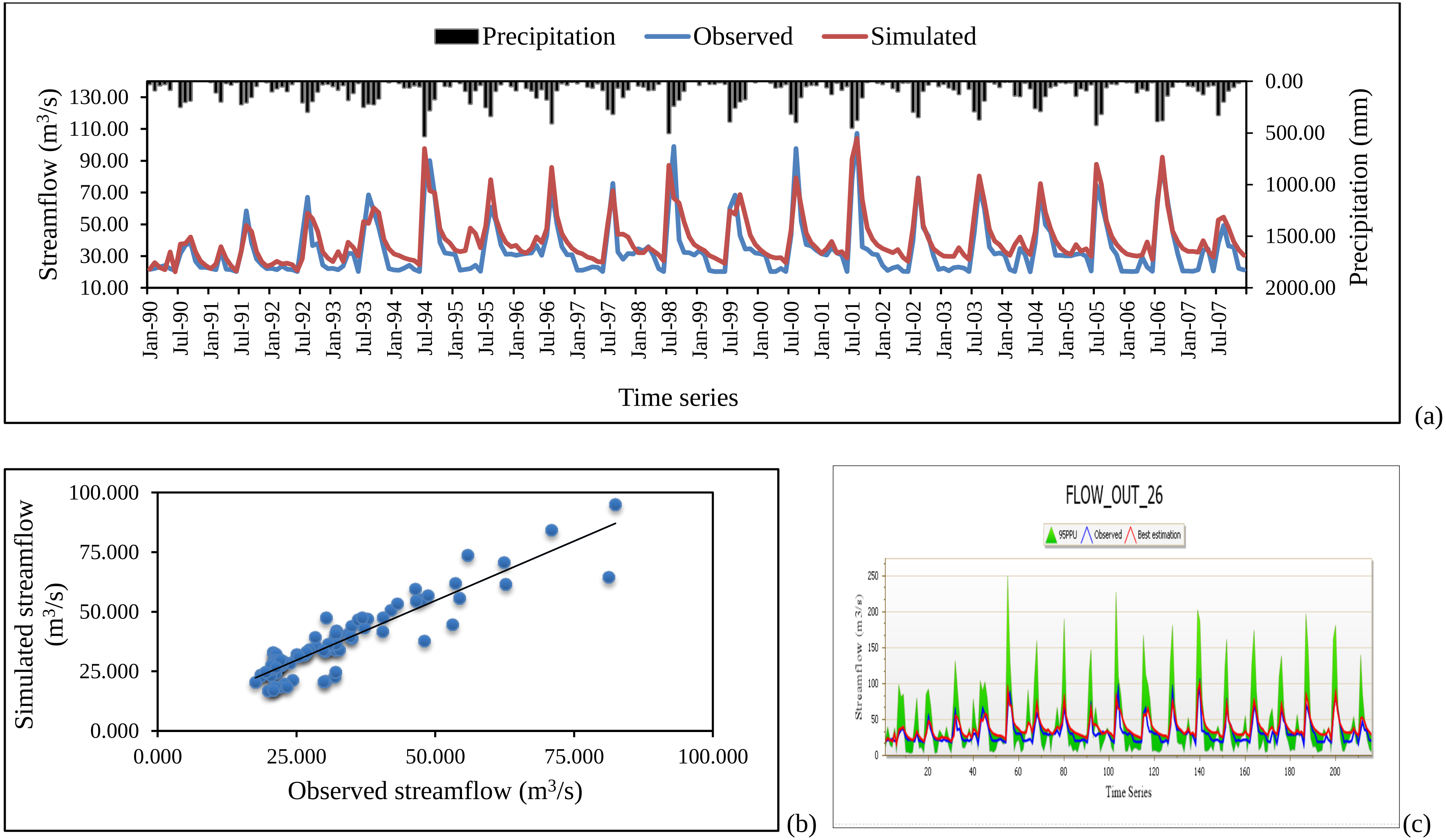

Figure 4.3 Observed and simulated streamflow hydrograph for calibration (a) and scatters plot of observed Vs simulated flow for calibration (b) and simulated vs observed average monthly flows generated from SWAT CUP during calibration (c)

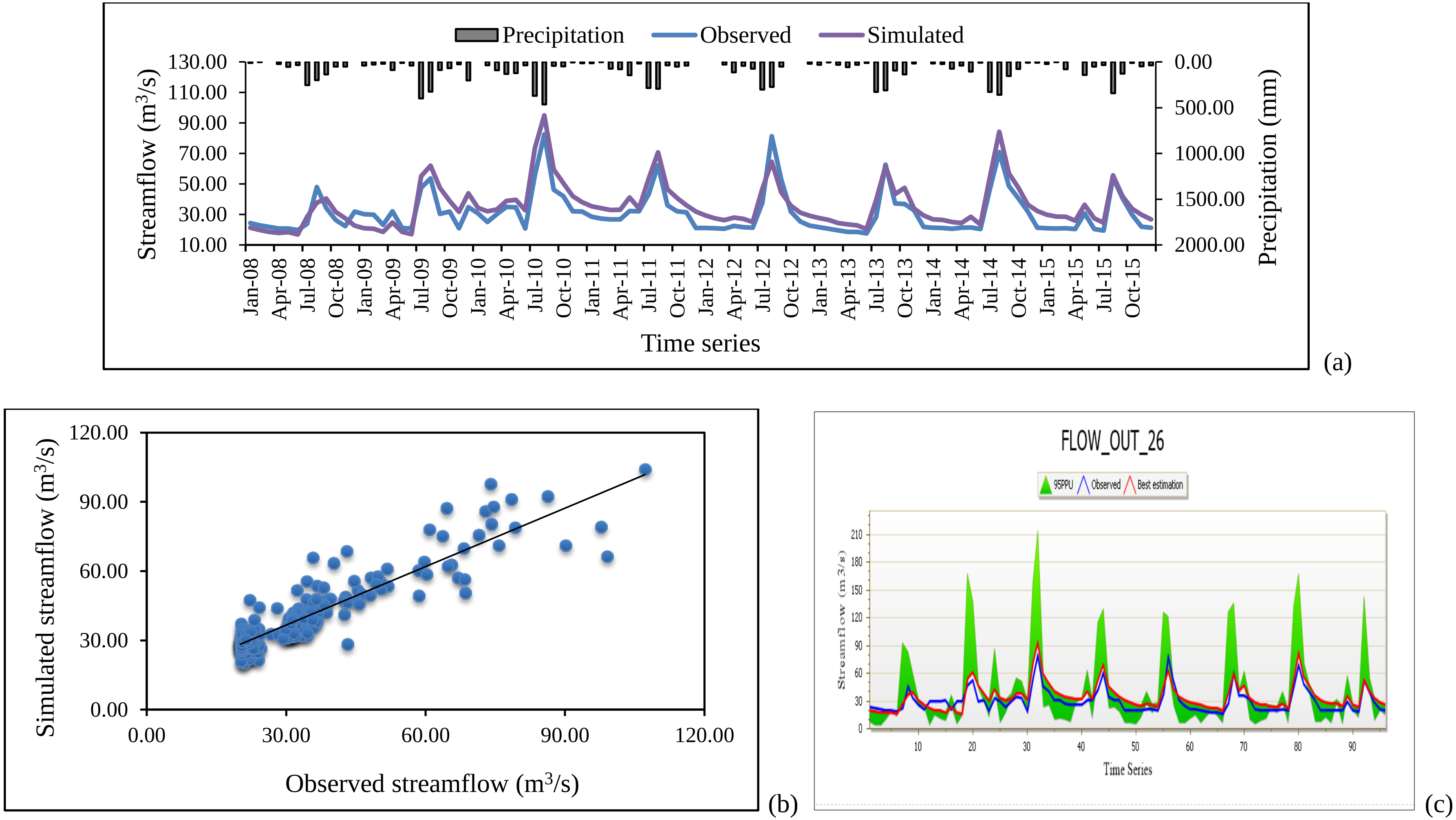

Figure 4.4 Observed and simulated streamflow hydrograph for validation (a) and scatters plot of observed Vs simulated flow for simulation (b) and simulated vs observed average monthly flows generated from SWAT CUP during simulation (c)

Every time the simulation was run after being calibrated for flow, the hydrographs were accurately represented. Some of the model parameters that are considered to have a limited influence on streamflow could be the cause of the uncertainty in the model simulation. Inconsistencies in the model simulation can also be caused by inconsistent hydro-metrological data, spatiotemporal data, including soil and LULC data, and other factors. However, the agreement between the measurement and simulation is typically extremely good, which is supported by R^2, NSE, and PBIAS. A result that complies with the model evaluation guidelines was thus produced (Moriasi *et al.*, 2007).

As a result, the SWAT model's ability to simulate the streamflow in the Borkena watershed was evaluated by comparing the observed and simulated streamflow during the calibration and validation periods.

Table 4.6 Statistical analysis for streamflow calibration and validation periods

Simulation Period	Model performance indicators			Uncertainty measures	
	R^2	NSE	PBIAS	p-factor	r-factor
Calibration (1990-2007)	0.82	0.69	-17.3	0.71	1.64
Validation (2008-2015)	0.81	0.65	-14.3	0.6	1.86

4.4 Sediment Yield Modelling

4.4.1 Sediment yield sensitivity analysis

Eight sediment parameters were obtained during the sensitivity analysis of sediment yield utilizing monthly observed sediment yield data in the SUFI-2 algorithm that was connected to SWAT-CUP using SUFI-2 in SWAT-CUP. The absolute SWAT values, which are shown in Appendix A.5, were used to determine the ranges of variation for these sediment yield characteristics. In the end, the calibration and validation of the sediment used six parameters with the greatest sensitive values. The six most sensitive sediment yield parameters during calibration and validation in the watershed were obtained from sensitivity analysis; ranks of sediment parameters were assigned depending on p-value and t-stat (Figure 4.5).

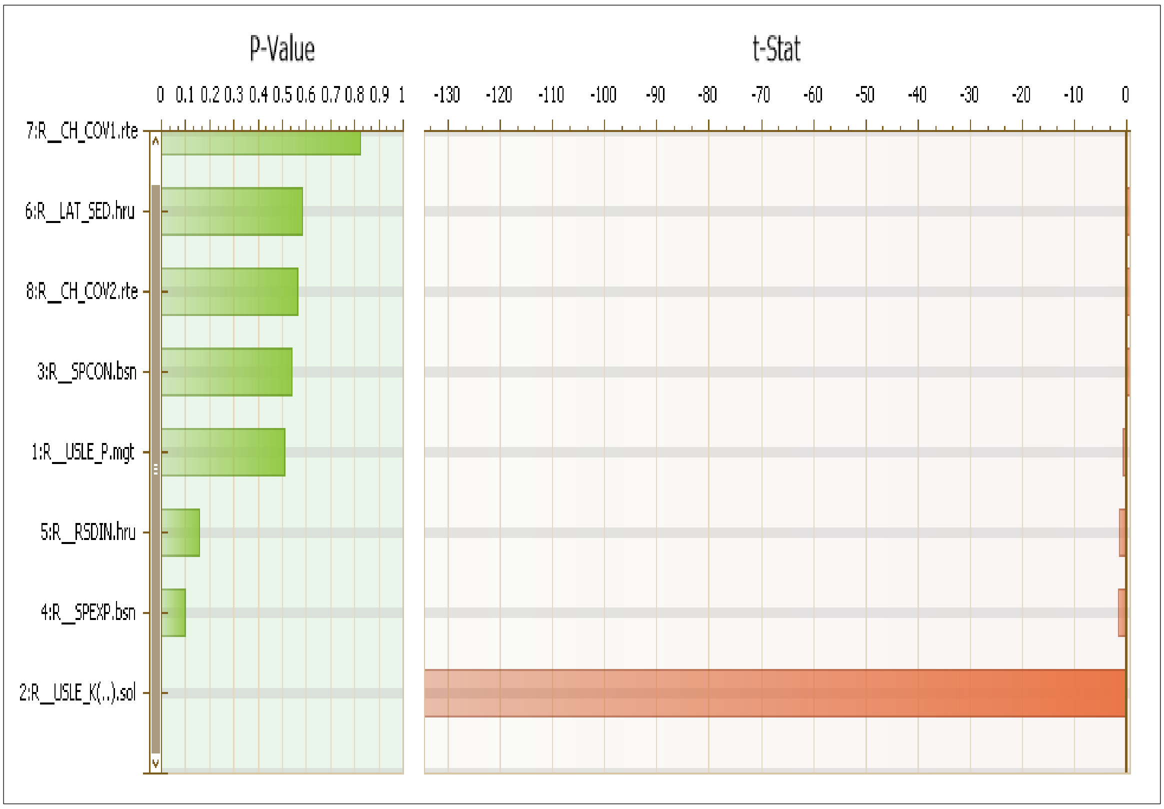

Figure 4.5 p-value and t-stat for sensitivity analysis of sediment yield

The most sensitive parameter among them was the USLE soil erodibility factor (USLE K), which was followed by the Exponent re-entrainment parameter in sediment routing (SPEXP. Bsn). were found to be the most sensitive factor, which is similar with other previous investigations (example, Choto and Fetene, 2019; Kidane *et al*., 2019; Aghsaei *et al*., 2020). Another crucial factor in sediment transport in the Borkena watershed is the exponent parameter for calculating sediment re-entrained in channel sediment routing (USLE P.mgt), channel sediment routing (SPCON), and initial residue cover (kg/ha) (RSDIN.hru).

Table 4.7 Sediment yield parameters sensitivity rank

Rank	Parameter_Name	Fitted_Value	Min_value	Max_value
1	USLE_K(..).sol	-0.5	-0.8	-0.2
2	SPEXP.bsn	1.3	1.2	1.3
3	RSDIN.hru	1.8	1.5	1.8
4	USLE_P.mgt	1.2	0.8	1.2
5	SPCON.bsn	0.0	0.0	0.0

4.4.2 Sediment yield calibration and validation

SWAT-CUP calibration and validation for monthly sediment yield were conducted after the model was calibrated and validated for streamflow. Like streamflow calibration, the model was also calibrated for sediment yield for the period 1990-2006 with a two-year warmup period from the years 1988-1989. The sediment calibration was done with calibration in a monthly time setup based on the sensitive sediment parameters identified after sediment sensitivity analysis. The SWAT model was found to simulate very well in the Borkena watershed (Swamp) stations with statistical measures computed between the simulated and observed monthly sediment loads for the calibration periods.

According to model performance evaluation criteria, the sediment simulation results for calibration and validation at Borkena watershed (Swamp outlate) station showed a very good performance with (R^2 = 0.81, NSE = 0.72, and PBIA = -14.6) for calibration and with (R^2 = 0.80, NSE = 0.70, and PBIA =-17.21) for validation. Uncertainty measure values during the calibration and validation periods were found to be Pfactor = 0.61 and R-factor = 0.71, and Pfactor = 0.72 and R-factor = 1.02. Observed and simulated sediment yield hydrograph and scatter plot at three stations during calibration and validation are presented in Figures 4.6 and 4.7, respectively.

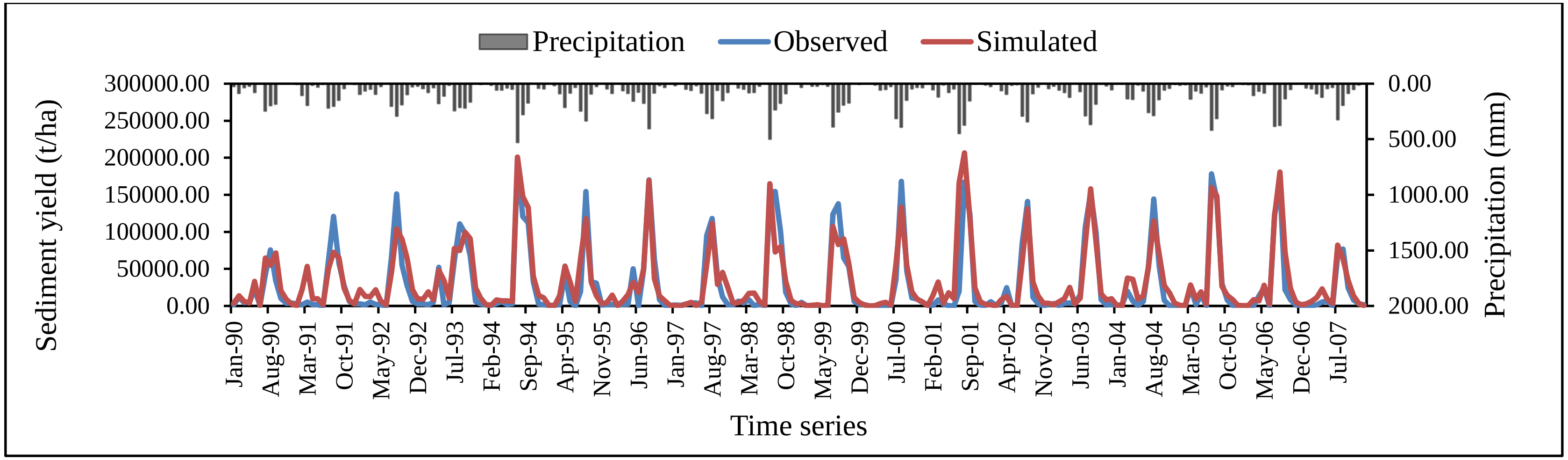

(a)

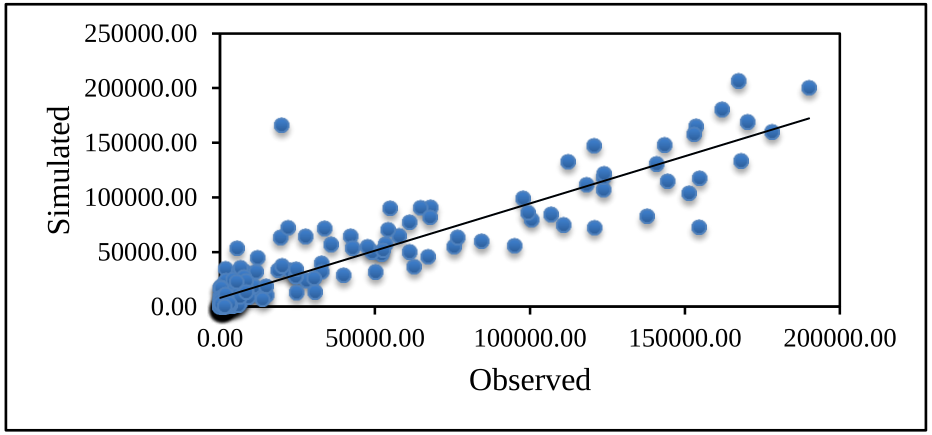

(b)

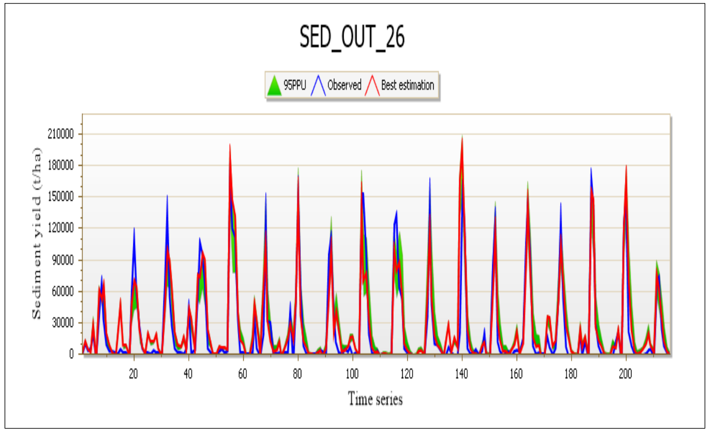

(c)

Figure 4.6 Observed and simulated sediment yield hydrograph for calibration (a) and scatters plot of observed Vs simulated Flow for calibration (b) and simulated vs observed sediment yield generated from SWAT CUP during calibration (c)

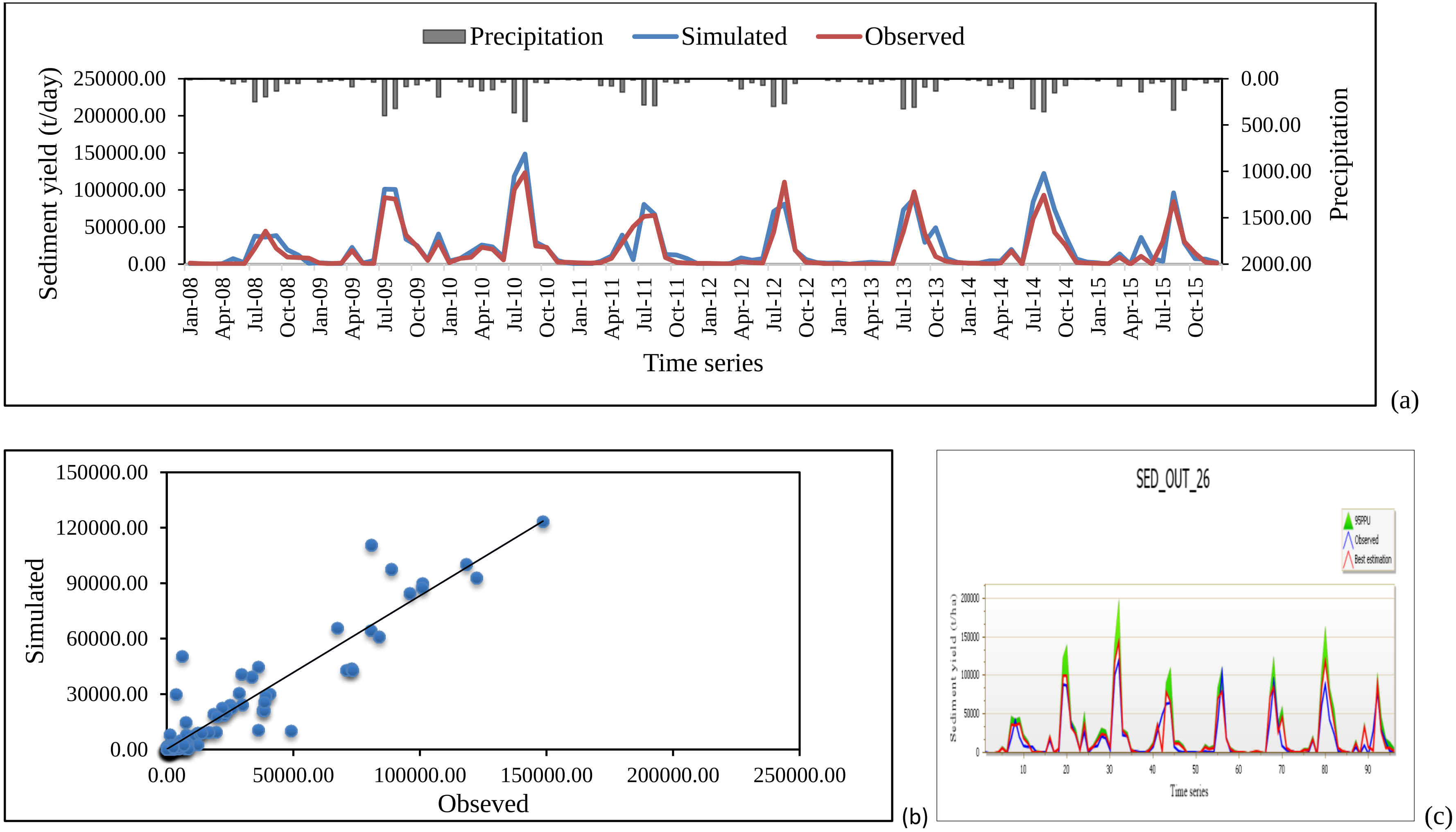

Figure 4.7 Observed and simulated sediment yield hydrograph for calibration (a) and scatters plot of observed Vs simulated flow for calibration (b) and simulated vs observed sediment yield generated from SWAT CUP during calibration (c)

4.5. Streamflow and Sediment Yield Responses to Land Use Land Cover Change

Based on historical LULC of 1990, 2006, and 2020, the calibration and validation SWAT model was used to assess the effect of land use and land cover (LULC) on streamflow and sediment output. The impact of LULC change on streamflow and sediment output at a specific watershed and sub-basins was examined using the long-term hydrologic simulation from the years 1988 to 2015 on a monthly basis.

4.5.1 Streamflow responses to land use land cover change

The catchment streamflow was affected by changes in land use and land cover that were discovered in the satellite image data from three separate years. In this study, the effect of LULC modification on streamflow in the Borkena watershed was evaluated. Additionally, the seasonal variation in streamflow throughout the rainy (July, August, and September) and dry (Jan, Feb, and March) months was evaluated. Figures 4.8 and 4.9, which exhibit the yearly streamflow and mean monthly streamflow comparison results for the land use and land cover maps from 1996, 2006, and 2020, respectively.

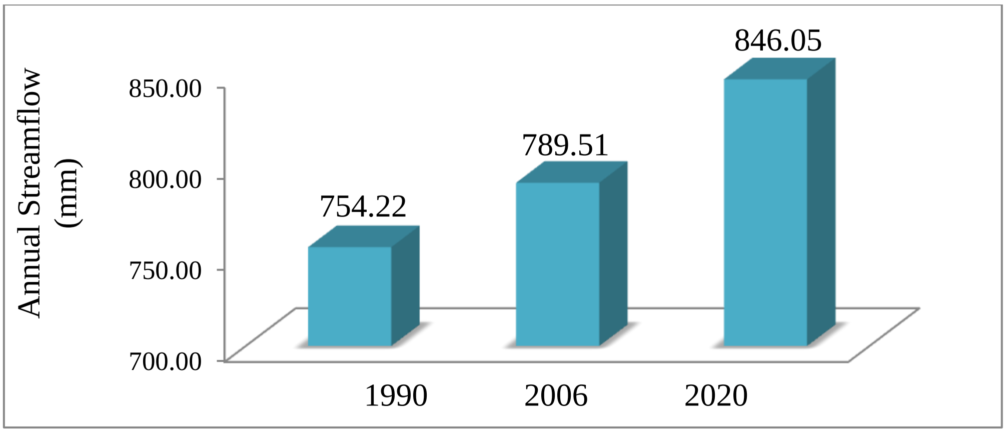

Figure 4.8 Annual simulated streamflowat different LULC

The result indicated that the annual streamflow from 1990 to 2006 LULC increased by 35.29 mm (4.68%) and increase from 2006 to 2020 LULC by 56.54 mm (6.68%). The combination led to a decrease in forested land and an increase in agricultural land from 2006 to 2020. In Ethiopia, Lake Tana Upper Blue Nile hydrological balance led to the conclusion that increased agricultural land expansion increased streamflow by reducing infiltration, but that forest areas have the highest potential to decrease streamflow due to improved land in watersheds and increased infiltration (Abeyou, 2008).

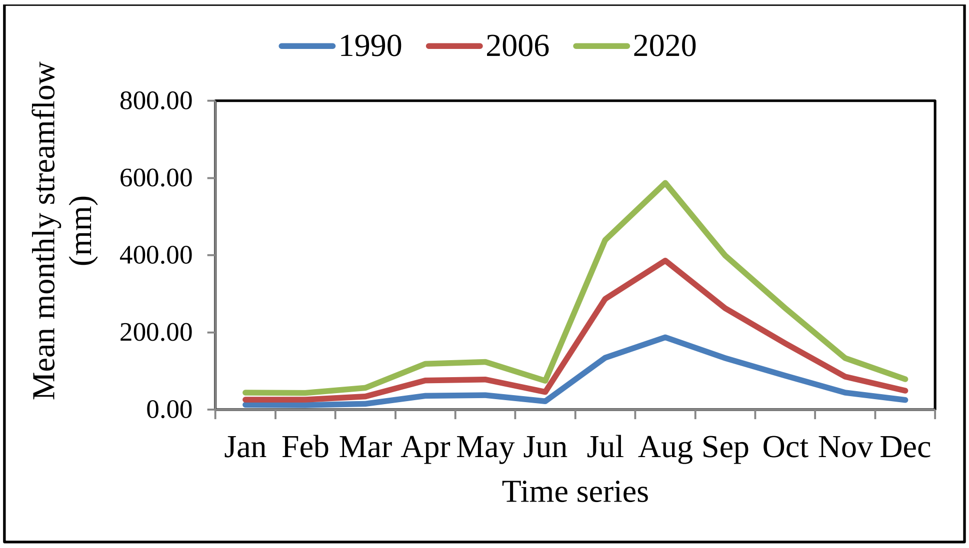

Figure 4.9 Mean monthly streamflowat different LULC

Based on three independent LULC, the yearly streamflow components of surface runoff (SURQ), groundwater flow (GWQ), lateral flow (LATQ), and evapotranspiration (ET) revealed temporal variability in the watershed (Table 4.8). The streamflow component SURQ indicated increasing up to 45.6% and 32.1 % for the period 1990-2006 and 2006-2020 respectively while GWQ, LATQ, and ET indicated decreasing trends. In other words, GWQ, LATQ, and ET contributions to streamflow decreased by 5.81%, 2.17%, and 1.27% for the year 1990-2006 and decreased by 11%, 2.9%, and 2.26% respectively during 2006-2020.

It was found that the streamflow component SURQ increased from 1990 to 2006, increasing from 88.7 mm to 129.2 mm. Surface runoff produced in 2006 was higher than in 1990 due to the expansion of agricultural land. At the loss of other land uses, there was a slight increase in agriculture and settlement in 2020, which led to an increase in surface runoff. While the amount of groundwater decreased from 305.75 mm in 1990 to 275.26 mm in 2006 as a result of the LULC change, this is attributable to the loss of forestland since forests increase groundwater levels by infiltrating precipitation and reducing runoff.

Table 4.8 Average annual basin water balance value and change

LULC	WY (mm)	SURQ (mm)	LAT Q (mm)	GWQ (mm)	ET (mm)	PERC (mm)
1990	754	88.7	353.8	324.6	371	324.6
2006	790	129.2	346.1	305.8	366	305.8
2020	846	161.3	336.4	275.3	358	275.3

It was Similar research was conducted by Serur and Adi (2022), who found that the Gidabo sub-basin showed higher temporal variability in terms of surface runoff (SURQ), groundwater flow (GWQ), lateral flow (LATQ), and evapotranspiration (ET) based on three independent LULC. The expansion of agricultural land, bare land, and built-up area over forest land and shrubland is directly responsible for the rise of SURQ and the declining trend of GWQ, LATQ, and ET. Additionally, Abebe (2005) found that as the area covered by forest cover reduced in the study of the Chemoga watershed in the Blue Nile basin, a considerable amount of surface runoff occurred during storm occurrences. According to studies by Tadele (2009) and Haile and Assefa, (2012), the extension of agricultural land, bare land, and settlement over forest and shrubland increases surface runoff.

4.5.2 Sediment Yield Responses to Land Use Land Cover Change

According to the annual sediment yield of the Borkena watershed, LULC was responsible for a significant amount of temporal fluctuation. Between 1990 and 2006, the yield of sediment increased by 81.4%, and from 2006 to 2020, it increased by 28.2%. The watershed generated a total annual sediment yield of 5.4 t/ha, 9.8 t/ha, and 12.6 t/ha, with simulated LULC of 1990, 2006, and 2020, respectively. Maximum sediment yield, according to Figure 4.10, is between July and September, while the minimum is between December and February. This is highly related to the temporal pattern of rain fall and surface runoff in the study area.

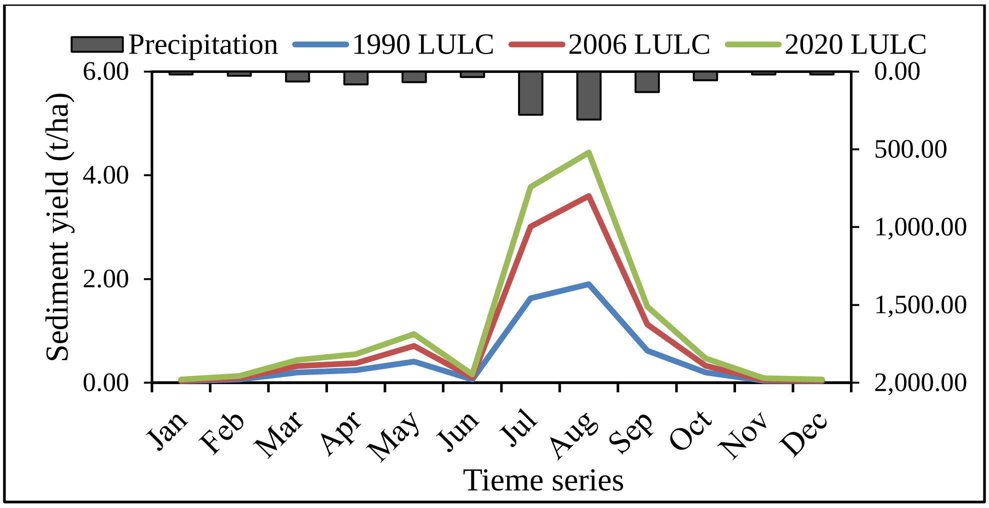

Figure 4.10 Mean monthly sediment yield for 1990, 2006 and 2020 LULC

The change in sediment yield in the watershed was obtained due to the increasing trend of agricultural, bareland, and settlement area over forestland, shrubland and grassland in the watershed, which increases surface runoff and sediment yield following rainfall events in the watershed. An increase in surface runoff during the study period resulted in an increase in sediment yield. Similar studies also support the results of this study. For example, Zeleke and Hurni (2001), Adi (2021) and Kidanu (2004) reported the continuous expansion of agricultural land, bareland, and settlement at the expense of vegetation cover in their study areas, which has increased the rate of soil erosion and sediment yield. Hence, LULC changes have a great impact on catchment soil erosion and sediment yield.

4.6 Spatial Distribution of Sediment Yield and Prioritization of Critical Sub-Basins

The climate, soil, slope, vegetation, and management practices are among the factors that affect surface runoff, soil erosion, and sedimentation. According to the SWAT model run with 2020 LULC, the watershed's total annual production of sediment that enters the Awash basin's downstream region is expected to be 470.59 t/yr. In a broad watershed, a small number of sub-watersheds are more crucial and accountable for significant runoff and soil losses. From 6.8 mm to 219.9 mm and 0.1 t/ha/yr to 71.23 t/ha/yr, respectively, the average annual surface runoff and sediment yield from each sub-basin varied. The study conducted to determine the rate of soil erosion in Ethiopia by Hurni (1985), the allowable soil loss amount for Ethiopia's diverse agro-ecological zones ranges from 2 to 22 t ha per year.

As a result, 6 of the 29 sub-basins in the Borkena watershed had simulated soil loss rates that were higher than the maximum allowable rate (22 t/ha/yr), indicating that sedimentation is a severe threat to the study region. According to the spatial distribution of sediment yield (Figure 4.13), six sub-basins (5, 7, 10, 11, 12, and 20) are shown to be the most important sediment sources, producing average annual sediment yields of over 40.74 t/ha/yr. According to the HRU distribution of the identified sub-basins, agricultural and bareland are the main governing factors for runoff and sediment potential areas.

Since surface runoff affects soil particle detachment and movement, there is a direct correlation between sediment yield and surface runoff. As shown in Figure 4.11, the majority of sub-watersheds with high levels of surface runoff also have high levels of sediment yield. Although some sub-basins, such as 10 and 20, produce tolerable annual average sediment yields while generating relatively high annual average surface runoff, others, such as 5, 7, 11, and 12, relatively produce low annual average surface runoff while generating high annual average sediment yields when compared to other sub-watersheds. This shows that land use, land cover, topography, soil properties, and management practices are all important influences on the formation of sediment yield and surface runoff alone is not the only major factor in sediment yield production.

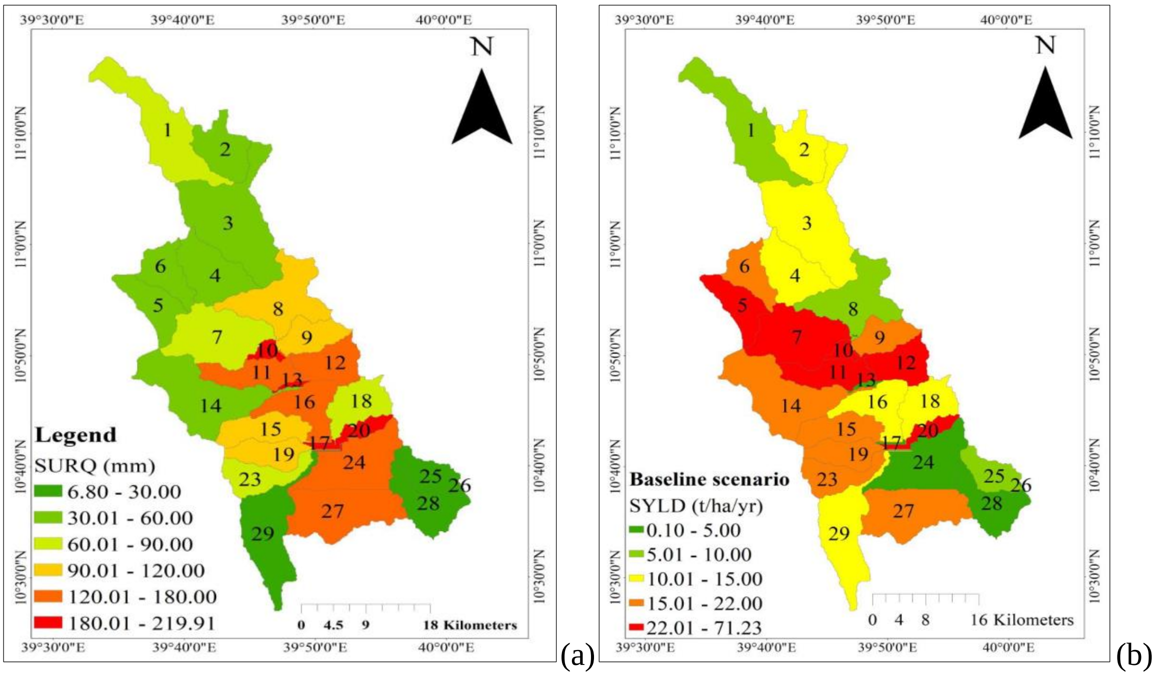

Figure 4.11 Spatial distribution of (a) surface runoff and (b) sediment yield in the study area

Sub-basin 5 creates relatively little surface runoff, but it is largely covered by agricultural land (61.9%), bareland (26.7%), and soil types with leptosols (47.1%). This sub-basin slope class has 20-40% dominance. On the other hand, sub-basin 19 generates a relatively high amount of surface runoff and produces a low amount of sediment yield because of the sub-coverage basins of leptosols (64.2%) and 55.5% forested land (with 65% having a slope class of 5 to 10%), which generates a comparatively high amount of surface runoff and a low amount of sediment output. Conclusion: Rather than surface runoff, land use and cover are the main contributors to the development of high sediment yields in sub-basins.

Tesema and Leta (2020) in Kesem dam watershed and Nadew *et al*. (2019) in Guder watershed also identified the sub-basins that generates a high amount of surface runoff but produce a low amount of sediment yield and finally, they concluded that surface runoff in alone has not to impact on sediment yield. As a result, high surface runoff does not automatically equate to high sediment production; instead, other factors such as land use, land cover, slope, and soil type play a role in sedimentation. For the purpose of watershed management to reduce the severity of sedimentation in the Borkena Watershed, six sub-basins numbers 5, 7, 11, 10, 12, and 20 were identified in this study as critical sources of sediment.4.7 Effectiveness of Best Management Practices Best management practices (BMPs) scenarios were taken into consideration and created based on the spatial variability of sediment source and sediment yield rate. The SWAT model was used to simulate the identified BMPs in order to determine their effectiveness in lowering the surface runoff and sediment production of the Borkena watersheds. Four alternative BMP scenarios were created and compared to the current state of this particular investigation (baseline scenario). A simulation was run for each scenario separately after changing the appropriate parameter values with the related management practices; a simulation was run for each scenario separately. Table 4.9 provides an illustration of the scenario employed and the provided parameters.

Table 4.9 Modified SWAT parameters

Scenarios	Description	Parameter Name		Calibrated Value	Modified Value
S0	Baseline	-		-	-
				0.00	3 m
S1	Filter strip	FILTERW		0.00	5 m
			Slope 0-5%	121.95	65 m
			Slope 5-10%	60.97	30 m
			Slope 10-20%	24.39	12 m
		SLSUBBSN	Slope > 20%	9.14	6 m
S2	Terracing	USLE_P		0.56	0.18
	Contour	CONT_CN		60	55
S3	farming	CONT_P		0.6	1.13
S4	Reforestation	5% AGRL, 10% FRST, and 60% BARR			

Scenario-0: Baseline

Baseline was implemented without best management practices to reflect the existing conditions. The baseline scenario reflects the current land management practices (2020 LULC) without conservation.

Scenario-1: Filter strip

Filter strip used to filter runoff and trap sediment in a specific agricultural area of identified key sub-basins on all agricultural HRUs, together with all soil types and slope classes. By allocating a FILTERW value of 3 m, which corresponds to the filter strip's width, the effect of the filter strip on sediment trapping was examined. As a result, the average annual sediment yield for critical subbasins was reduced from 40.74 t/ha/year to 20.09 t/ha/year after treatment with a 3 m wide filter strip, with an average reduction capacity of 57.1%. According to Gashaw *et al.*, (2021), at Abbay (upper Blue Nile) Basin, indicated the implementation of 3m wide filter strips for critical subbasins and reported a 13.7% mean annual sediment yield reduction for the critical subbasins from the baseline scenario.

Implementing a 5 m wide filter strip in critical sub-basins reduced the average annual sediment yield from 40.74 t/ha/ year to 17.5 t/ha/year, with an average of 57.1% reduction capacity. These results are consistent and similar with the previous research work in Ethiopian highlands by Abraham and Nadew (2018) at Guder watershed.

Scenario-2: Parallel Terracing

The average annual sediment yields from crucial sediment-yielding sub-basins were decreased by 27.68% by using the terracing management option. The average sediment yield rate of the subbasins was considerably decreased from 40.74 t/ha/year to 11.28 t/ha/year, as shown in Table 10, which illustrates how terracing affected each crucial area. Gashaw *et al.* (2021) showed a 72.3% annual average sediment yield reduction by implementing parallel terracing compared to the baseline scenario, which is similar to previous research in the Guder watershed.

Scenario-3: Contour farming

By enhancing surface roughness, installing contours on pastures, shrubland, and agricultural land increases infiltration. Runoff's speed and erosive power are subsequently decreased as a result. According to Table 4.10, the contour farming management option reduced sediment yields from high sediment yielding subbasins by 63.6%, or reduced the sediment yield rate from 40.74 t/ha/year to 14.84 t/ha/year. According to a different study by Kefay *et al.* (2022) that investigated the impact of contour farming and filter strips on ecosystem services, contour farming reduces yearly sediment yield by about 35.8% on average. As a result, the findings of this investigation were somewhat similar to those of previous studies.

Scenario-4: Reforestation

Simulated results show how reforestation affects the decline in sediment yield. By covering the soil from the direct impact of raindrops and promoting infiltration, a good vegetative cover offers the best, most affordable, and long-lasting protection against erosion (Morris and Fan, 1998). Due to rising food demand and population expansion, it is difficult and impracticable to convert agricultural land into evergreen forestland. In order to determine the amount of sediment yield reduction in the Borkena watershed, reforestation of 5% of agricultural land, 10% of shrubland, and 60% of bare land in sediment-prone regions from the most recent (2020) LULC was taken into account.

Reforestation reduced the annual average sediment yield from 40.74 t/ha/y to 26.96 t/ha/yr (Table 4.10) or by 33.8% compared with the baseline scenario. Betrie *et al*.

(2010) and Choto and Fetene (2019) also shown the reduction of sediment yield by 11% in the Blue Nile basin and 32.3% in the Gojeb watershed of Ethiopian highlands respectively by applying reforestation.

Table 4.10 Summary of sediment reduction with filter strip, parallel terracing, contour farming and reforestation simulation.

Critical (hotspot) subbasin	Baseline t/ha/y	After Filter strips 3 m t/ha/y	After Filter strips 5 m t/ha/y	After Parallel Terracing t/ha/y	After contouring t/ha/y	After Reforestation t/ha/y
5	24.5	12.1	10.5	6.8	8.9	16.18
7	24.4	12.0	10.5	6.8	8.9	16.16
10	71.2	35.1	30.5	19.7	26.0	47.15
11	43.2	21.3	18.5	12.0	15.7	28.58
12	57.7	28.5	24.7	16.0	21.0	38.20
20	23.4	11.6	10.0	6.5	8.5	15.51

4.8 Evaluation of Best Management Practices.

When conservation measures were implemented, the results were compared to the simulation's result under the current conditions (baseline scenario). According to Figures 4.10 and 4.11, the implemented watershed management options (reforestation, filter strips, terracing, and reforestation) had a significant impact on the key sub-basins' reduced sediment yield as compared to the baseline scenario. The effects of each management approach on the reduction of sediment yield are summarized in Table 4.12.

Table 4.11 Comparison best management practices in the study area

Scenario	BMPs		Sediment yield (t/ha/yr)	Reduction (%)
S0	Baseline		12.57	-
		3 m	6.201	50.67
S1	Filter strip	5 m	5.390	57.12
S2	Terracing		3.479	72.32
S3	Contour farming		4.581	63.56
S4	Reforestation		8.320	33.81

Overall, the study finds that allowing reforestation has the lowest potential to reduce sediment in the watershed's important subbasins, reducing just around 33.8% of the mean annual sediment load. Although becoming the least effective, this scenario has demonstrated more constant reduction characteristics than the others. Following filter strips 3 m wide, which reduced the mean annual sediment load by about 33.8%, and filter strips 5 m wide, which reduced the mean annual sediment load by about 57.12%, which was higher than terracing but lower than reforestation (63.56%). Critical subbasins showed the greatest reduction in contouring, which was lowered by 72.32%. This reduction was superior to others.

This indicates that improvements characterized by the control and reduction of soil erosion may be made through the application of terracing. This is in line with previous findings (Bracmort *et al*., 2006; Briak *et al*., 2019; Betrie *et al*., 2010; Fetene *et al*., 2019; Tesema and Leta, 2020). As a result, the downstream system of the watershed is greatly influenced by the choice of sediment management options. In general, the analysis found that at all hotspots in this watershed area, terracing was more effective than other management techniques. The findings would help policymakers, practitioners, and other accountable stakeholders implement the best BMPs within the watershed and in other watersheds that seem to be similar.

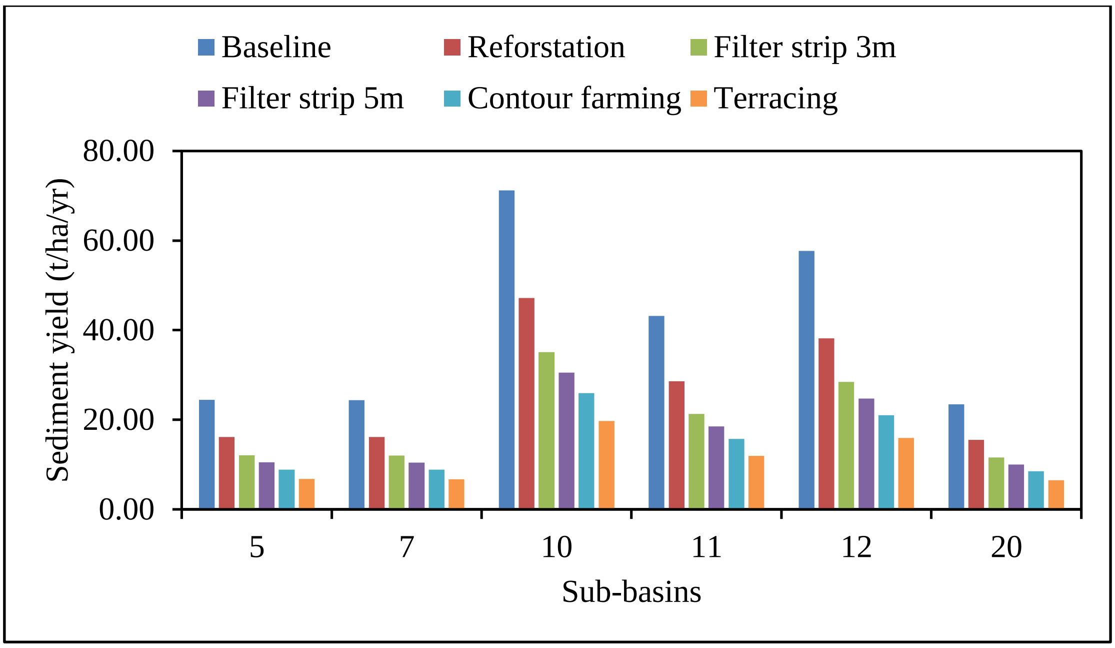

Figure 4.12 Comparison of best management practices in critical sub-basins

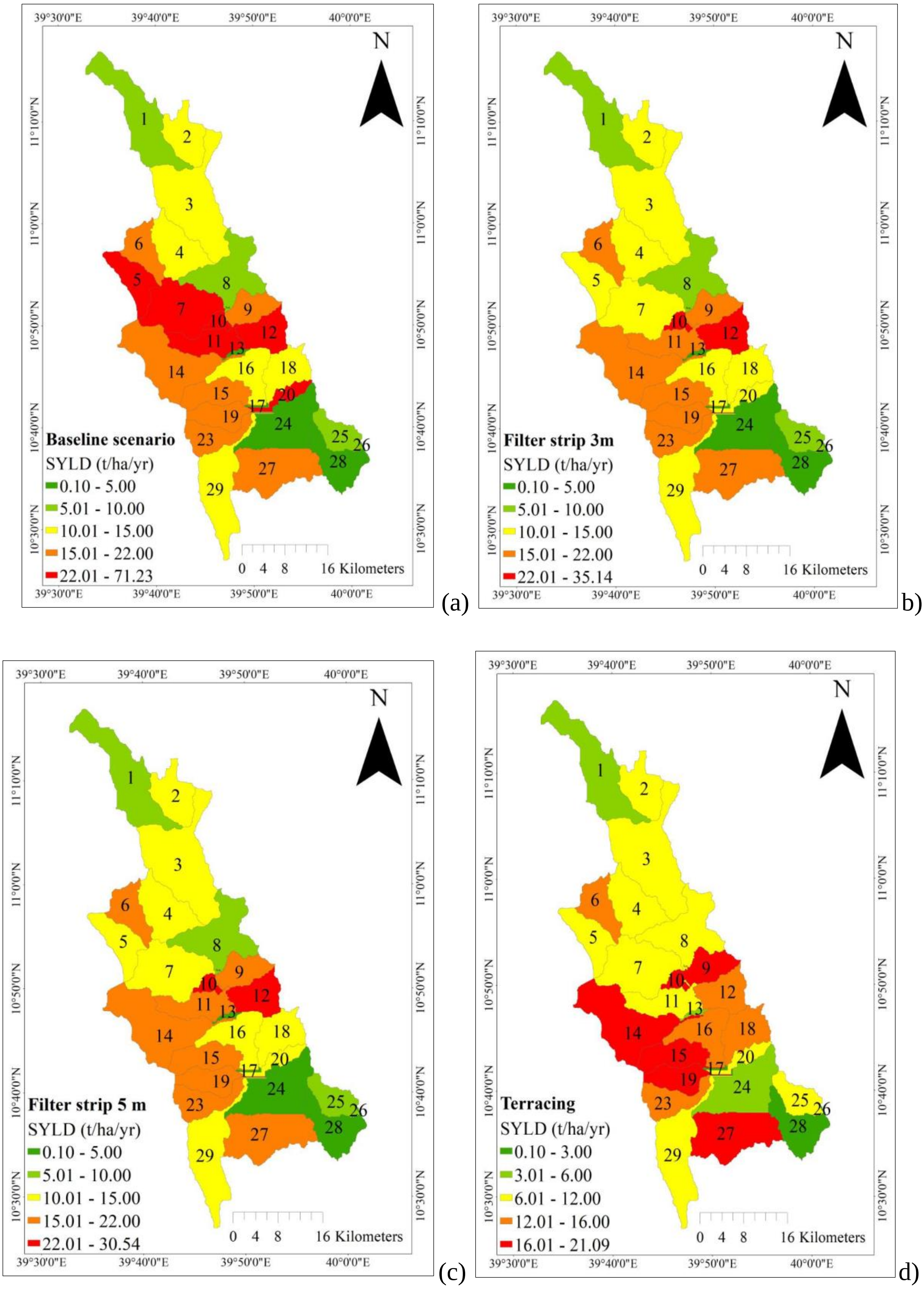
39°30'0"E
39°40'0"E
39°50'0"E
40°0'0"E
11°10'0"N
11°0'0"N
10°50'0"N
10°40'0"N
10°30'0"N
N
Baseline scenario
SYLD (t/ha/yr)
0.10 - 5.00
5.01 - 10.00
10.01 - 15.00
15.01 - 22.00
22.01 - 71.23
0 4 8 16 Kilometers
(a)
Filter strip 3m
SYLD (t/ha/yr)
0.10 - 5.00
5.01 - 10.00
10.01 - 15.00
15.01 - 22.00
22.01 - 35.14
b)
Filter strip 5 m
SYLD (t/ha/yr)
0.10 - 5.00
5.01 - 10.00
10.01 - 15.00
15.01 - 22.00
22.01 - 30.54
(c)
Terracing
SYLD (t/ha/yr)
0.10 - 3.00
3.01 - 6.00
6.01 - 12.00
12.01 - 16.00
16.01 - 21.09
d)

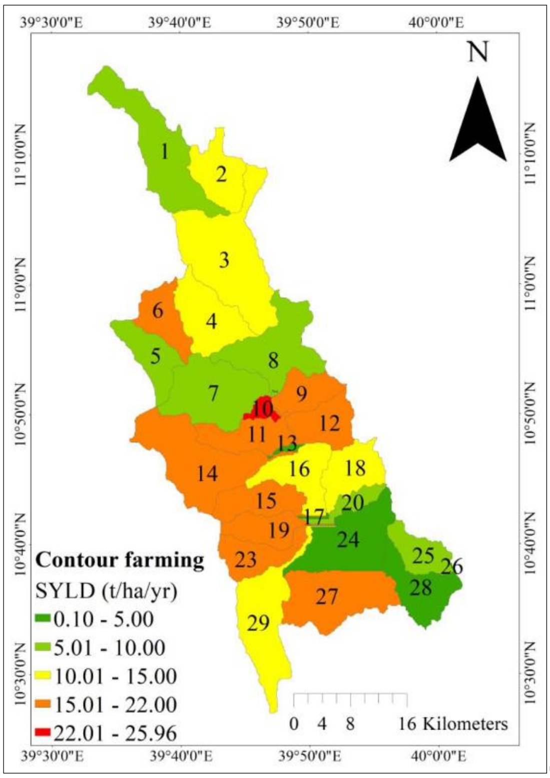

(e)

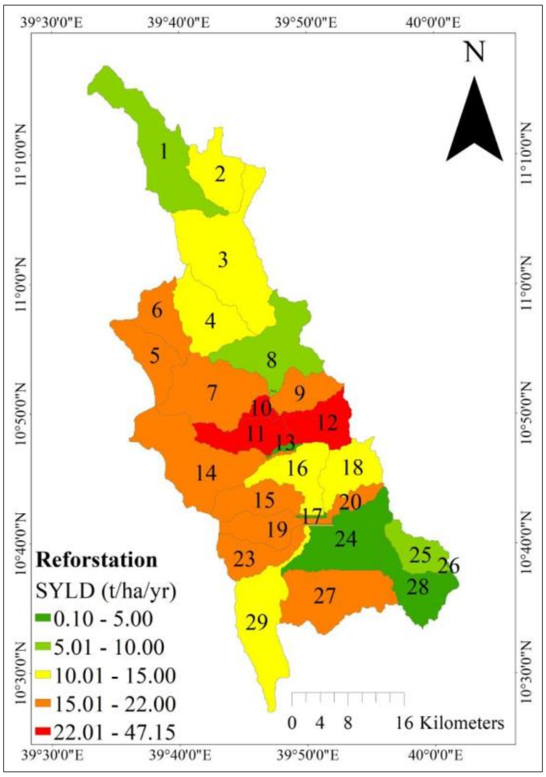

(f)

Figure 4.13 Comparison of best management practices sediment yield spatial distribution

5. CONCLUSIONS AND RECOMMENDATIONS

5.1 Conclusions

The objective of this paper was to assess how changes in land use and cover affected streamflow and sediment yield in the Borkena watershed. Best management techniques were also proposed to minimize sediment yield. The SWAT hydrology model was chosen to analyze the effects of changes in land use and land cover on streamflow and sediment yield for this particular study. To conduct this research, ERDAS Imagine 2014 with integrated GIS was used to categorize the remote sensing data from 1990, 2006, and 2020. Additionally, the LULC change during the past 31 years (1990–2020) was examined, and the Borkena watershed was used to evaluate the SWAT model's performance in order to examine the watershed's hydrological response to changes in land use and land cover. Finally, it was determined how land use and land cover affected streamflow. On the other hand, the semi-distributed model SWAT was used for data preparation, sensitivity analysis, calibration, validation, and evaluation of model performance. These evaluations were carried out before the effects of changing land use and land cover on the watershed's streamflow were examined.

There were increases in cropland, settlement area, and bareland, but there were decreases in forestland, grassland, shrubland, and water bodies for the years from 1990-2020. The decreasing trends of forestland, grassland, and shrubland, and the increasing trends of cropland, bareland, and settlement in the study watershed happened due to population pressure.

The SWAT model was calibrated and verified to evaluate the effect of LULC change streamflow and sediment yield in this watershed. Using SWAT-CUP, a SWAT model's streamflow and sediment yield were calibrated for the years 1990–2007 and validated for 2008–2015. The performance of the SWAT model was evaluated using different model performance indicators and found to be R^2 = 0.82, NSE = 0.69, PBIAS = -17.3, P-factor = 0.71, and R-factor = 1.64 for streamflow calibration; R^2 = 0.81, NSE = 0.65, PBIAS =-14.3, P-factor = 0.66, and R-factor = 1.86 for streamflow validation. Similarly, R^2 = 0.81, NSE = 0.72, PBIAS = -14.6, P-factor = 0.61, and Rfactor = 0.71 for sediment yield calibration. R^2= 0.8, NSE= 0.7, PBIAS= -17.2, Pfactor= 0.72 and R-factor= 1.02 for sediment yield validation. The finding confirmed that the SWAT model was found to be in the acceptable range. Thus, the model simulation result provides confidence for the further application of the model to analyse hydrologic response due to spatiotemporal watershed characteristics in Borkena watersheds.

LULC changes are recognized to have major impacts on hydrological processes, such as streamflow and sediment yield. Comparison of simulated outputs of the model using 1990, 2006 and 2020 LULC indicated an increase of average annual water yield by 35.3 mm (4.7%) and 56.5 mm (7.2%) during the periods 1990-2006 and 2006-2020, respectively. The LULC on sediment yield was increased by 4.4 t/ha (81.4%) during 1990-2006 and 2.8 t/ha (28.2%) during 2006–2020. Variation in topography, soil type, land use, land cover, and rainfall characteristics over the watershed results in spatial variability in surface runoff and sediment yield. Hence, out of 29 sub-basins, six sub-basins (5, 7, 10, 11, 12, and 20) produced the highest sediment yield and produced an average annual sediment yield of above 40.74 t/ha/yr. Those sub-watersheds require attention for best management practices in the watershed to reduce the severity of sedimentation in the Borkena watershed.

Accordingly, four BMPs, namely filter strips, terracing, contour farming, and reforestation, were simulated and tested using the SWAT model concerning sediment yield reduction. The result revealed that the terracing management option was the most effective conservation measure with a 72.32% sediment yield reduction efficiency. Next to terracing, countor farming was the most effective measure, which reduced about 63.56% of sediment yield. Implementing filter strips 5 m and 3 m wide reduced sediment yield by 57.12% and 50.67%, respectively, whereas reforestation reduced sediment yield by 33.81%.

5.2 Recommendation

Generally, from this specific study, the following recommendations could improve similar research for future work:

- In this study the model simulation manly considered the LULC change effect by assuming all other variables constant. But change in climate, slope and soil management activities will also contribute great impact on rainfall runoff process of the watershed. Therefore, there is a need for further research to ascertain the hydrological impacts of climate change, slope and soil in the watershed.
- Sustainable and adaptable strategies for future water resource management are required to reduce tremendous pressure on the hydrological system of the Borkena watershed.
- Sediment reduction methods like terracing, contouring, reforestation, and filter strips must be taken under consideration in order to reduce sedimentation problems in the Borkena watershed.

REFERENCES

Abbaspour, K. C., Vaghefi, S. A., & Srinivasan, R. (2017). A guideline for successful calibration and uncertainty analysis for soil and water assessment: A review of papers from the 2016 international SWAT conference. *Water (Switzerland)*, *10*(1). https://doi.org/10.3390/w10010006

Abbaspour, K. C., Vejdani, M., Haghighat, S., & Yang, J. (2007). SWAT-CUP calibration and uncertainty programs for SWAT. *MODSIM 2007 International Congress on Modelling and Simulation, Modelling and Simulation Society of Australia and New Zealand*, 1596–1602.

Abraham, T., & Nadew, B. (2018). Impact of land use land cover dynamics on water balance, Lake Ziway watershed, Ethiopia. *Hydrol Current Res*, *9*(309), 2.

Adepoju, M. O., Millington, A. C., & Tansey, K. T. (2006). Land use/land cover change detection in metropolitan lagos (Nigeria): 1984-2002. *American Society for Photogrammetry and Remote Sensing - Annual Conference of the American Society for Photogrammetry and Remote Sensing 2006: Prospecting for Geospatial Information Integration*, *1*, 8–14.

Adi, K. A. (2021). Modelling Hydrological Response to Land Use Land Cover Change and Developing Best Management Practices in the Gidabo Watershed, Ethiopia. *MSc Thesis Adama Science and Technology University, 112.*

Akbari, S., & Singh, R. (2012). Hydrological modelling of catchments using MIKE SHE. *IEEE-International Conference on Advances in Engineering, Science and Management*, 335–340.

Al-Doski, J., Mansorl, S. B., & Shafri, H. Z. M. (2013). Image classification in remote sensing. *Department of Civil Engineering, Faculty of Engineering, University Putra, Malaysia*, *3*(10).

Ali, H. (2009). Land use and land cover change, drivers and its impact: *A comparative study from Kuhar Michael and Lenche Dima of Blue Nile and Awash Basins of Ethiopia*. Cornell University.

Ali Saleh, & Bing Du. (2013). Application of SWAT and HSPF within BASINS program for the Upper North Bosque River watershed. *January 2002*. https://doi.org/10.13031/2013.10387

Amsalu A., Stroosnijder L., Graaff, J de., 2007. Long-term dynamics in land resource use and the driving forces in the Beressa watershed, highlands of Ethiopia. *Journal of Environmental Management. 83(4), 448–459.*

Arnold, J. G., & Fohrer, N. (2005). SWAT2000: current capabilities and research opportunities in applied watershed modelling. *Hydrological Processes: An International Journal*, *19*(3), 563–572.

Arnold, J. G., Moriasi, D. N., Gassman, P. W., Abbaspour, K. C., White, M. J., Srinivasan, R., Santhi, C., Harmel, R. D., Van Griensven, A., & Van Liew, M. W. (2012). SWAT: Model use, calibration, and validation. *Transactions of the ASABE*, *55*(4), 1491–1508.

Arnold, J. G., Williams, J. R., & Maidment, D. R. (1995). Continuous-time water and sediment-routing model for large basins. *Journal of Hydraulic Engineering*, *121*(2), 171–183.

Asselman, N. E. M. (2000). Fitting and interpretation of sediment rating curves. *Journal of Hydrology*, *234*(3–4), 228–248.

Awash Basin Authority. (2017). Awash River Basin Strategic Plan Main Report. *Awash Basin Authority: Amhara, Ethiopia.*

Berihun, M. L., Tsunekawa, A., Haregeweyn, N., Dile, Y. T., Tsubo, M., Fenta, A. A., Meshesha, D. T., Ebabu, K., Sultan, D., & Srinivasan, R. (2020). Evaluating runoff and sediment responses to soil and water conservation practices by employing alternative modeling approaches. *Science of the Total Environment*, *747*, 141118.

Beven, K. J. (2000). Uniqueness of place and process representations in hydrological modelling. *Hydrology and Earth System Sciences*, *4*(2), 203–213.

Bewket, W., & Sterk, G. (2005). Dynamics in land cover and its effect on stream flow in the Chemoga watershed, Blue Nile basin, Ethiopia. *Hydrological Processes*, *19*(2), 445–458. https://doi.org/10.1002/hyp.5542

Bruijnzeel, L. A. (1990). Hydrology of moist tropical forests and effects of conversion: a state of knowledge review. *Hydrology of Moist Tropical Forests and Effects of Conversion: A State of Knowledge Review.*

Bicknell, B. R., Imhoff, J. C., Donigian, A. S., and Johanson., R. C. (1997). Hydrological simulation program - FORTRAN (HSPF): *User's manual for release 11. EPA-600/R-97/080. Athens, Ga.: U.S. Environmental Protection Agency*.

Borah, D. K., M. Bera, M., and Xia., R. (2004). Storm event flow and sediment simulations in agricultural watersheds using DWSM. *Trans. ASAE 47(5). 1539-1559.*

Chen, S. M., Wang, Y. M., & Tsou, I. (2013). Using artificial neural network approach for modelling rainfall–runoff due to typhoon. *Earth System Science*, *122*, 399–405. http://dx.doi.org/10.1007/s12040-013-0289-8

Choto, M., & Fetene, A. (2019). Impacts of land use/land cover change on stream flow and sediment yield of Gojeb watershed, Omo-Gibe basin, Ethiopia. *Remote Sensing Applications: Society and Environment*, *14*(January), 84–99. https://doi.org/10.1016/j.rsase.2019.01.003

Choubin, B., Soleimani, F., Pirnia, A., Sajedi-Hosseini, F., Alilou, H., Rahmati, O., Melesse, A. M., Singh, V. P., & Shahabi, H. (2019). Effects of drought on vegetative cover changes: Investigating spatiotemporal patterns. *Extreme Hydrology and Climate Variability: Monitoring, Modelling, Adaptation and Mitigation*, *2*, 213–222. https://doi.org/10.1016/B978-0-12-815998-9.00017-8

Daba, M. H. and S. You (2018). "Assessment of Climate Change Impacts on River Flow Regimes in the Upstream of Awash Basin, Ethiopia: *Based on IPCC Fifth Assessment Report (AR5) Climate Change Scenarios." Hydrology 7(4): 98.*

Deshmukh, C., Saikia, T., Bakshi, A., Amare-Kadam, P., Baisane, C., & Parikh, P. (2005). Imatinib mesylate in chronic myeloid leukemia: a prospective, single arm, non-randomized study. *The Journal of the Association of Physicians of India*, *53*, 291–295.

Dwarakish, G. S., & Ganasri, B. P. (2015). Impact of land use change on hydrological systems: A review of current modeling approaches. *Cogent Geoscience*, *1*(1). https://doi.org/10.1080/23312041.2015.1115691

El-Nasr, A. A., Arnold, J. G., Feyen, J., & Berlamont, J. (2005). Modelling the hydrology of a catchment using a distributed and a semi-distributed model. *Hydrological Processes*, *19*(3), 573–587. https://doi.org/https://doi.org/10.1002/hyp.5610

Elfert, S., & Bormann, H. (2010). Simulated impact of past and possible future land use changes on the hydrological response of the Northern German lowland Hunte catchment. *Hydrology*, *383*, 245–255. http://dx.doi.org/10.1016/j.jhydrol.2009.12.040

Esa, E., Assen, M., & Legass, A. (2018). Implications of land use/cover dynamics on soil erosion potential of agricultural watershed, northwestern highlands of Ethiopia. *Environmental Systems Research*, *7*(1). https://doi.org/10.1186/s40068-018-0122-0

Garg, S. K., Weinzimer, S. A., Tamborlane, W. V, Buckingham, B. A., Bode, B. W., Bailey, T.

S., Brazg, R. L., Ilany, J., Slover, R. H., & Anderson, S. M. (2017). Glucose outcomes with the in-home use of a hybrid closed-loop insulin delivery system in adolescents and adults with type 1 diabetes. *Diabetes Technology & Therapeutics*, *19*(3), 155–163.

Gashaw, T., Tulu, T., Argaw, M., Worqlul, A. W., Tolessa, T., & Kindu, M. (2018). Estimating the impacts of land use/land cover changes on Ecosystem Service Values: The case of the Andassa watershed in the Upper Blue Nile basin of Ethiopia. *Ecosystem Services*, *31*, 219–228.

Gebrehiwet, K. B. (2004). Land use and land cover changes in the central highlands of Ethiopia: The case of Yerer Mountain and its surroundings. *Unpublished MSc. Project Report.*

Geremew, A. A. (2013). Assessing the impacts of land use and land cover change on hydrology of watershed: *a case study on Gigel-Abbay Watershed, Lake Tana Basin, Ethiopia*.

Gessesse, B., & Bewket, W. (2014). Drivers and implications of land use and land cover change in the central highlands of Ethiopia: Evidence from remote sensing and socio-demographic data integration. *Ethiopian Journal of the Social Sciences and Humanities*, *10*(2), 1–23.

Gudmundsson, B. (2001). Initial National Communication of Ethiopia to the United Nations Framework Convention on Climate Change (UNFCCC)'. *National Meteorological Services Agency June*.

Haile E, & Assefa. (2012). The impact of land use change on the hydrology of Angereb Watershed. *International Journal of Water Sciences. 1: 1-7.*

Hurni, H. (1985). Erosion–productivity–conservation systems in Ethiopia. *IV International Conference on Soil Conservation November 3-9, 1985 Maracay, Venezuela, January 1985*, 654–674.

Hurni, H., Abate, S., Bantider, A., Debele, B., Ludi, E., Portner, B., Yitaferu, B., & Zeleke, G. (2010). *Land degradation and sustainable land management in the highlands of Ethiopia*.

Ikbal, M., Atasoy, M., Pirim, I., Aliagaoglu, C., Karatay, S., & Erdem, T. (2006). The alteration of sister chromatid exchange frequencies in Behçet's disease with and without HLA-B51. *Journal of the European Academy of Dermatology and Venereology*, *20*(2), 149–152.

Jansen, L. J. M., & Di Gregorio, A. (2002). Parametric land cover and land-use classifications as tools for environmental change detection. *Agriculture, Ecosystems & Environment*, *91*(1–3), 89–100.

Kassa, G. (2003). GIS-based analysis of land use/land cover, land degradation and population changes-a study of Boru Metero area of South Wello, Amhara region. *Unpublished MSc Thesis, School of Graduate Studies, Addis Ababa University*.

Kassa, T., & Forech, G. (2009). Watershed Hydrological Responses to Changes in Land Use and Land Cover , and Management Practices at Hare Watershed , Ethiopia. *Ph.D Thesis, University of Siegen, Germany*, 229.

Kefay, T., Abdisa, T., & Tumsa, B. C. (2022). Prioritization of Susceptible Watershed to Sediment Yield and Evaluation of Best Management Practice: A Case Study of Awata River, Southern Ethiopia. *Applied and Environmental Soil Science, 2022*. https://doi.org/10.1155/2022/1460945

Khoshru, B., Mitra, D., Khoshmanzar, E., Myo, E. M., Uniyal, N., Mahakur, B., Mohapatra, P. K. Das, Panneerselvam, P., Boutaj, H., & Alizadeh, M. (2020). Current scenario and future prospects of plant growth-promoting rhizobacteria: An economic valuable resource for the agriculture revival under stressful conditions. *Journal of Plant Nutrition*, *43*(20), 3062–3092.

Kode, A., Manavalan, J. S., Mosialou, I., Bhagat, G., Rathinam, C. V, Luo, N., Khiabanian, H., Lee, A., Murty, V. V, & Friedman, R. (2014). Leukaemogenesis induced by an activating β-catenin mutation in osteoblasts. *Nature*, *506*(7487), 240–244.

Lemma, H., Frankl, A., van Griensven, A., Poesen, J., Adgo, E., & Nyssen, J. (2019). Identifying erosion hotspots in Lake Tana Basin from a multisite Soil and Water Assessment Tool validation: Opportunity for land managers. *Land Degradation & Development*, *30*(12), 1449–1467.

Li, L. J., Jiang, D. J., Li, J. Y., Liang, L. Q., & Zhang, L. (2007). Advances in hydrological response to land use/land cover change. *Journal of Natural Resources*, *22*(2), 211–224.

Metaferia, G. (2019). Impact of land use land cover change on hydrology of Borkena Watershed, Ethiopia. *MSc Thesis, Addis Abeba university school of civil and environmental engineering, Ethiopia,87.*

Moriasi, D. N., Arnold, J. G., Van Liew, M. W., Bingner, R. L., Harmel, R. D., & Veith, T. L. (2007). Model evaluation guidelines for systematic quantification of accuracy in watershed simulations. *Transactions of the ASABE*, *50*(3), 885–900.

Neitsch, S. ., Arnold, J. ., Kiniry, J. ., & Williams, J. . (2011). Soil & Water Assessment Tool Theoretical Documentation Version 2009. In *Texas Water Resources Institute*.

https://doi.org/10.1016/j.scitotenv.2015.11.063

Neitsch, S. L. (2005). Soil and water assessment tool. *User's Manual Version 2005*, *476*.

Ponce-Hernandez, R., & Oumer, A. (2009). A Model-based approach to predicting the effects of global warming 4 degrees and beyond on ecosystem primary productivity, land degradation and food security at national scale: Case Study Ethiopia. *Trent University, Ontario*.

Prakasam, C. (2010). Land use and land cover change detection through remote sensing approach: A case study of Kodaikanal taluk, Tamil nadu. *International Journal of Geomatics and Geosciences*, *1*(2), 150.

Raes, D., Willems, P., & Gbaguidi, F. (2006). RAINBOW–A software package for hydrometeorological frequency analysis and testing the homogeneity of historical data sets. *Proceedings of the 4th International Workshop on Sustainable Management of Marginal Drylands. Islamabad, Pakistan*, *2731*, 12.

Reid, J. M., Monaghan, P., & Ruxton, G. D. (2000). Resource allocation between reproductive phases: the importance of thermal conditions in determining the cost of incubation. *Proceedings of the Royal Society of London. Series B: Biological Sciences*, *267*(1438), 37–41.

Sarkar, A., & Kumar, R. (2012). Artificial neural networks for event-based rainfall–runoff modeling. *Water Resource and Protection*, *4*, 891–897. http://dx.doi.org/10.4236/jwarp.2012.410105

SCS. (1972). USDA Soil Conservation Service. In *National Engineering Handbook Section 4 Hydrology*.

Serur, A. B., & Adi, K. A. (2022). Multi-site calibration of hydrological model and the response of water balance components to land use land cover change in a rift valley Lake Basin in Ethiopia. *Scientific African*, *15*, e01093. https://doi.org/10.1016/J.SCIAF.2022.E01093

Shawl Abebe, D. (2020). Modeling the Hydrology of Borkena Watershed , Awash Basin , Ethiopia. *International Journal of Advanced Research in Basic Engineering Sciences and Technology (IJARBEST)*, *6*(9), 29–40.

Shawul, A. A., Chakma, S., & Melesse, A. M. (2019). The response of water balance components to land cover change based on hydrologic modeling and partial least squares regression (PLSR) analysis in the Upper Awash Basin. *Journal of Hydrology: Regional*

Studies, *26*(August). https://doi.org/10.1016/j.ejrh.2019.100640

Shirke, Y., Kawitkar, R., & Balan, S. (2012). Artificial neural network-based runoff prediction model for a reservoir. *Engineering Research and Technology*, *1*(3), 1–4.

Sivakami, C., Meenakshi, S. M., & Sundram, A. (2010). Application of RS and GIS for Land Use/Land Cover Mapping & Change Detection in Madurai District TN. *Indian Geotechnical Conference–2010, GEOtrendz*.

Taddese, G. (2001). Land degradation: a challenge to Ethiopia. *Environmental Management*, *27*(6), 815–824.

Tekle, K., & Hedlund, L. (2000). Land cover changes between 1958 and 1986 in Kalu District, southern Wello, Ethiopia. *Mountain Research and Development*, *20*(1), 42–51.

Tesema, T. A., & Leta, O. T. (2020). Sediment Yield Estimation and Effect of Management Options on Sediment Yield of Kesem Dam Watershed, Awash Basin, Ethiopia. *Scientific African*, *9*, e00425. https://doi.org/10.1016/j.sciaf.2020.e00425

Tilahun, A., & Teferie, B. (2015). A GIS based slope analysis for recommended soil and water conservation techniques in Sekela District, Amhara State, Ethiopia. *Ijaar*, *3*, 45–54.

Tsegaye, B. (2019). Effect of land use and land cover changes on soil erosion in Ethiopia. *International Journal of Agricultural Science and Food Technology*, *5*(1), 26–34.

Ullrich, A., & Volk, M. (2009). Application of the Soil and Water Assessment Tool (SWAT) to predict the impact of alternative management practices on water quality and quantity. *Agricultural Water Management*, *96*(8), 1207–1217.

Use, L., Change, L. C., Hydrology, W., Study, C., Basin, U. A., Awash, U., Tool, W. A., LULC, T., Awash, U., The, U., Awash, M. S., Author, S. P., & Author, S. P. (2021). *owToc Impact of Land Use / Land Cover Change on Watershed Hydrology : A Case Study of Upper Awash Basin , Ethiopia*. *2021*(October), 1–28.

Vasiliades, L., & Loukas, A. (2009). Hydrological response to meteorological drought using the Palmer drought indices in Thessaly, Greece. *Desalination*, *237*(1–3), 3–21.

Wagayehu, B., & Lars, D. (2003). Soil and water conservation decision of subsistence farmers in the Eastern highlands of Ethiopia: a case study of the Hunde-Lafto. *Journal of Agricultural Economics*, *18*(1), 125–133.

Wang, S., Zhang, Z., McVicar, T. R., Zhang, J., Zhu, J., & Guo, J. (2012). An event-based approach to understanding the hydrological impacts of different land uses in semi-arid catchments. *Journal of Hydrology*, *416–417*, 50–59. https://doi.org/10.1016/j.jhydrol.2011.11.035

Wassie, S. B. (2020). Natural resource degradation tendencies in Ethiopia: a review. *Environmental Systems Research*, *9*(1), 1–29.

Yesuf, H. M., Assen, M., Melesse, A. M., & Alamirew, T. (2015). Detecting land use/land cover changes in the Lake Hayq (Ethiopia) drainage basin, 1957-2007. *Lakes and Reservoirs: Research and Management*, *20*(1), 1–18. https://doi.org/10.1111/lre.12082

Yesuph, A. Y., & Dagnew, A. B. (2019a). Land use/cover spatiotemporal dynamics, driving forces and implications at the Beshillo catchment of the Blue Nile Basin, North Eastern Highlands of Ethiopia. *Environmental Systems Research*, *8*(1). https://doi.org/10.1186/s40068-019-0148-y

Yesuph, A. Y., & Dagnew, A. B. (2019b). Soil erosion mapping and severity analysis based on RUSLE model and local perception in the Beshillo Catchment of the Blue Nile Basin, Ethiopia. *Environmental Systems Research*, *8*(1), 1–21.

Yuan, M. (2001). Representing complex geographic phenomena in GIS. *Cartography and Geographic Information Science*, *28*(2), 83–96.

Zeleke, G., & Hurni, H. (2001). Implications of land use and land cover dynamics for mountain resource degradation in the Northwestern Ethiopian highlands. *Mountain Research and Development*, *21*(2), 184–191.

Zhu, C. (2011). TRACE : Tennessee Research and Creative Exchange Land Use / Land Cover Change and Its Hydrological Impacts from 1984 to 2010 in the Little River Watershed , *Tennessee*. 1–85.

APPENDIX

Appendix-A

Appendix A.1 Average annual rainfall of station in the study area

Year	Kombolcha	Majete	Kemissie	Cheffa	Dessie	Harbu
1988	1198.3	1139.0	1131.4	1099.35	1376.3	1054.0
1989	1169.1	1018.5	754.4	878.5	1128.8	974.5
1990	892.8	1018.6	1209.0	1382.2	884.9	758.5
1991	754.0	930.1	1240.9	1345.1	979.5	1264.3
1992	1040.1	1126.0	1016.5	1114.2	1166.1	1284.1
1993	1280.0	1106.0	1114.6	1087.8	1319.9	1200.0
1994	1185.1	991.7	929.5	1277.3	1292.2	1138.7
1995	1096.0	1352.3	1145.1	1103.4	1190.5	1143.3
1996	1027.5	1344.9	958.4	1358.2	1194.1	1160.8
1997	1001.5	1256.1	1352.3	1271.8	1100.7	1064.9
1998	998.1	1295.2	1149.5	1508.6	1282.6	1301.0
1999	972.5	1242.7	901.6	865	1128.0	941.8
2000	961.5	1146.4	867.2	1008.6	1121.5	937.0
2001	987.6	1120.6	1244.3	1613.9	1307.8	1138.3
2002	893.9	1177.9	975.2	1127.5	1016.7	1023.3
2003	991.4	1214.9	956.9	1158.9	1268.7	1054.0
2004	908.2	1060.0	1011.0	1331.5	1154.9	1112.0
2005	975.1	1148.8	898.1	748.3	1179.8	893.8
2006	1131.1	1343.6	1186.0	963.4	1236.0	1120.0

2007	910.5	1243.3	1015.9	1312.4	1053.7	882.0
2008	821.3	916.0	817.8	821.15	811.5	816.0
2009	961.3	1044.2	771.4	903.95	1327.3	1096.1
2010	896.4	1065.5	1345.8	1188.3	1359.0	1210.7
2011	1007.3	743.0	809.8	752.4	1035.1	800.4
2012	969.7	1059.5	758.7	886.25	899.7	1200.0
2013	1010.0	1140.5	1111.0	1013.6	1043.5	946.3
2014	1108.0	1306.8	1172.8	1760.3	1192.1	680.1
2015	749.1	873.3	675.9	913.95	893.8	802.9
2016	1144.8	1394.5	1213.4	1349.2	1155.2	803.4
2017	1007.2	1237.2	739.2	988.2	1055.9	1385.1
2018	1107.9	1387.5	1005.4	871.05	1290.8	1100.3
2019	1181.6	1032.3	1023.4	989.35	1191.2	1091.1
2020	1041.8	1091.3	816.3	953.8	1127.4	965.0

Appendix A.2 Parameters used in a streamflow sensitivity analysis

Rank	Parameter Name	Description
1	CN2.mgt	Moisture condition II curvenumber
2	HRU_SLP.hru	Average slope steepness (m/m)
3	SOL_K(..).sol	Saturated hydraulic conductivity of the soil layer
4	GW_DELAY.gw	Delay time for aquifer recharge
5	GW_REVAP.gw	Groundwater "revap" coefficient
6	SOL_AWC(..).sol	Available water capacity of the soil layer
7	SLSUBBSN.hru	Average slope length.
8	ALPHA_BF.gw	Base flow alpha-factor
9	CANMX.hru	Maximum canopy storage
10	ESCO.hru	Soil evaporation compensation factor
11	RCHRG_DP.gw	Deep aquifer percolation fraction
12	SOL_Z..sol	Depth from soil surface to bottom of layer
13	GWQMN.gw	Shallow a aquifer for flow (mm)
14	OV_N.hru	Manning's roughness coefficient for overland flow
15	SURLAG.bsn	Surface runoff lag coefficient
16	EPCO.hru	Plant uptake compensation factor.
17	CH_K2.rte	Channel effective hydraulic conductivity(mm/hr)
18	REVAPMN.gw	Threshold depth of water in the shallow aquifer for"revap"
19	BIOMIX.mgt	Biological mixing efficiency

Appendix A.3 Parameters used in sediment yield sensitivity analysis

Parameter Name	t-Stat	P-Value	Description
USLE_K(..).sol	-134.51	0.00	USLE soil erodibility factor (USLE_K)
SPEXP.bsn	-1.66	0.10	Exponent re-entrainment parameter in sediment routing (SPEXP. Bsn)
RSDIN.hru	-1.43	0.15	Initial residue cover (kg/ha) (RSDIN.hru)
USLE_P.mgt	-0.66	0.51	Exponent parameter for calculating sediment re-entrained in channel sediment routing (USLE_P.mgt)
SPCON.bsn	0.62	0.54	channel sediment routing (SPCON)
CH_COV2.rte	0.58	0.56	Channel cover factor. (CH_COV2)
LAT_SED.hru	0.55	0.58	Sediment concentration in lateral flow and groundwater flow. (LAT_SED)
CH_COV1.rte	-0.23	0.82	Channel erodibility factor. (CH_COV1)

Appendix A.4 Sub basins Surface Runoff and Sediment Yield distribution

Subbasins	SURQ (mm)	SYLDt/ha/Year	Subbasins	SURQ (mm)	SYLDt/ha/Year
1	66.40	5.73	16	161.79	12.52
2	57.00	11.94	17	214.14	0.73
3	49.50	10.67	18	72.95	12.55
4	30.13	11.95	19	117.88	21.09
5	50.55	24.45	20	183.84	23.43
6	51.02	15.52	21	162.59	0.10
7	81.32	24.41	22	198.73	0.29
8	92.05	6.55	23	69.60	15.39
9	109.67	18.18	24	156.68	3.17
10	218.34	71.23	25	19.52	6.32
11	153.05	43.18	26	9.93	0.13
12	145.57	57.71	27	158.27	16.02
13	219.91	3.50	28	6.80	1.99
14	41.01	20.80	29	27.49	10.50
15	117.55	20.53			

Appendix A.5 Monthly average basin water balance value

Months	RF (mm)	SUR Q (mm)			LAT Q (mm)			WY (mm)			ET (mm)			SY (t/ha)		
		1990	2006	2020	1990	2006	2020	1990	2006	2020	1990	2006	2020	1990	2006	2020
Jan	19.66	0.29	0.48	0.77	5.64	5.64	5.49	12.16	13.52	18.19	7.1	7.14	6.72	0.03	0.04	0.06
Feb	27.79	0.71	1.11	1.61	8.09	8.09	7.86	11.35	13.92	18.11	9.96	9.99	9.64	0.06	0.09	0.13
Mar	65.47	2.67	3.91	5.3	19.5	19.4	18.8	25.1	28.85	32.66	18.5	18.3	17.4	0.2	0.32	0.44
Apr	83.34	3.83	5.65	7.65	25.1	25	24.2	35.63	39.45	43.46	30	29.3	27.3	0.24	0.38	0.55
May	68.67	4.47	6.66	8.61	21	20.7	20	37.06	40.83	45.18	44.8	42.7	38.8	0.41	0.71	0.94
Jun	36.7	0.71	1.2	1.91	10.4	10.4	10.2	21.85	23.72	28.71	42.4	40.8	40.9	0.06	0.1	0.16
Jul	278.05	29.3	43	52.3	92.9	90.4	87.8	134.3	152.64	152.00	40.3	40.5	41.4	1.63	3.01	3.77
Aug	308.03	32.7	46.9	56.9	99.6	96.1	93.5	187.3	198.96	201.45	42	42.2	42.9	1.9	3.6	4.44
Sep	131.72	9.36	13.5	17.1	42.3	41.5	40.3	133.1	129.23	137.36	39.1	39.2	40.1	0.62	1.12	1.47
Oct	56.38	3.61	5.2	6.73	17.9	17.6	17.1	88.05	83.24	91.29	39.1	38.9	40.4	0.2	0.33	0.47
Nov	19.91	0.55	0.84	1.25	5.87	5.85	5.69	44.05	41.50	48.18	36	35.6	37.1	0.04	0.05	0.09
Dec	19.42	0.56	0.84	1.24	5.81	5.8	5.63	24.54	24.35	29.75	21.8	21.6	23.7	0.03	0.04	0.06

Appendix-B

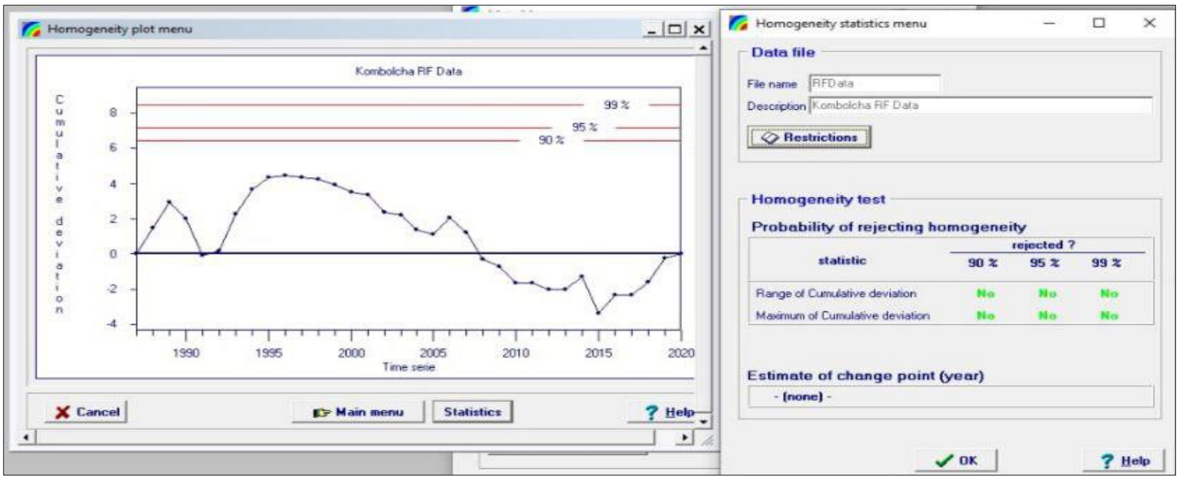

Appendix B.1 Homogeneity test plot at station Kombolcha

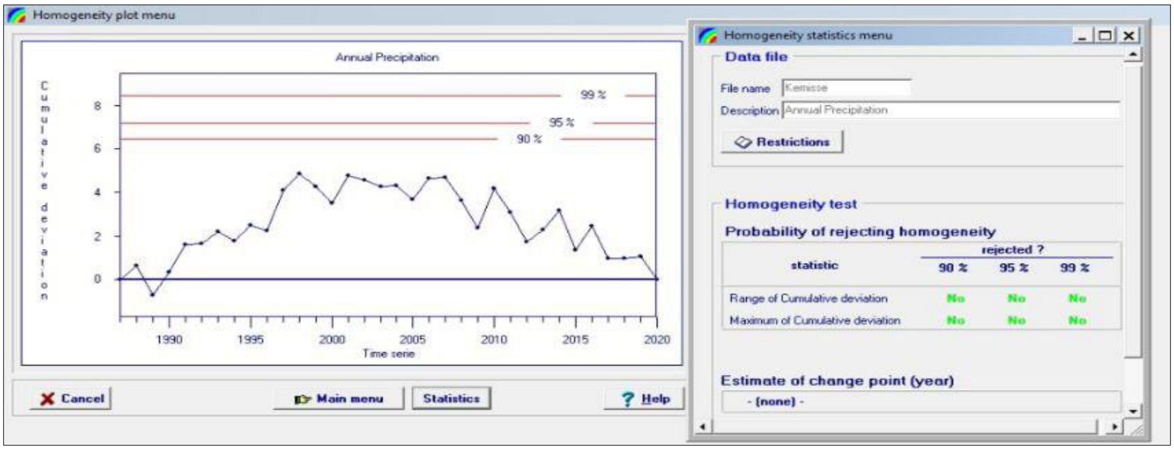

Appendix B.2 Homogeneity test plot at station Kemisse

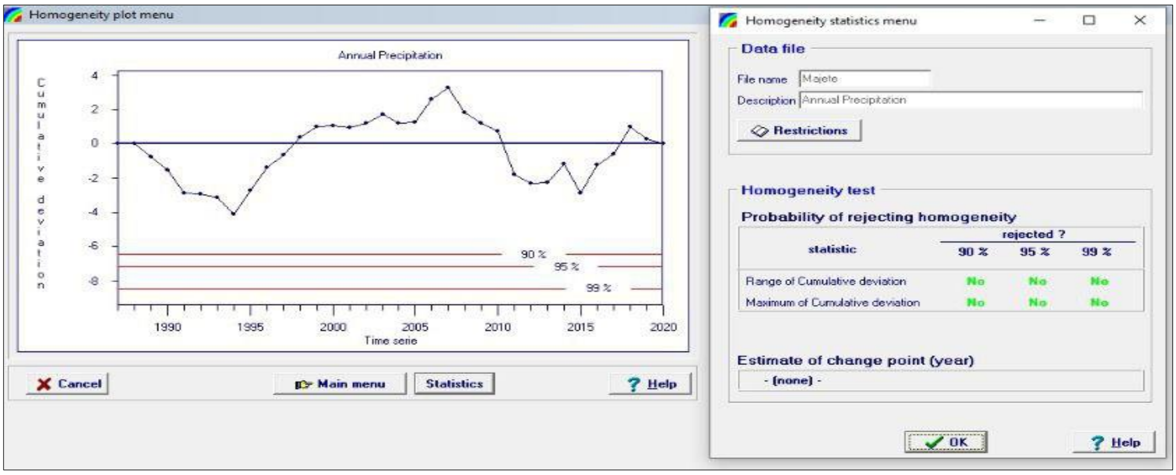

Appendix B.3 Homogeneity test plot at station Majete

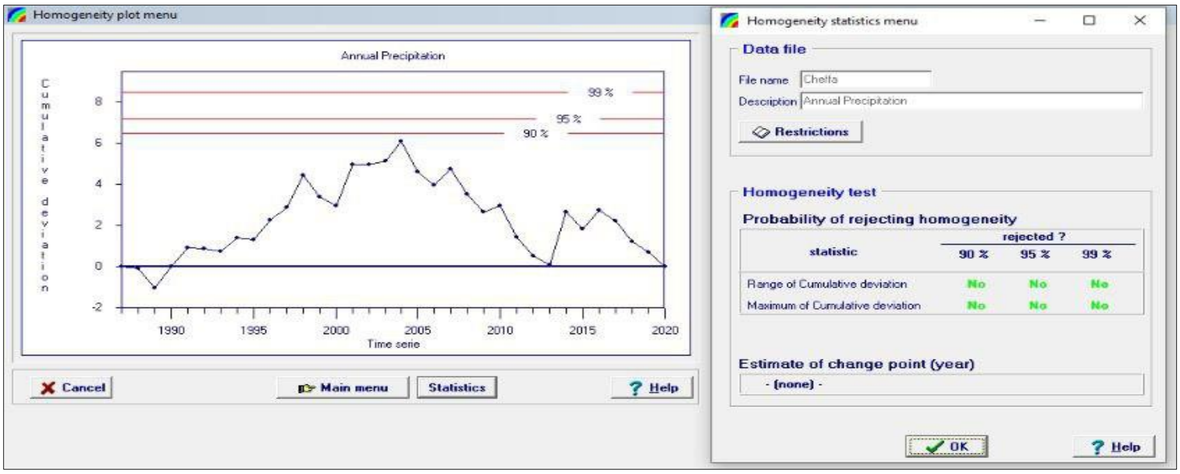

Appendix B.4 Homogeneity test plot at station Cheffa

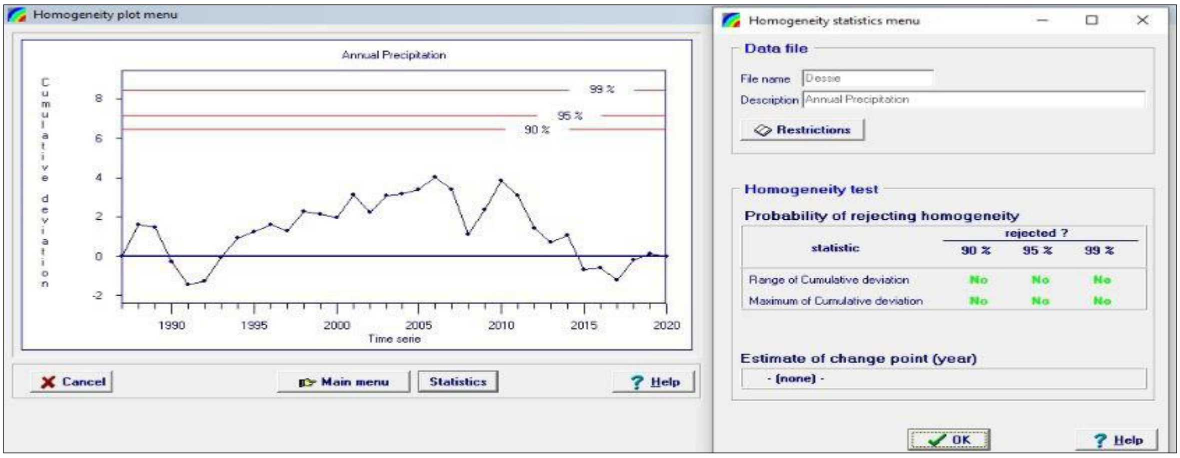

Appendix B.5 Homogeneity test plot at station Dessie

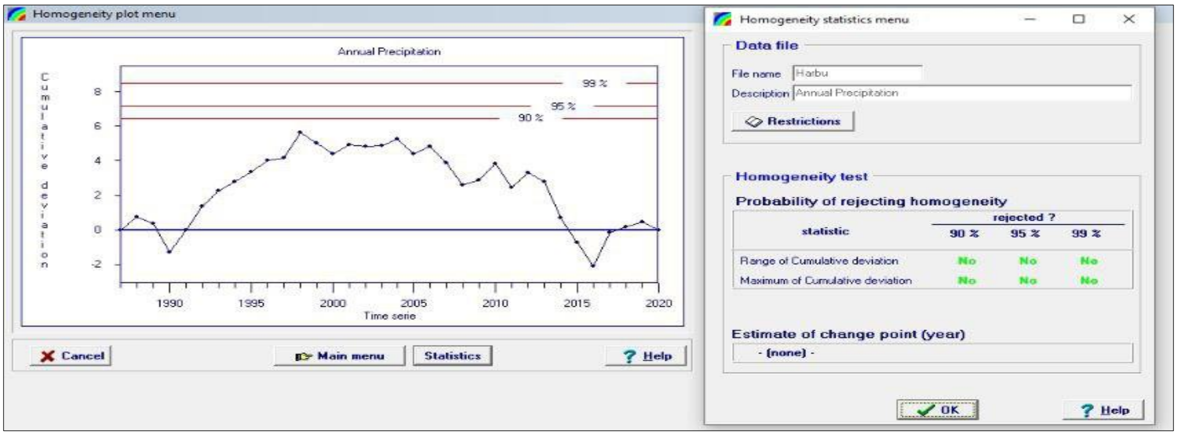

Appendix B.6 Homogeneity test plot at station Harbu